

Equal-spin supercurrents and magnetization dynamics in high-temperature superconductor/ferromagnet hybrids

Javier E. Villegas

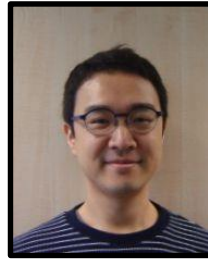
Unité Mixte de Physique CNRS/Thales, France



THALES

université
PARIS-SACLAY

Acknowledgements



**D. Sanchez, S. J. Carreira, S. Mesoraca, M.-W. Yoo, V. Rouco, X. Palermo,
A. Balan, K. Seurre, A. Sander, A. Anane & Javier E. Villegas**
Unité Mixte de Physique CNRS, Thales, **FRANCE**

**G. Orfila, A. Cuellar, M. Cabero, L. Marcano, M. Rocci, J. Garcia-Barriocanal
F. Gallego, J. Tornos, A. Rivera, J. M. Gonzalez-Calbet, C. Leon & J. Santamaria**
Universidad Complutense Madrid, **SPAIN**

S. Valencia
Helmholtz-Zentrum Berlin, **GERMANY**

F. Mompean, M. Garcia-Hernandez
ICMM-CSIC, **SPAIN**

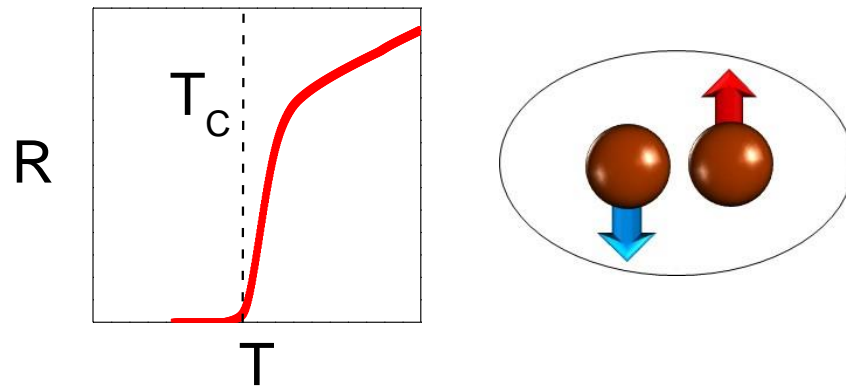
C. Feuillet-Palma, N. Bergeal & J. Lesueur
ESPCI-Paris, **FRANCE**

A. I. Buzdin
Université de Bordeaux, **FRANCE**



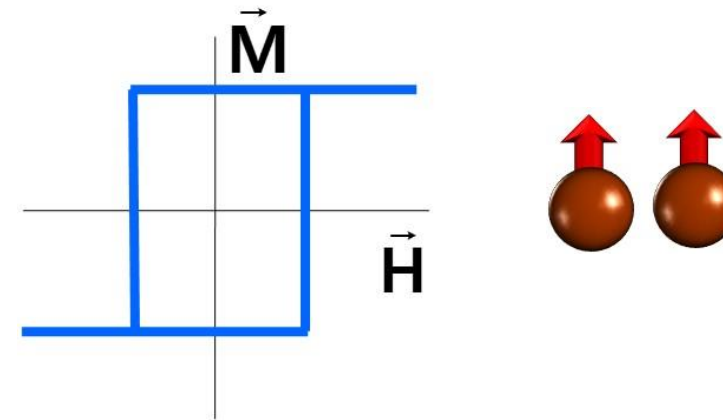
Superconductor/ferromagnet hybrids

Superconductor



Large resistance variation
Coherent transport

Ferromagnet



Memory
Spin-polarized transport

→ OPPORTUNITIES FOR SPINTRONICS

Main goals in the area



Spin-polarized supercurrents for spintronics

Matthias Eschrig *Physics Today*, 64 43 (2011)

A marriage between superconductivity and ferromagnetism is opening the door for new spin-based applications.

Mesoscopic magnetism and superconductivity

Ali C. Basaran, Javier E. Villegas, J.S. Jiang, Axel Hoffmann, and Ivan K. Schuller



REVIEW ARTICLES

PUBLISHED ONLINE: 2 APRIL 2015 | DOI: 10.1038/NPHYS3242

Superconducting spintronics

Jacob Linder^{1*} and Jason W. A. Robinson^{2*}



Volume 40, Issue 11 (Mesoscale Materials, Phenomena, and Functionality)

November 2015, pp. 925-932

Main goals in the area



Spin-polarized supercurrents for spintronics

Matthias Eschrig *Physics Today*, 64 43 (2011)

A marriage between superconductivity and ferromagnetism is opening the door for new spin-based applications.

Mesoscopic magnetism and superconductivity

Ali C. Basaran, Javier E. Villegas, J.S. Jiang, Axel Hoffmann, and Ivan K. Schuller



Superconducting spintronics

Jacob Linder^{1*} and Jason W. A. Robinson^{2*}

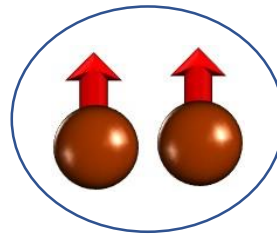


Volume 40, Issue 11 (Mesoscale Materials, Phenomena, and Functionality)

November 2015, pp. 925-932

A) SPIN-POLARIZED SUPERCURRENTS

- Equilibrium
- Low-dissipation spin transport
- Spin torques
- Phase coherence effects (Josephson)
- Large spin signals (spin valves)



Main goals in the area



Spin-polarized supercurrents for spintronics

Matthias Eschrig *Physics Today*, 64 43 (2011)

A marriage between superconductivity and ferromagnetism is opening the door for new spin-based applications.

Mesoscopic magnetism and superconductivity

Ali C. Basaran, Javier E. Villegas, J.S. Jiang, Axel Hoffmann, and Ivan K. Schuller



REVIEW ARTICLES

PUBLISHED ONLINE: 2 APRIL 2015 | DOI: 10.1038/NPHYS3242

Superconducting spintronics

Jacob Linder^{1*} and Jason W. A. Robinson^{2*}

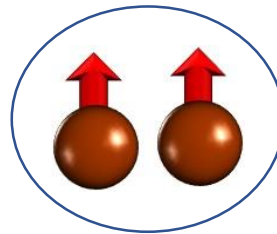
MRS Bulletin

Volume 40, Issue 11 (Mesoscale Materials, Phenomena, and Functionality)

November 2015, pp. 925-932

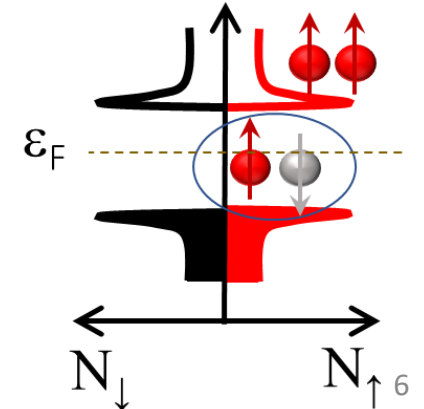
A) SPIN-POLARIZED SUPERCURRENTS

- Equilibrium
- Low-dissipation spin transport
- Spin torques
- Phase coherence effects (Josephson)
- Large spin signals (spin valves)



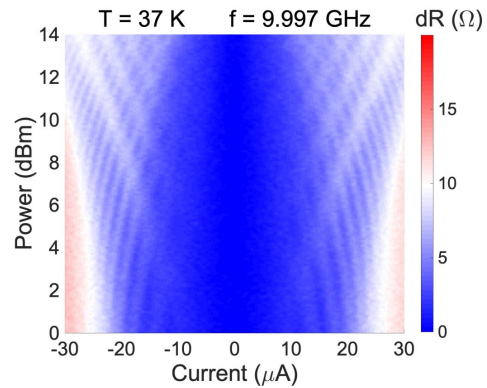
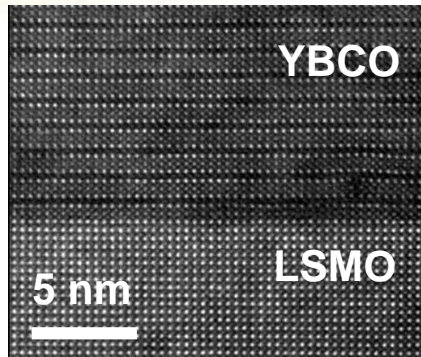
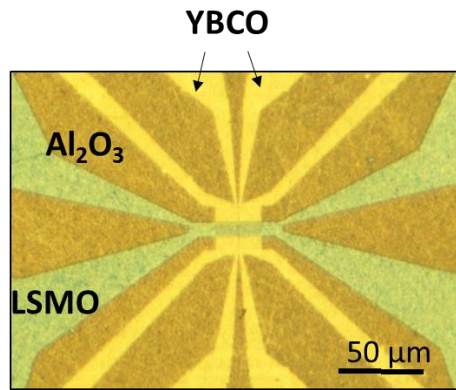
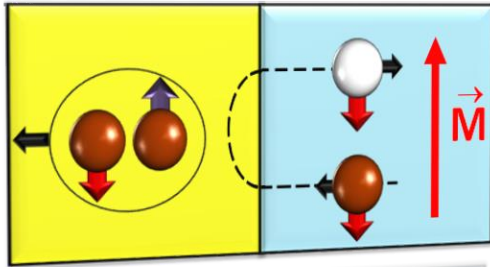
B) SPIN-POLARIZED QUASIPARTICLES

- Non-equilibrium
- Quantum protection
- Enhanced spin lifetimes
- Enhanced spin Hall effects
- Dynamic coupling



The talk in a nutshell

Proximity effect

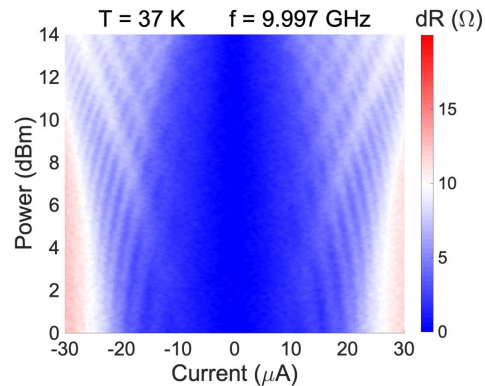
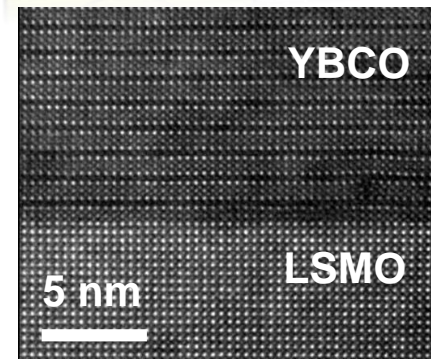
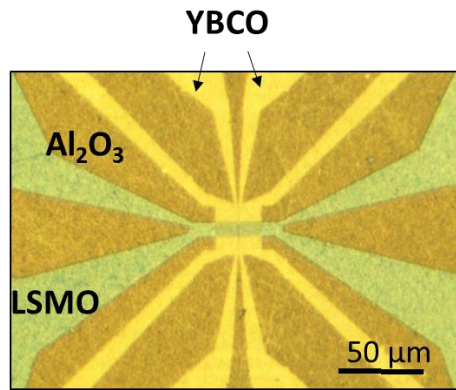
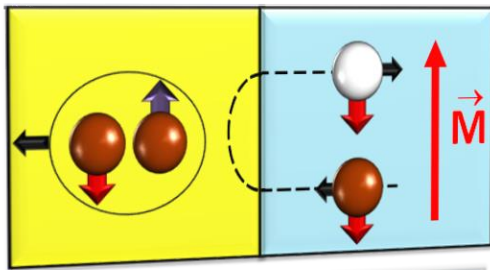


Fully spin-polarized, high- T_c Josephson supercurrents
Quantum phase coherence effects

Sanchez-Manzano *et al.* Nature Materials (2022)

The talk in a nutshell

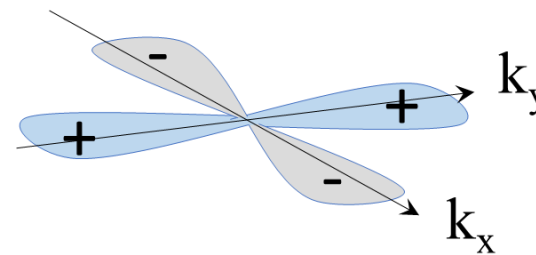
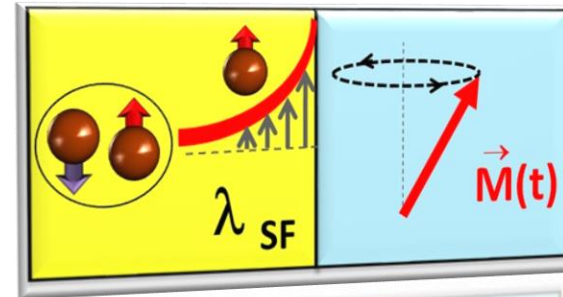
Proximity effect



Fully spin-polarized, high- T_c Josephson supercurrents
Quantum phase coherence effects

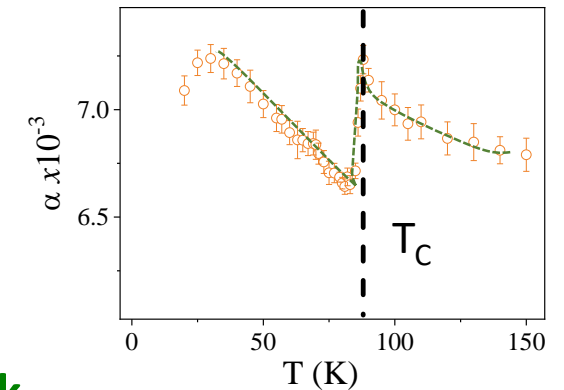
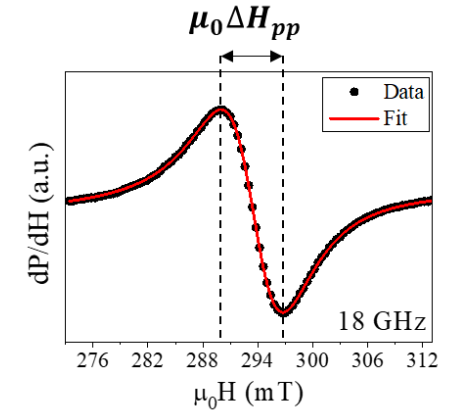
Sanchez-Manzano *et al.* Nature Materials (2022)

Dynamic coupling



Tunable spin sink
d-wave effects

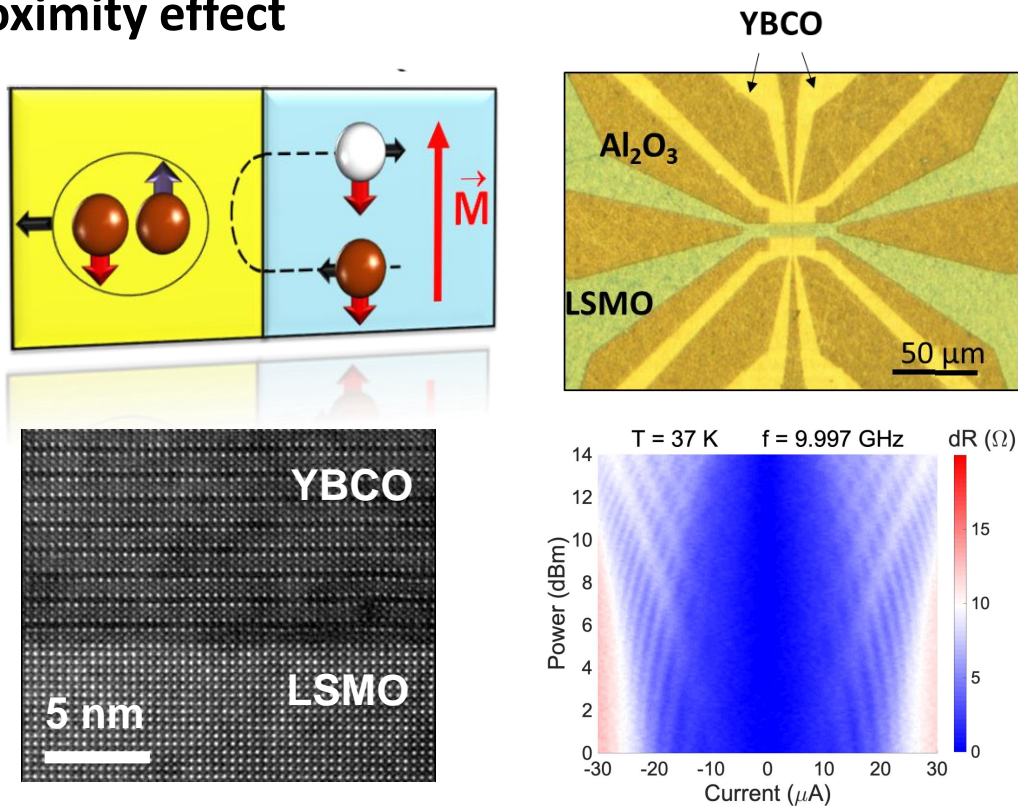
Carreira *et al.* PRB (2021)



→ OPPORTUNITIES FOR HIGH- T_c SUPERCONDUCTING SPINTRONICS 8

The talk in a nutshell

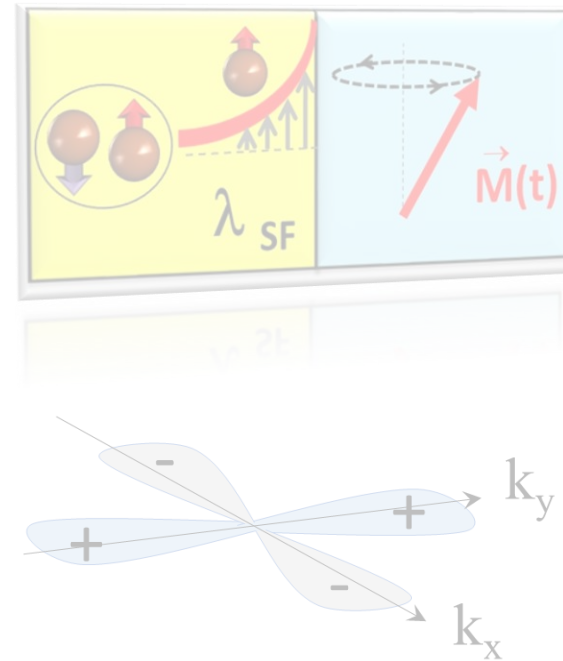
Proximity effect



Fully spin-polarized, high- T_c Josephson supercurrents
Quantum phase coherence effects

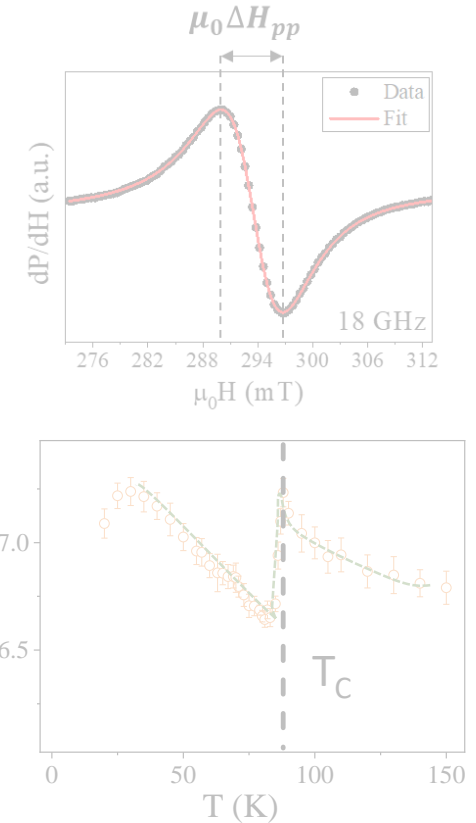
Sanchez-Manzano *et al.* Nature Materials (2022)

Dynamic coupling



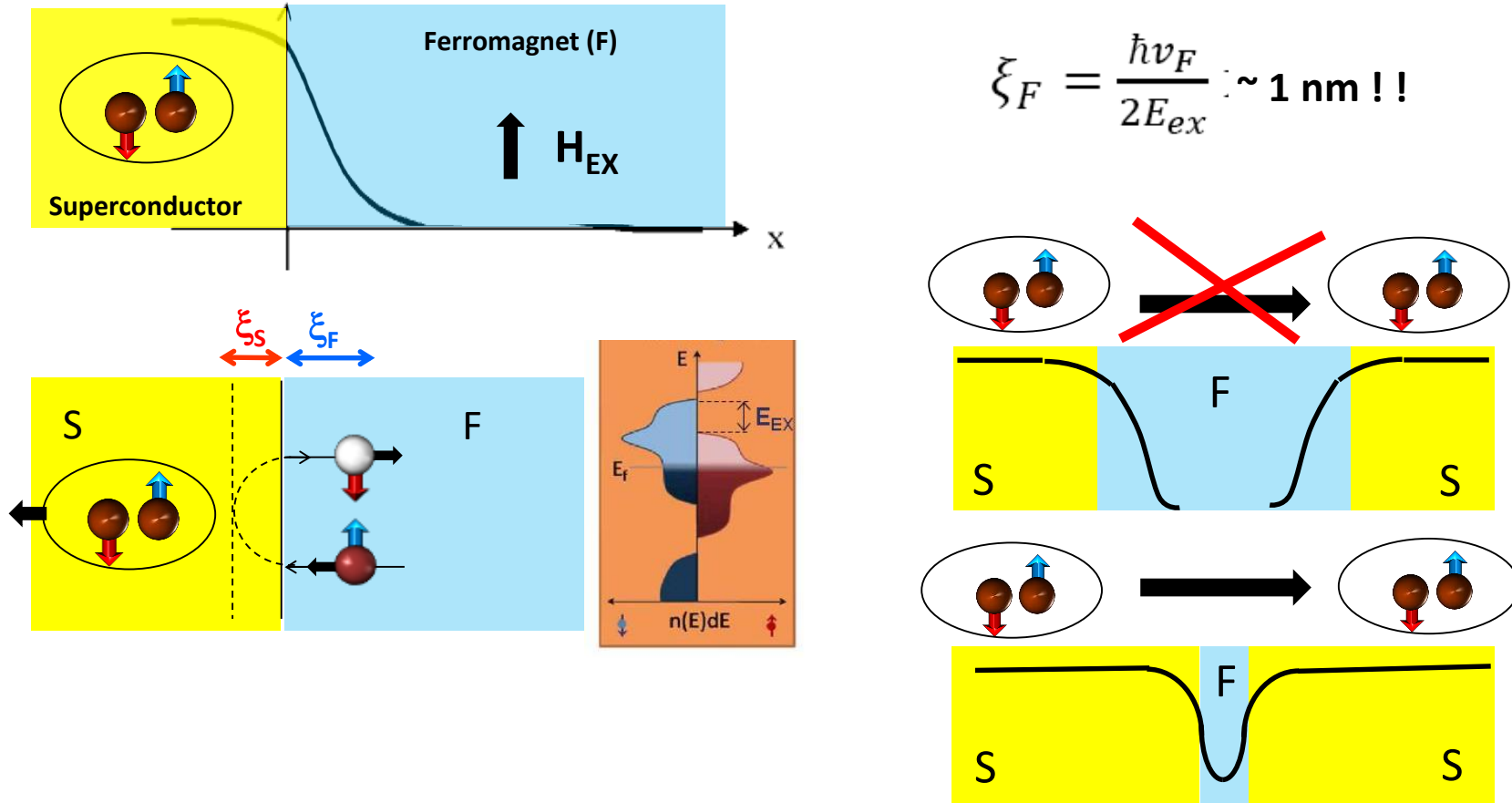
Tunable spin sink
d-wave effects

Carreira *et al.* PRB (2021)

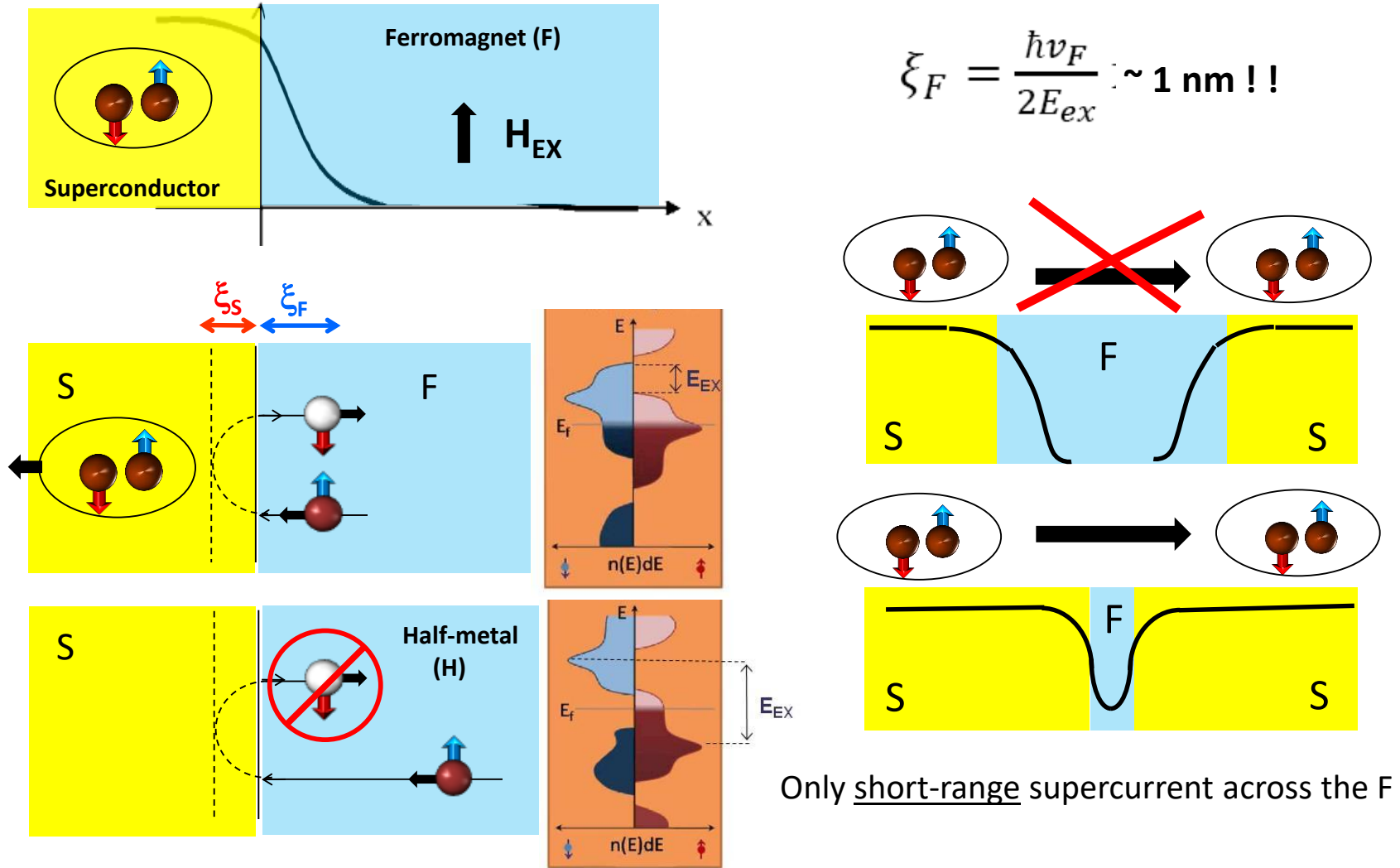


→ OPPORTUNITIES FOR HIGH- T_c SUPERCONDUCTING SPINTRONICS 9

Conventional proximity effect in ferromagnets

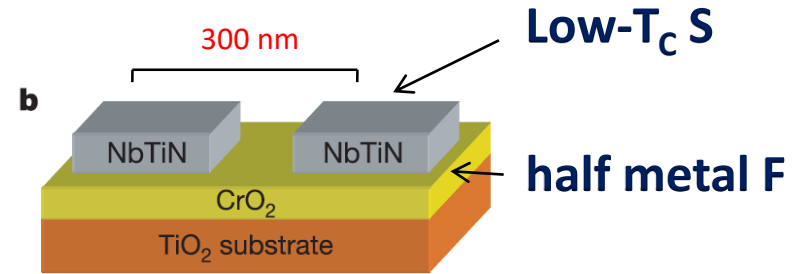
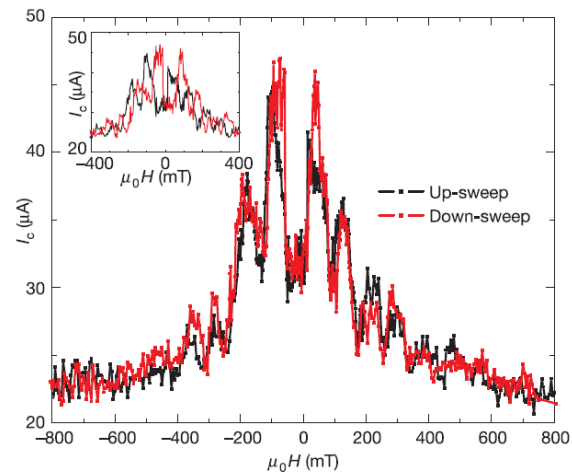


Conventional proximity effect in ferromagnets

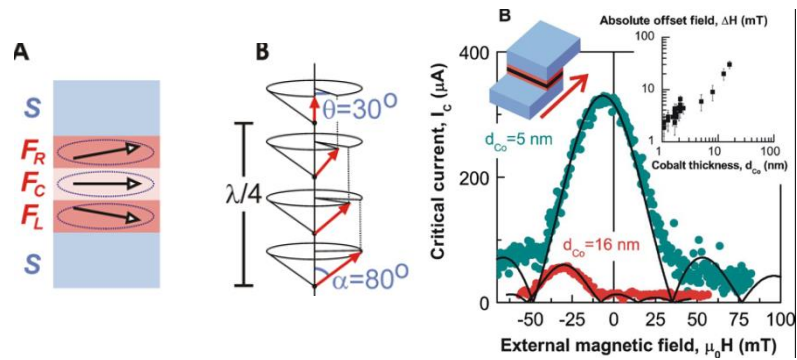


→ NO SINGLET SUPERCURRENTS ACROSS HALF-METALS

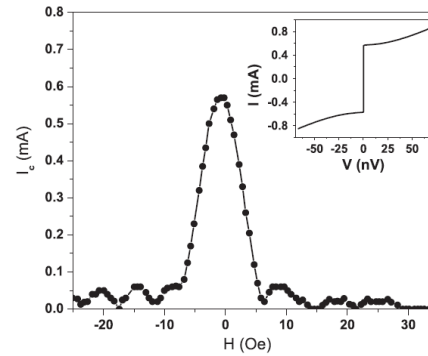
Early experiments with low- T_c superconductors



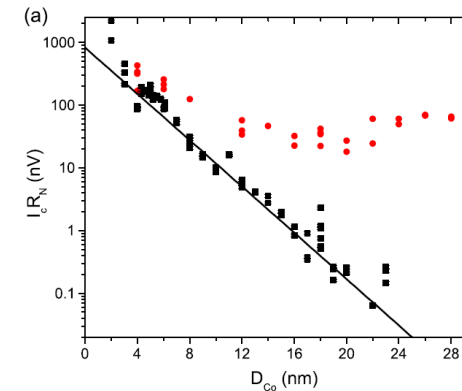
R. S. Keizer et al. Nature 439 (2006)



J. W. A. Robinson et al, Science (2010)



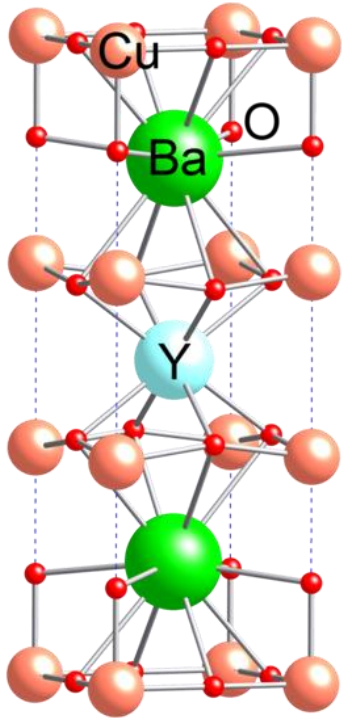
T. Khaire et al, PRL 104, 137002 (2010)



See also: Anwar et al. PRB (2010) & Sprungmann et al. PRB (2010)

→ LONG-RANGE JOSEPHSON COUPLING ACROSS STRONG F

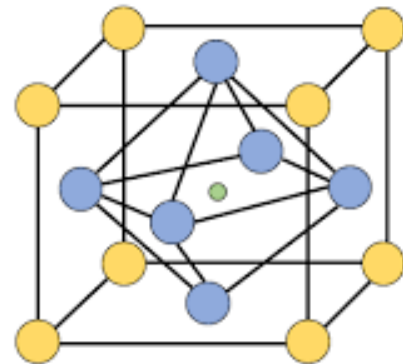
Aim: the case of high- T_C superconductors



Superconductor: YBa₂Cu₃O₇ (YBCO)

- d-wave
- high- T_C

Ferromagnets: La_{0,7}Sr_{0,3}MnO₃ (LSMO) or La_{0,7}Ca_{0,3}MnO₃

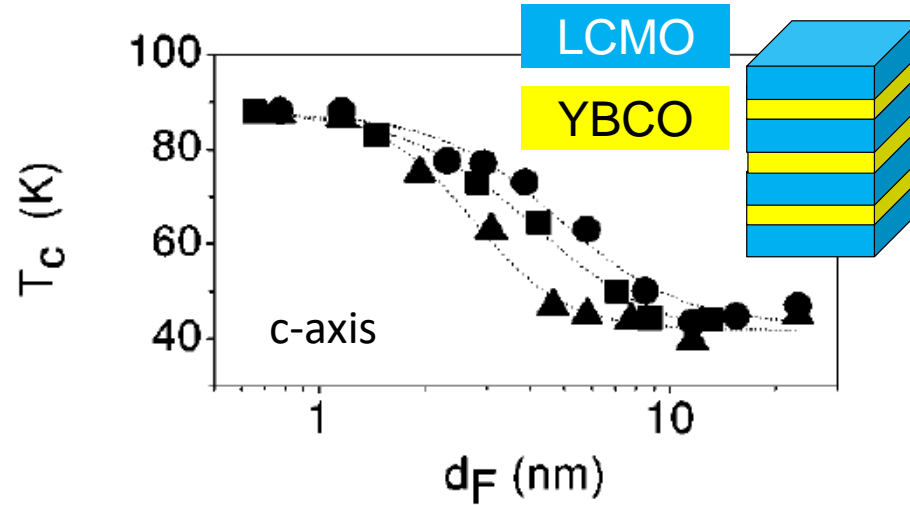


- La³⁺/ Sr²⁺
- O²⁻
- Mn³⁺/ Mn⁴⁺

- Half-metal
(100% spin-polarized)

Long-range proximity effect in $\text{YBa}_2\text{Cu}_3\text{O}_7/\text{La}_{2/3}\text{Ca}_{1/3}\text{MnO}_3$

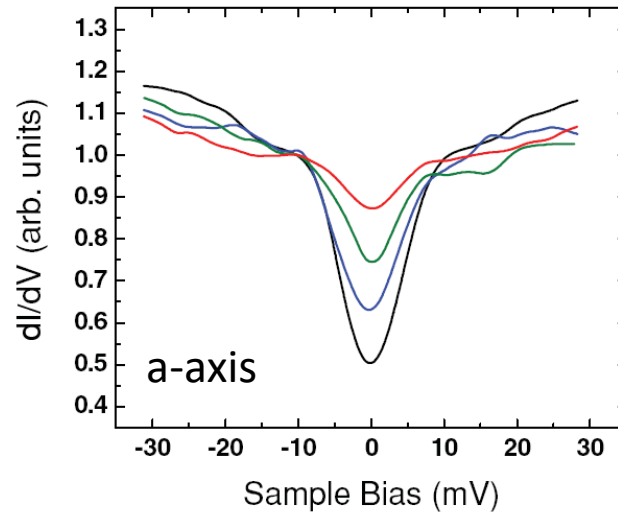
high-temperature superconductor / half-metal ferromagnet



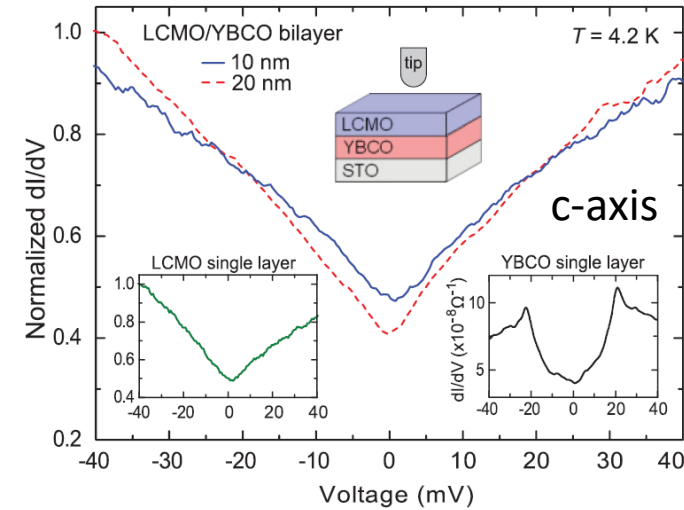
Sefrioui, JEV *et al.* PRB 67, 214511 (2003)

Peña *et al.* PRB 69, 224502 (2004)

T_c DEPRESSION \rightarrow PROXIMITY EFFECT



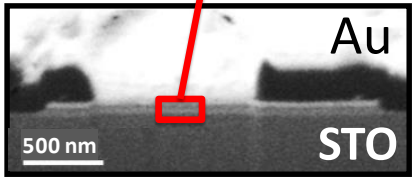
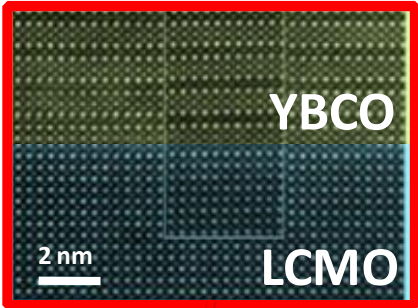
Kalcheim *et al.* Phys. Rev. B 83, 064510 (2011)



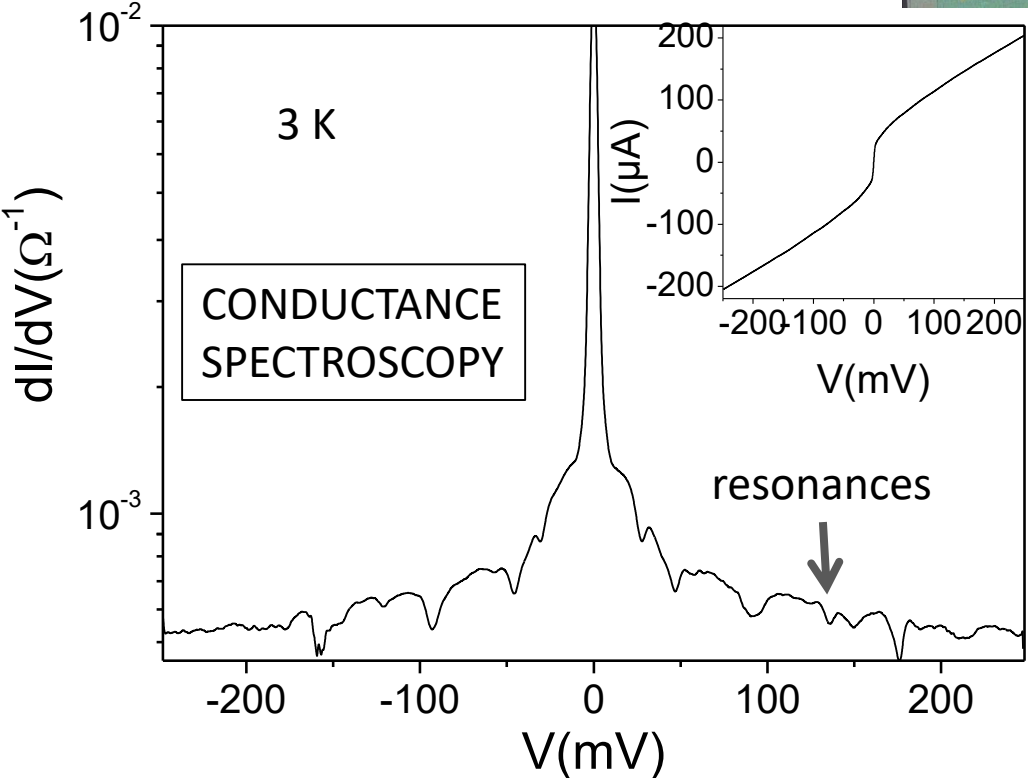
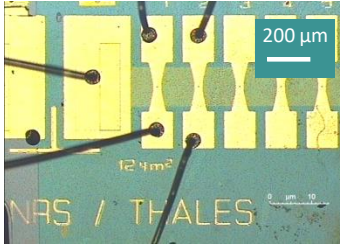
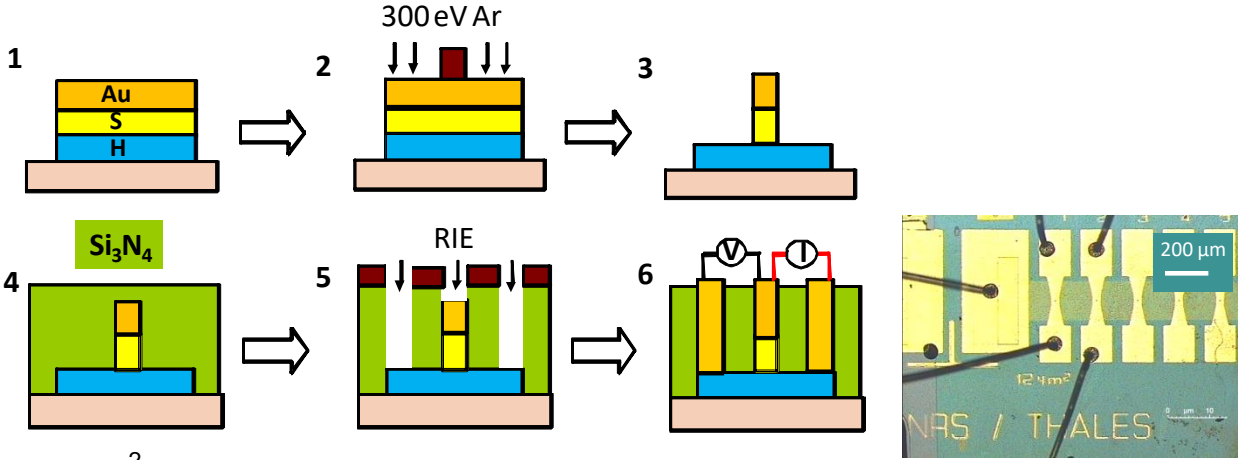
Fridman *et al.* Phys. Rev. B 84, 104522 (2011)

High- T_C /half-metal junctions

$\text{YBa}_2\text{Cu}_3\text{O}_7$
 $\text{La}_{2/3}\text{Ca}_{1/3}\text{MnO}_3$

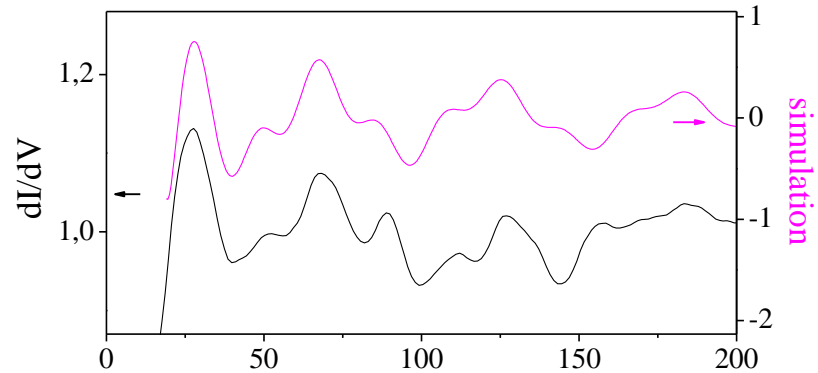


grown by
 Santamaria's group
 (UCM Spain)

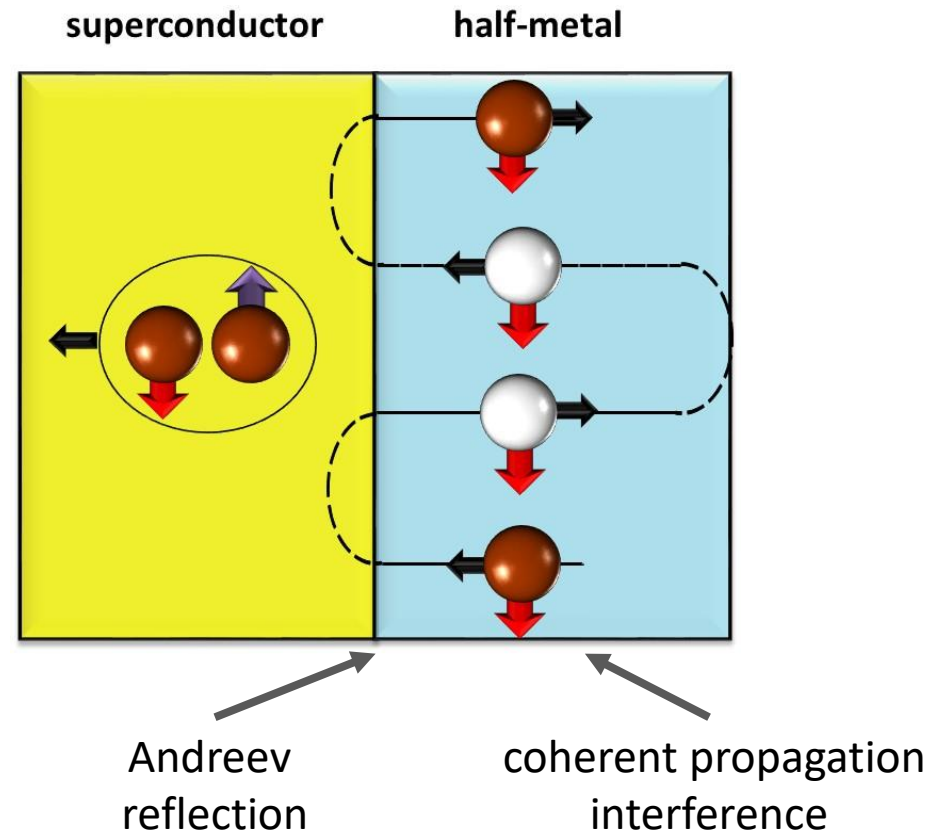


Equal-spin Andreev reflection

Tomasch & McMillan-Rowell resonances



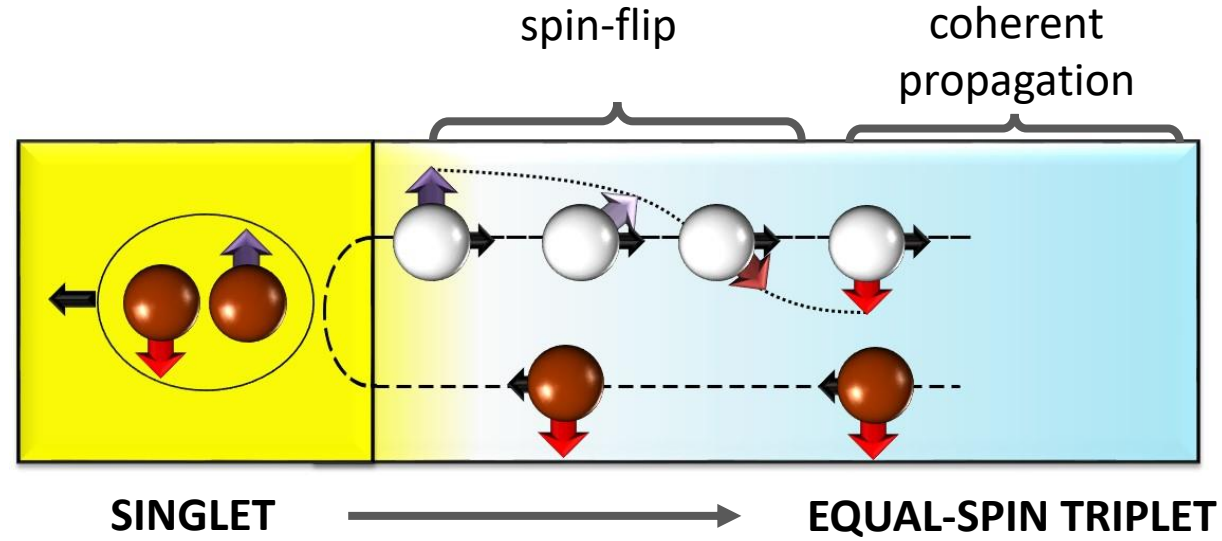
$$V_m = V_0 + \frac{m\hbar v_F^N}{4d_N}$$



→ ANDREEV REFLECTION

→ PHASE COHERENT, SPIN-POLARIZED CHARGE TRANSPORT

Equal-spin triplets: physical origin



ARTICLES *Nat. Phys.* **4**, 138-143 (2008).

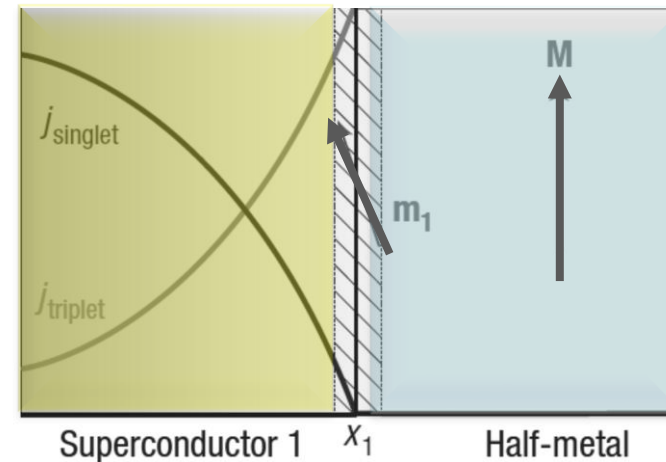
Triplet supercurrents in clean and disordered half-metallic ferromagnets

MATTHIAS ESCHRIG* AND TOMAS LÖFWANDER†

Bergeret et al. *Rev. Mod. Phys.* **77**, 1321-1373 (2005)

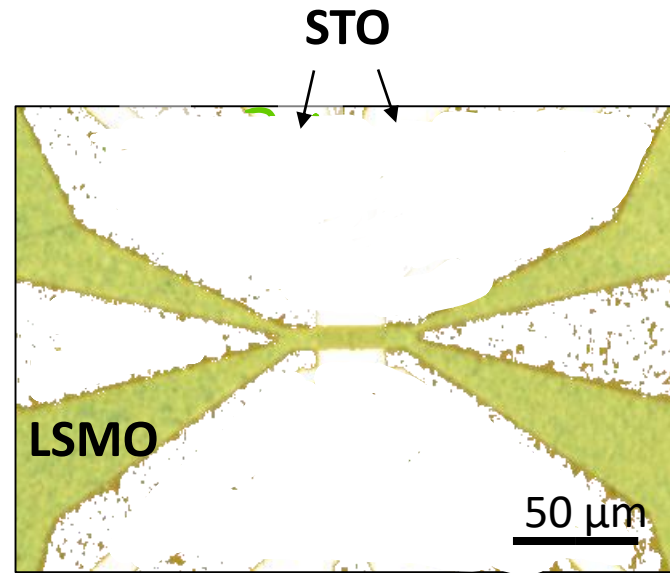
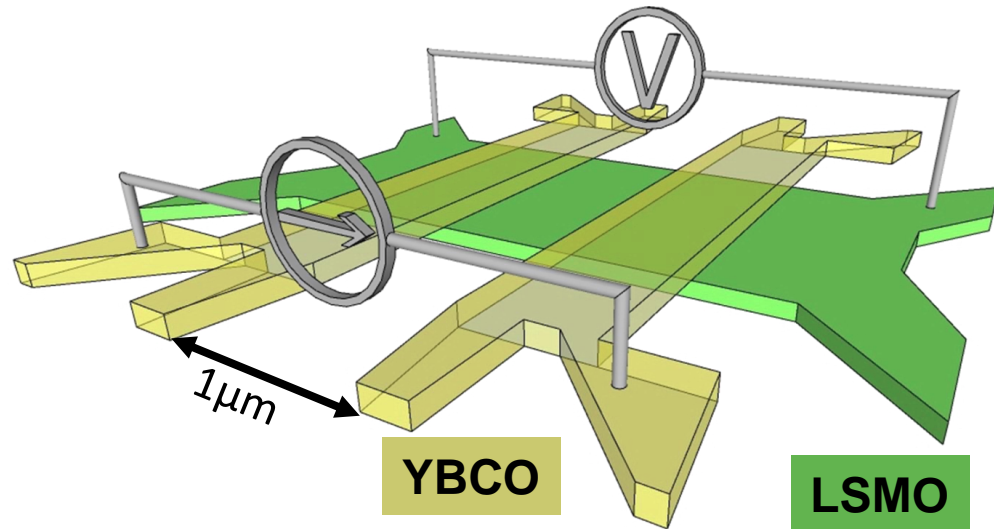
Buzdin et al. *Phys. Rev. B* **76** 060504 (2007)

Linder et al. *Phys. Rev. B* **81**, 174526 (2010)



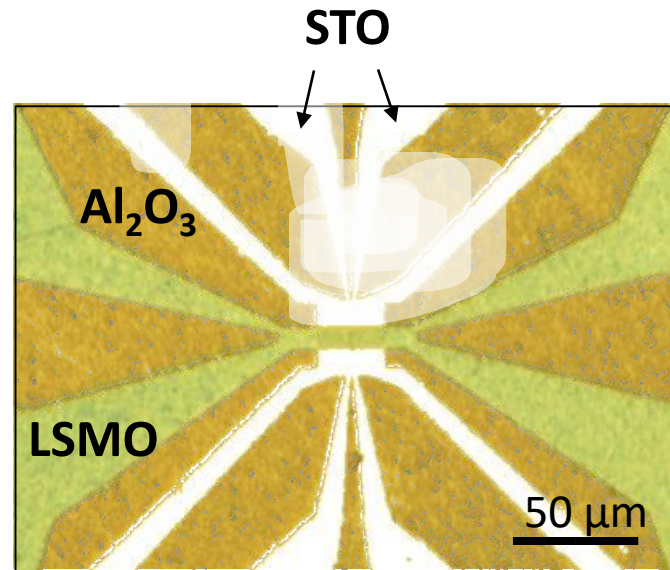
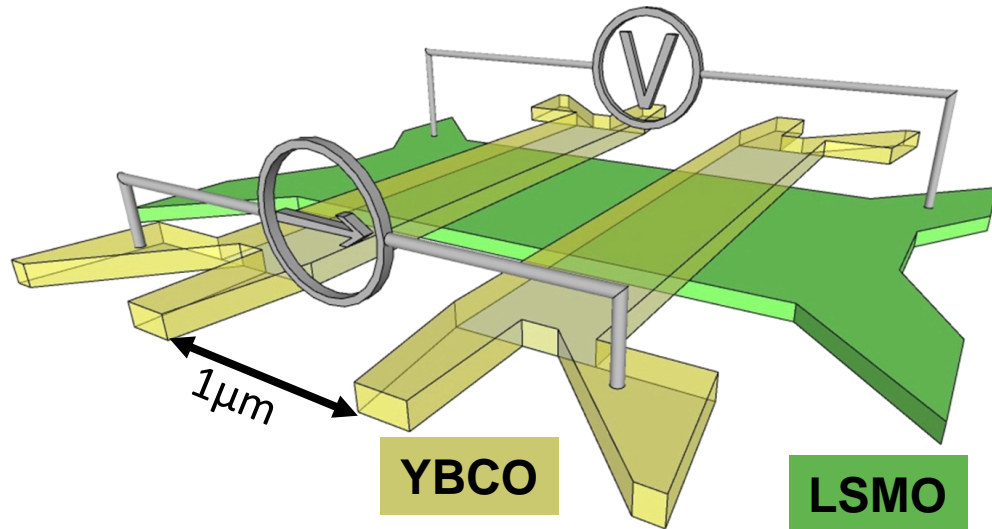
→ **MAGNETIC INHOMOGENEITY YIELDS SPIN-FLIP**

Fabrication of planar Josephson junctions



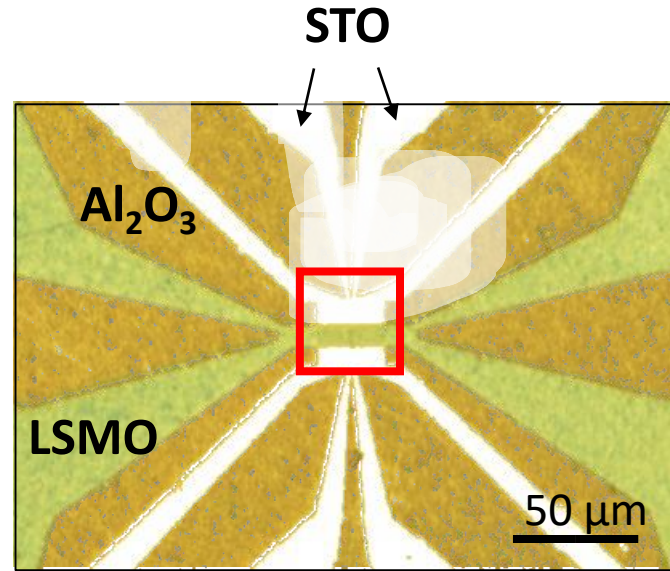
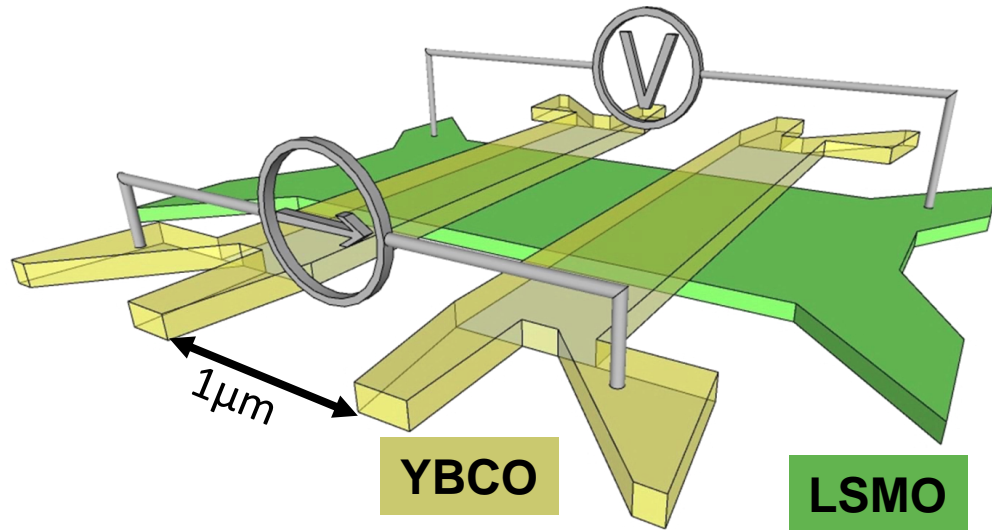
→ PLD GROWTH OF LSMO AND LITHOGRAPHY

Fabrication of planar Josephson junctions

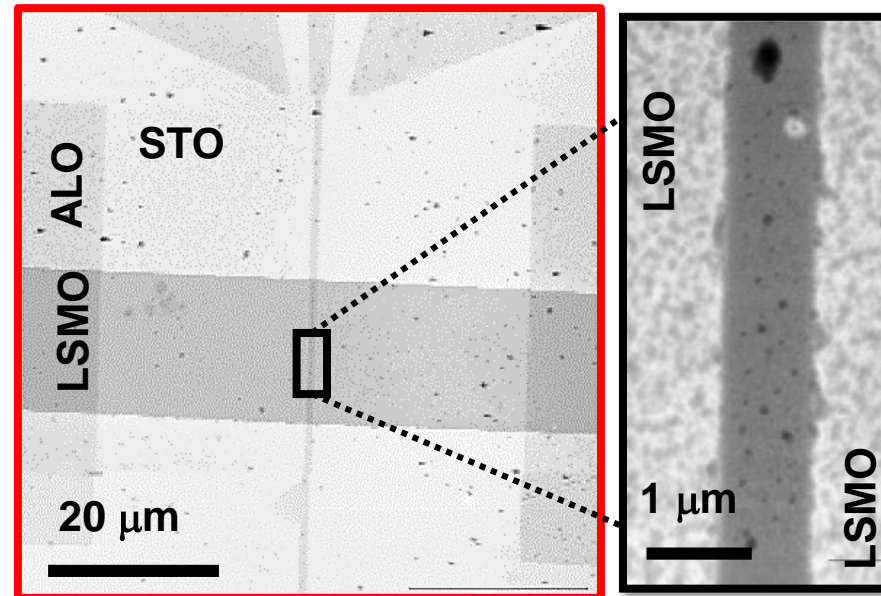


→ E-BEAM LITHOGRAPHY
→ DEPOSITION OF AMORPHOUS ALUMINA

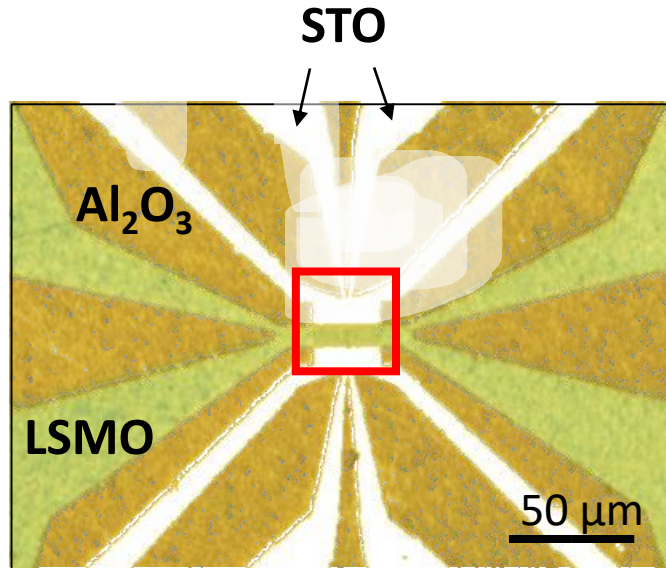
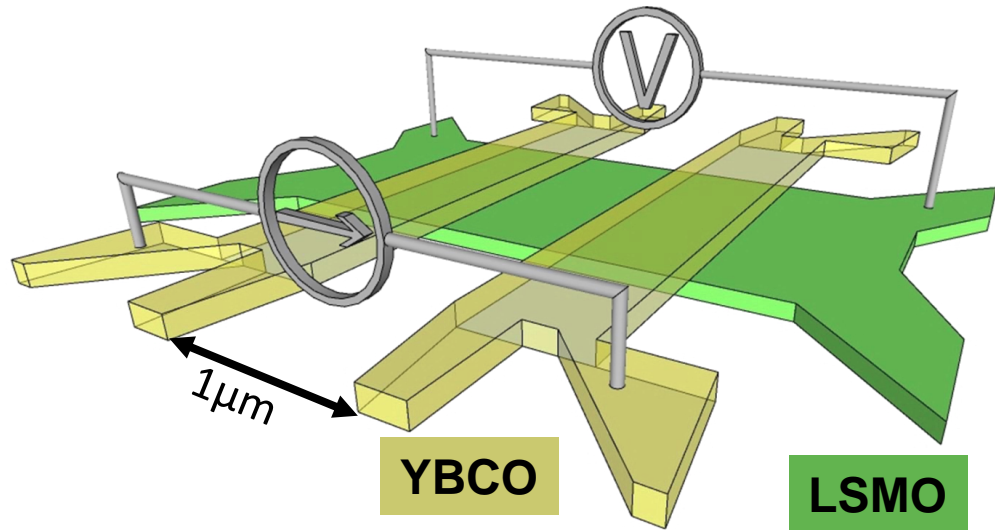
Fabrication of planar Josephson junctions



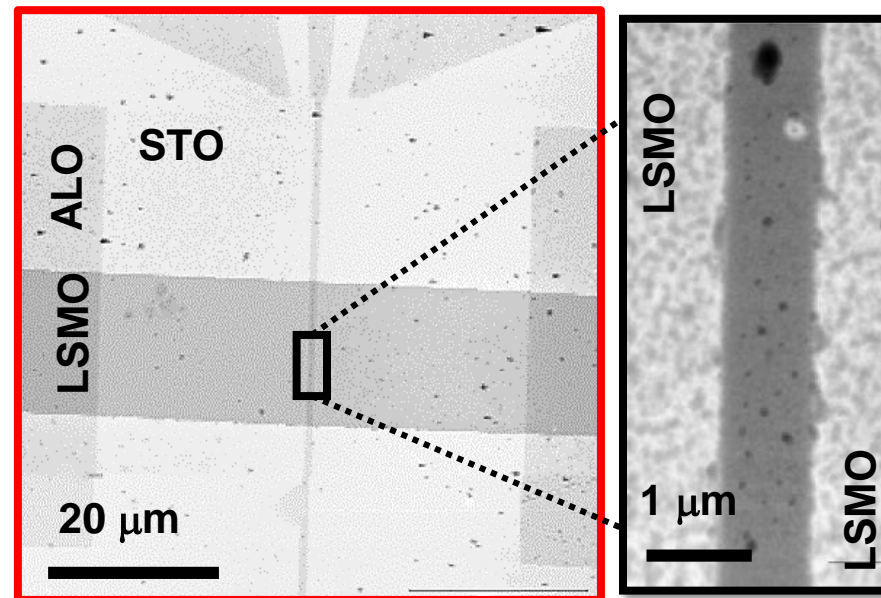
→ AMORPHOUS ALUMINA MASK



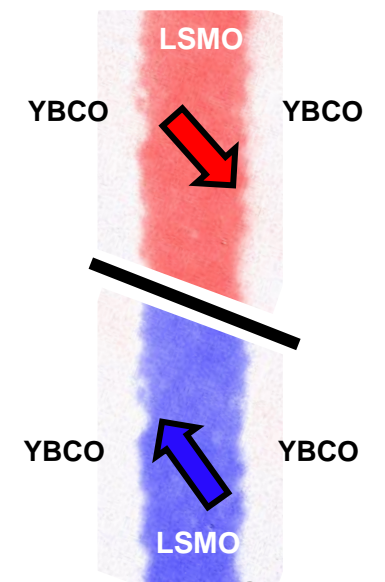
Fabrication of planar Josephson junctions



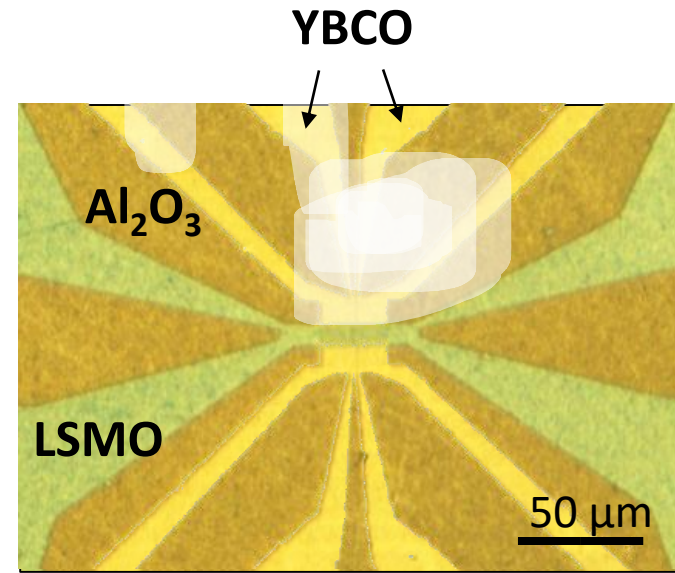
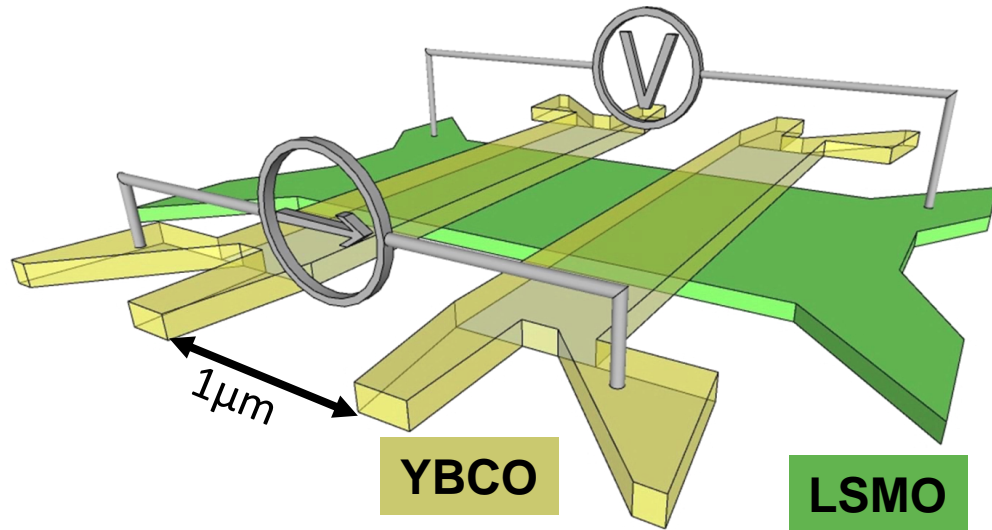
→ AMORPHOUS ALUMINA MASK
→ LSMO REMAINS MAGNETIC



XMCD-PEEM



Fabrication of planar Josephson junctions

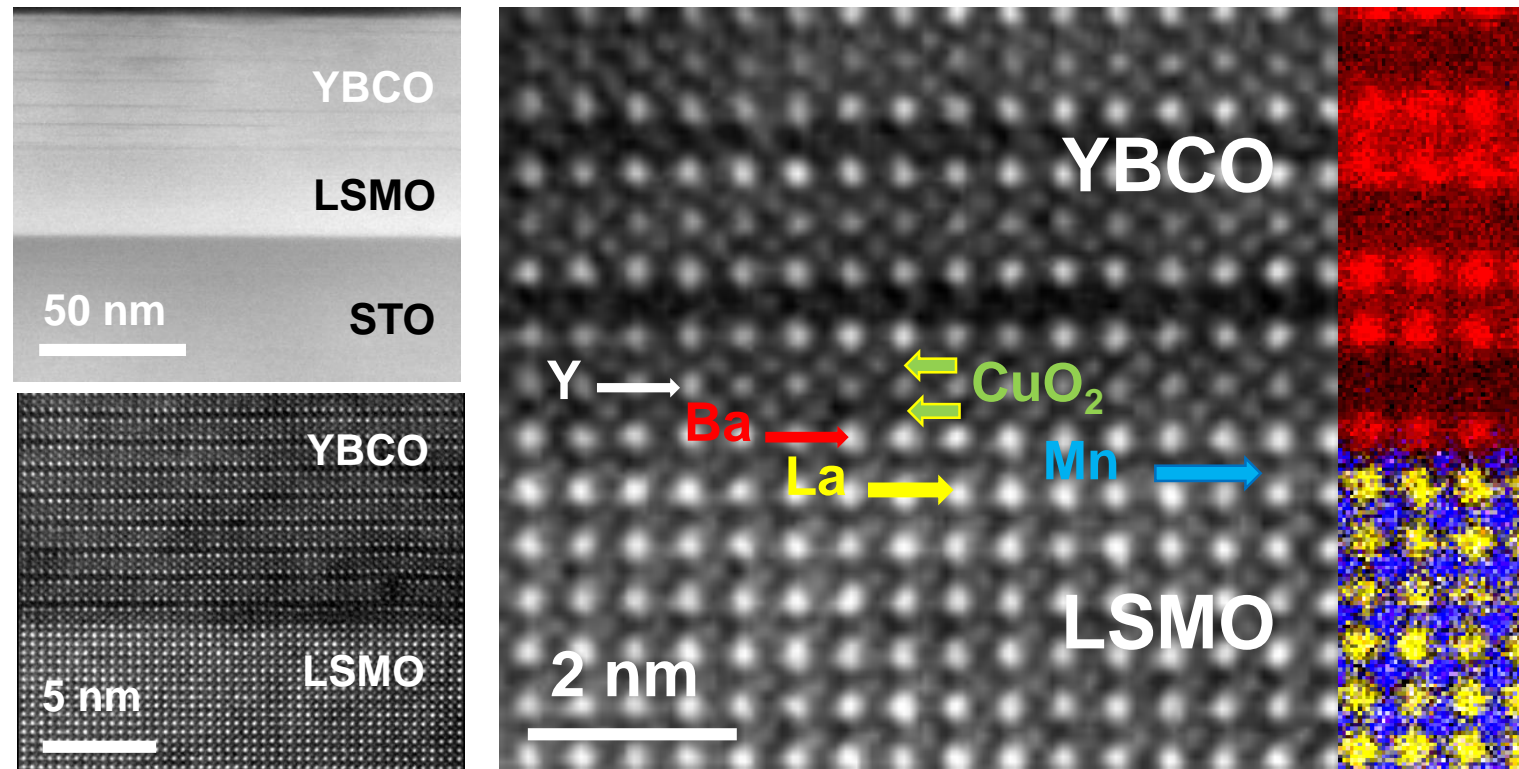


→ PLD GROWTH OF EPITAXIAL YBCO

Interface quality

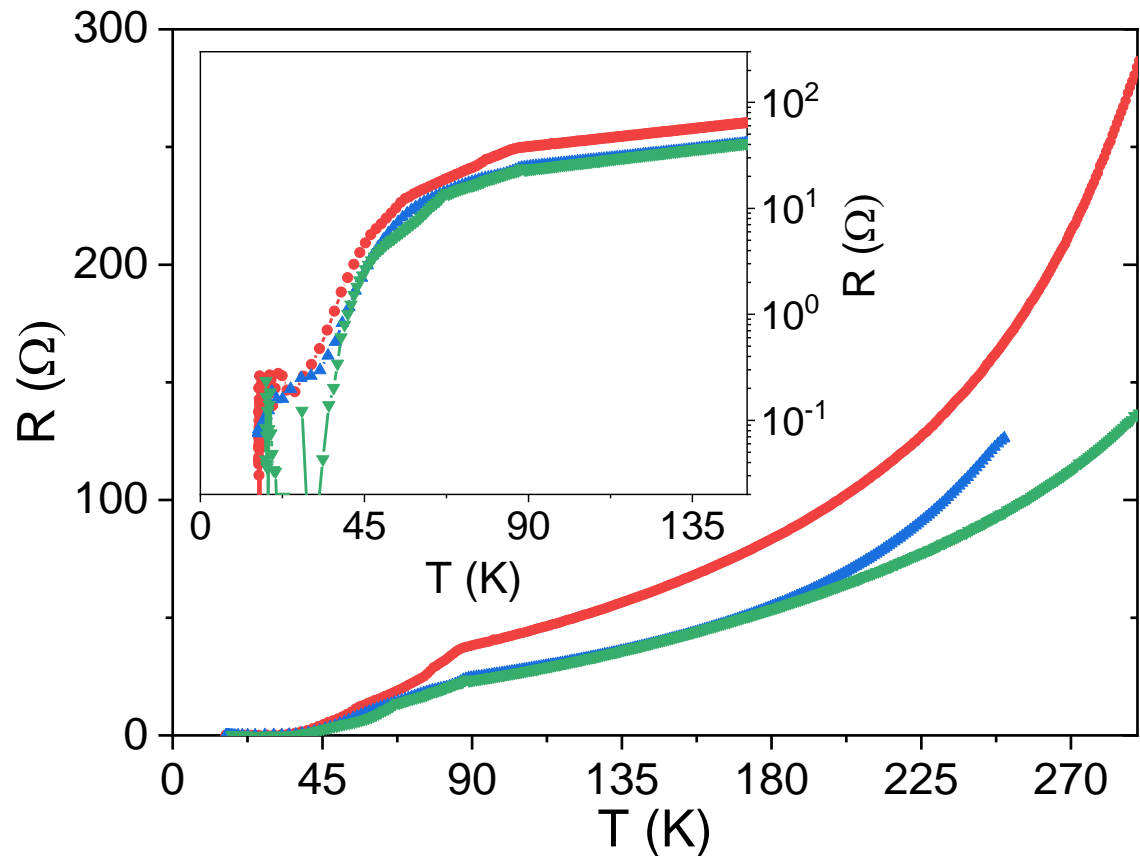
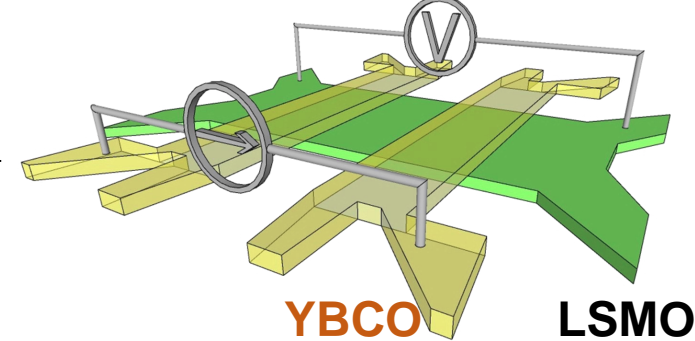
Z-contrast

EELS

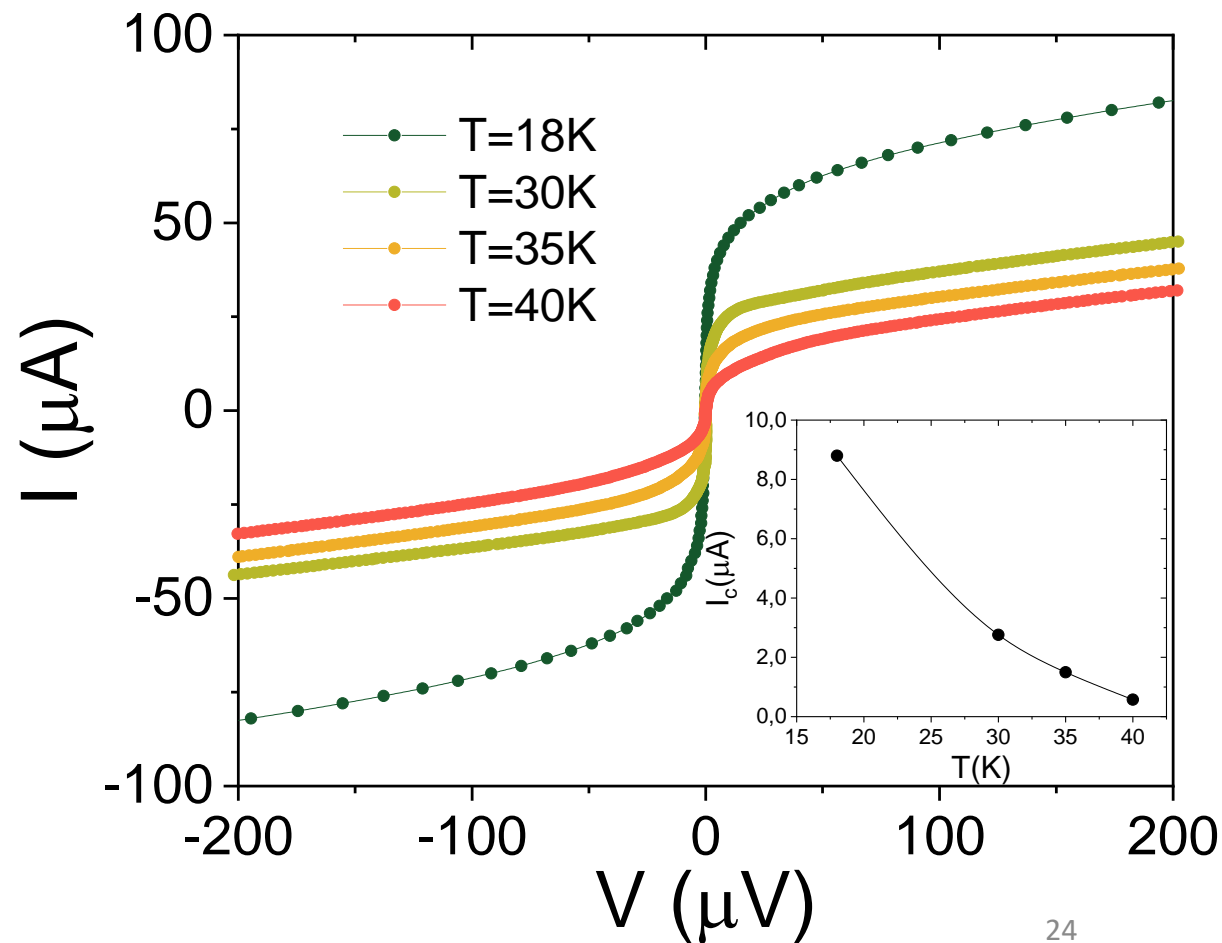


→ HIGH QUALITY INTERFACES DESPITE EX-SITU GROWTH

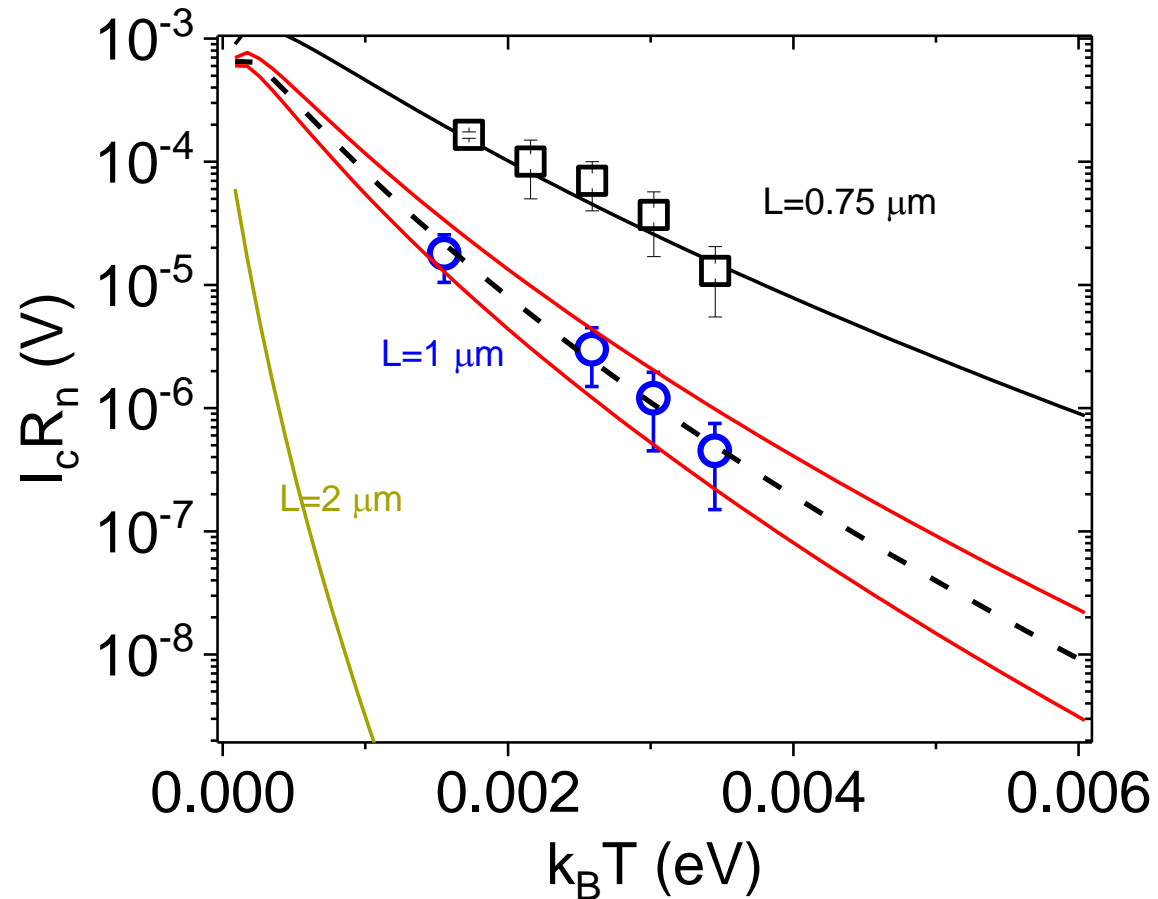
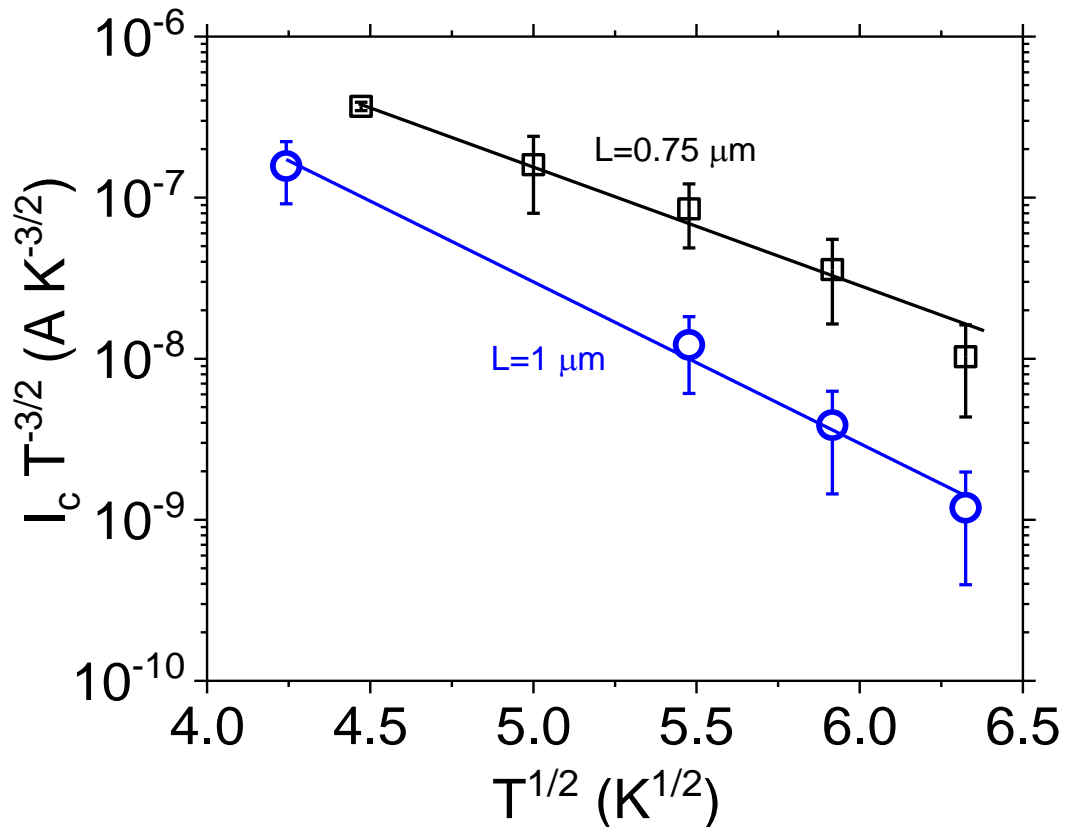
Supercurrents across the device



→ ZERO RESISTANCE STATE AT ~ 40K



Size of critical current



$$I_c \propto T^{3/2} \exp(\sqrt{2\pi k_B T / E_{Th}}) \rightarrow \ln(I_c) - \frac{3}{2} \ln(T) \text{ vs } \sqrt{T}$$

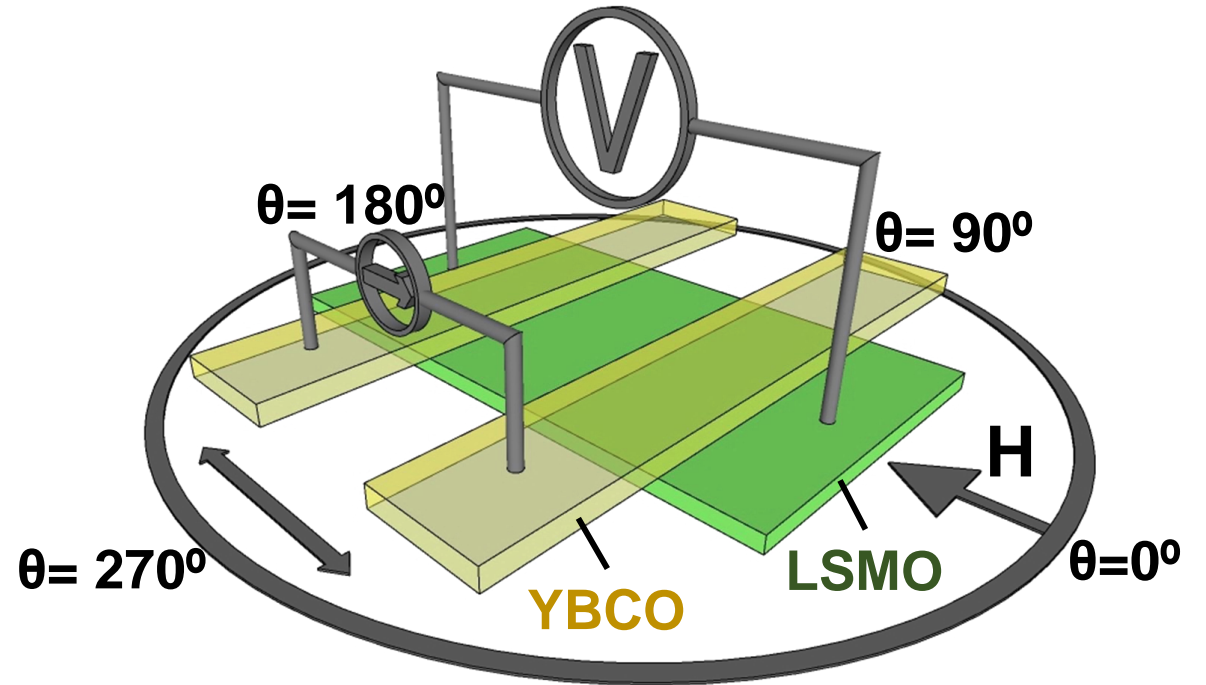
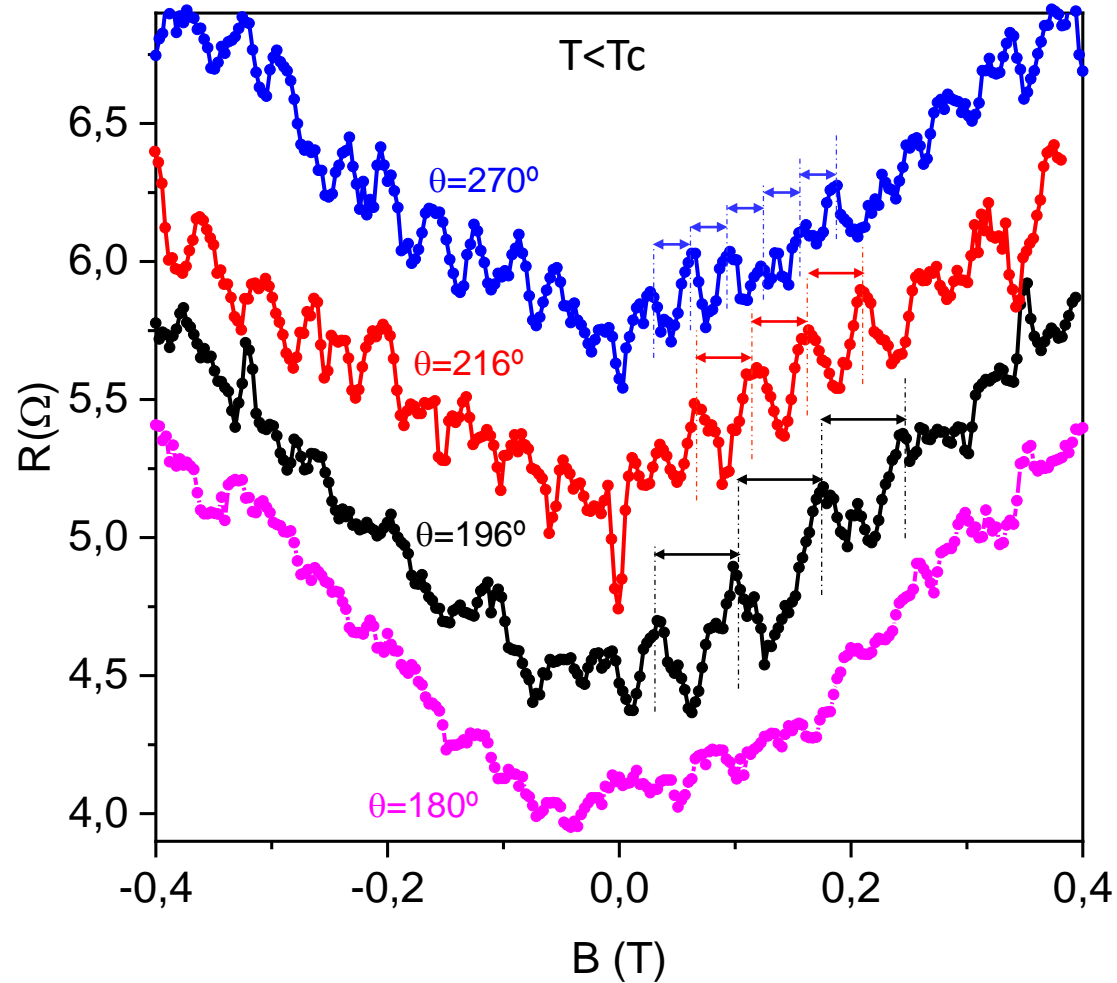
$$E_{Th} = 100 \pm 10 \mu\text{eV} \text{ (for } 1 \mu\text{m)}$$

From: Anwar et al, Appl. Phys. Lett. 100, 052602 (2012)

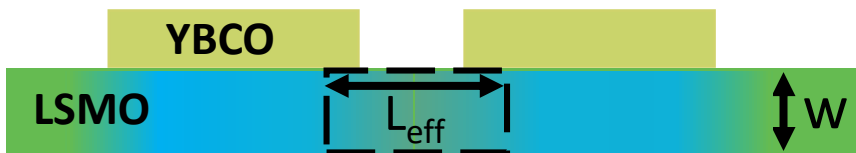
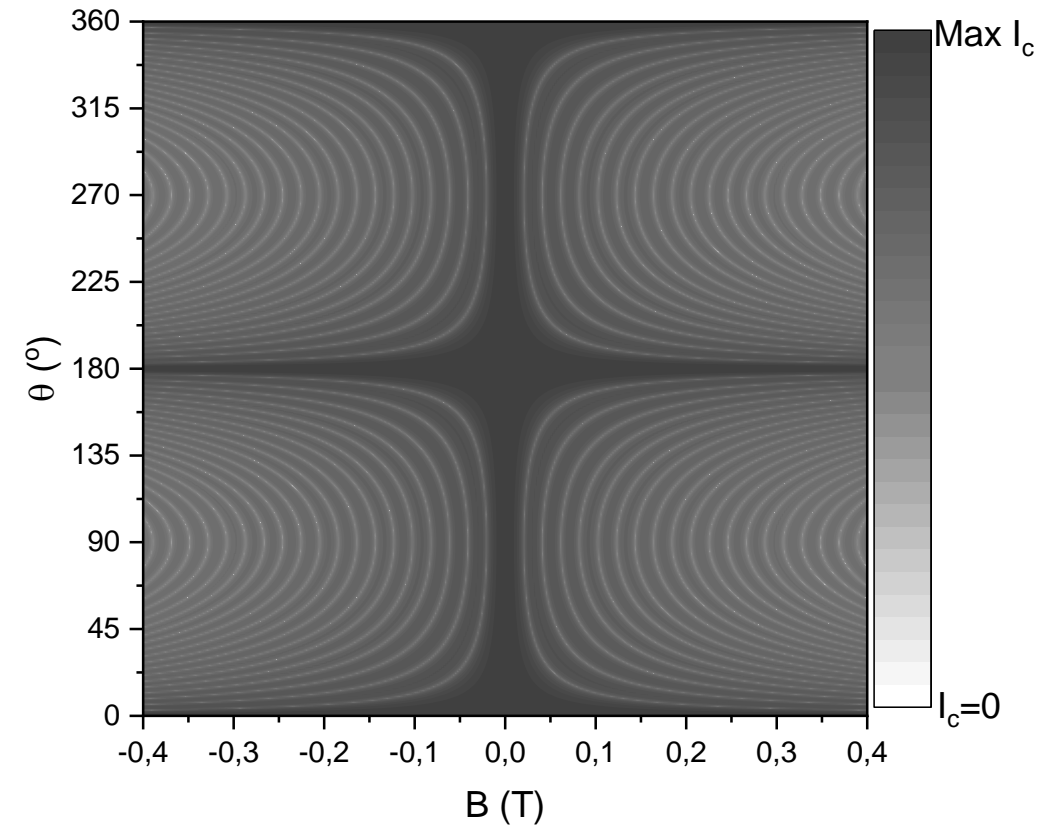
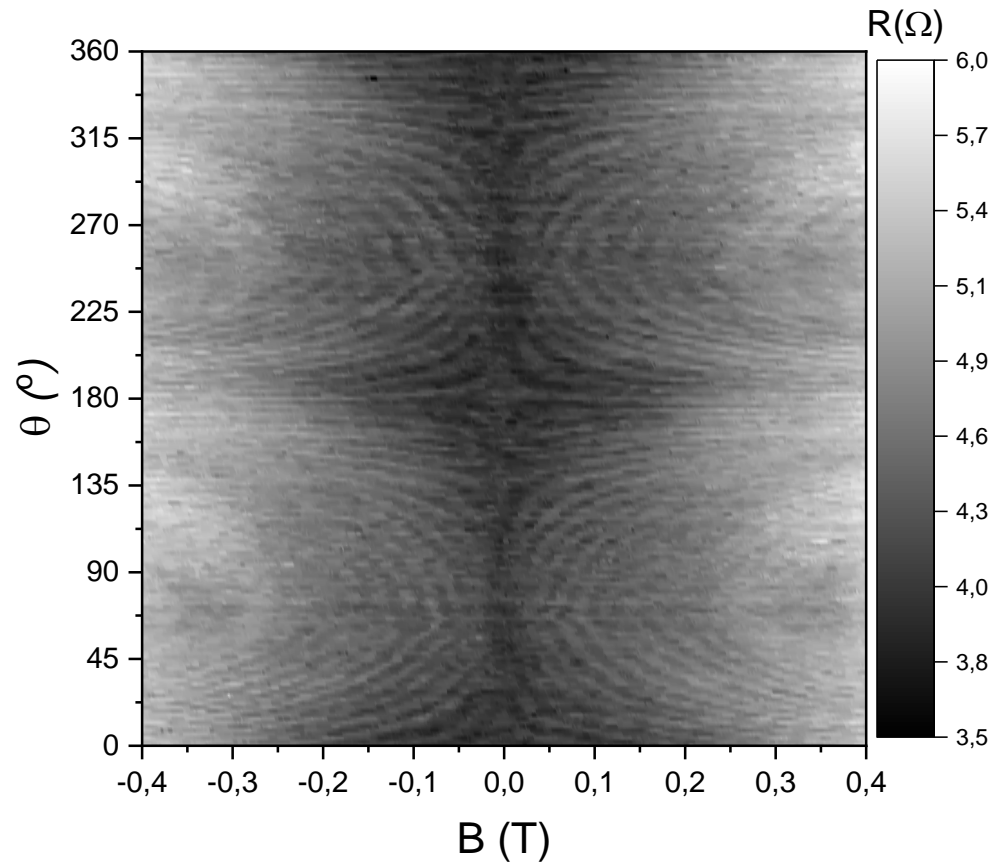
$$e I_c R_n = \frac{32}{3 + 2\sqrt{2}} E_{Th} \left[\frac{2\pi k_B T}{E_{Th}} \right]^{3/2} e^{-[2\pi k_B T / E_{Th}]^{1/2}}$$

From: Dubos et al, Phys. Rev. B 63, 064502 (2001)

Magnetic flux quantization: angular dependence



Magnetic flux quantization: angular dependence

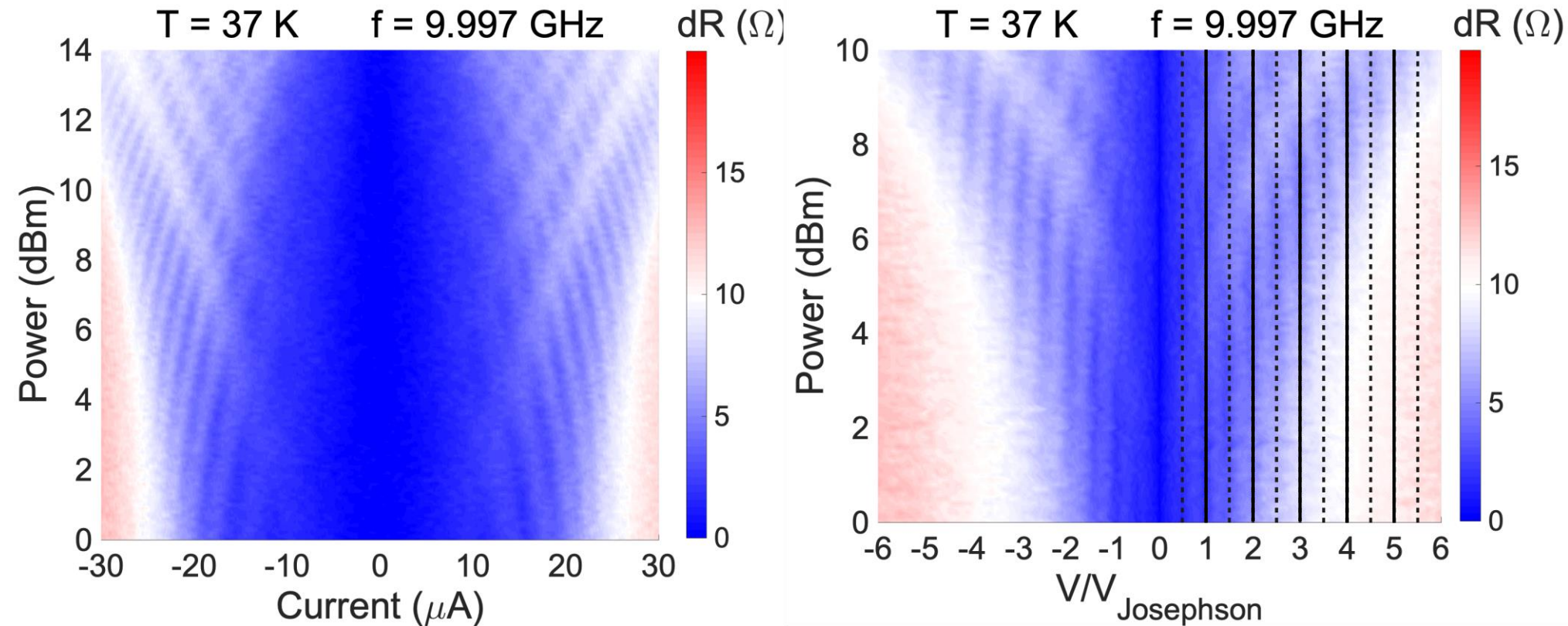


$$I_c = I_0 \left| \frac{\sin\left(\frac{\pi\phi}{\phi_0}\right)}{\left(\frac{\pi\phi}{\phi_0}\right)} \right| = I_0 \left| \frac{\sin\left(\frac{\pi H_{\perp} w L}{\phi_0}\right)}{\left(\frac{\pi H_{\perp} w L}{\phi_0}\right)} \right| = I_0 \left| \frac{\sin\left(\frac{\pi H \sin\theta w L}{\phi_0}\right)}{\left(\frac{\pi H \sin\theta w L}{\phi_0}\right)} \right|$$

$$L_{\text{eff}} = 3,4 \mu\text{m}$$

$$L_{\text{eff}} = L_{\text{junction}} + 2\lambda_{\text{YBCO}}$$

Shapiro steps: quantum interference



$$V_{\text{Josephson}} = n \frac{\hbar\omega}{4e}$$

$$I_c = I_0 \left| \frac{\sin\left(\frac{2\pi\phi}{\phi_0}\right)}{\left(\frac{2\pi\phi}{\phi_0}\right)} \right|$$

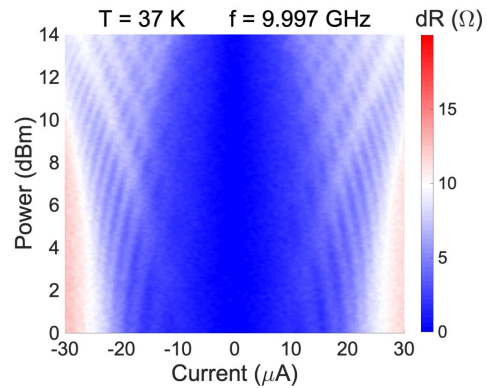
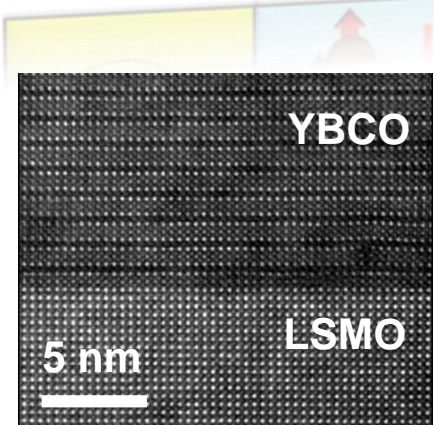
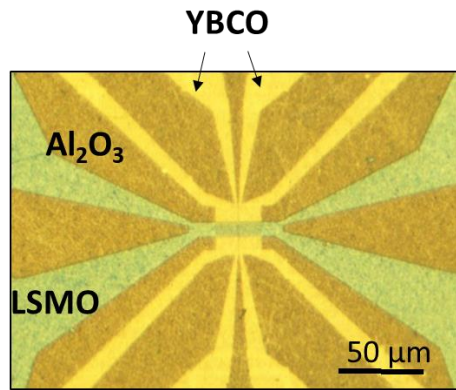
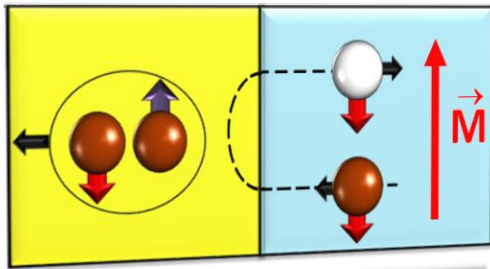
Half integer Shapiro steps \rightarrow Second harmonic component

Richard, C., Houzet, M. & Meyer, J. S. *Phys. Rev. Lett.* **110**, 1–5 (2013).

Can explain $L_{\text{eff}} = 2 \times (L_{\text{junction}} + 2\lambda_{\text{YBCO}})$

The talk in a nutshell

Proximity effect

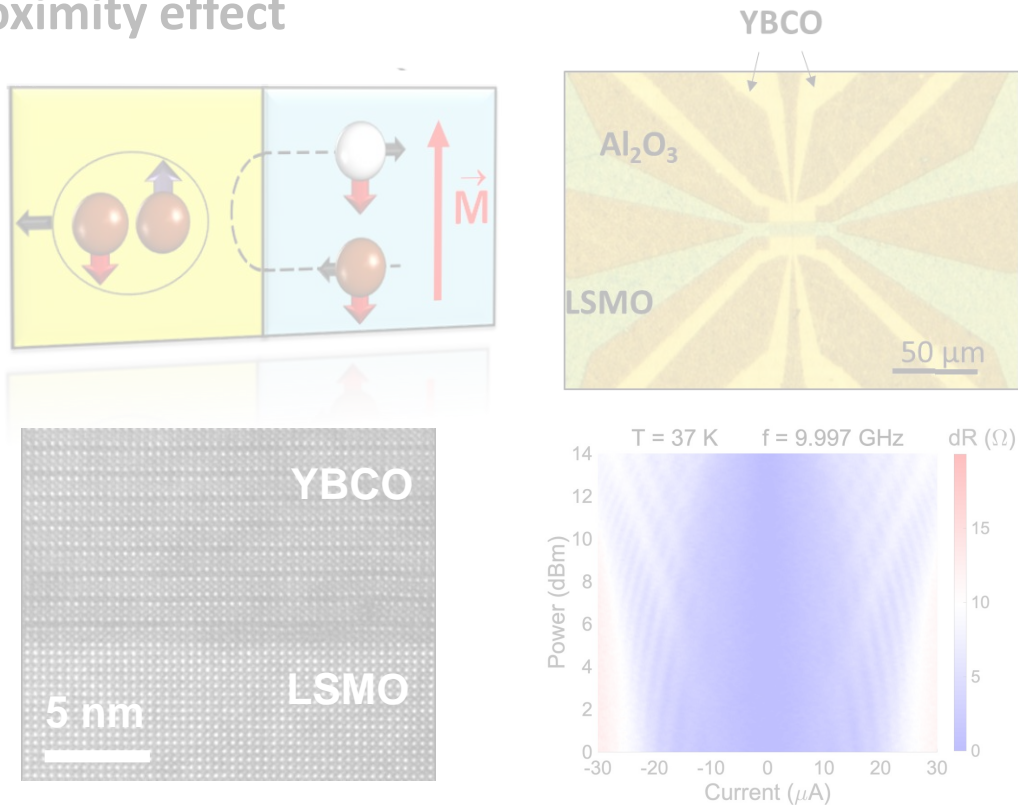


Fully spin-polarized, high- T_c Josephson supercurrents
Quantum phase coherence effects

Sanchez-Manzano *et al.* Nature Materials (2022)

The talk in a nutshell

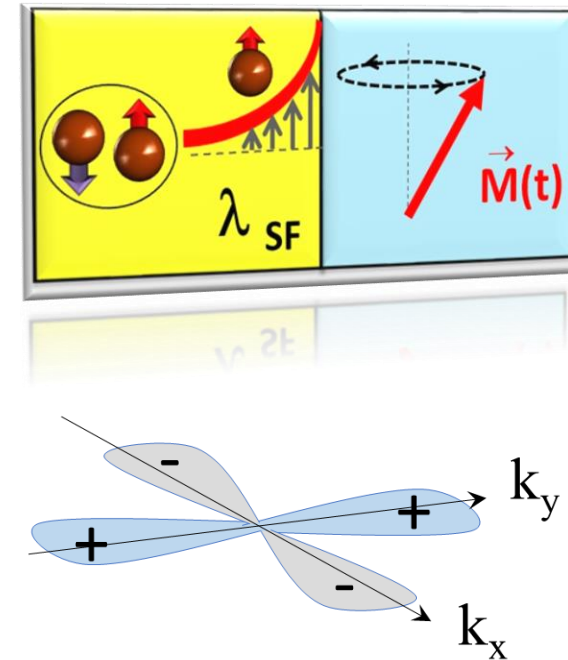
Proximity effect



Fully spin-polarized, high- T_C Josephson supercurrent
Quantum phase coherence effects

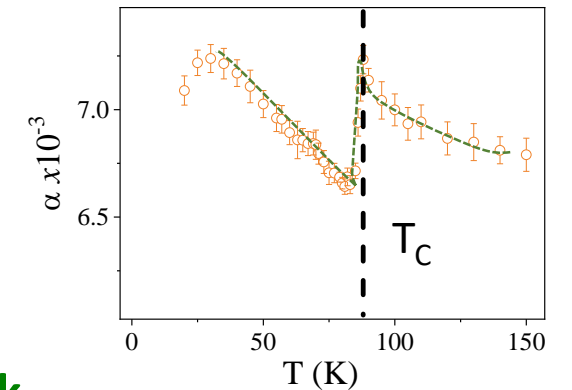
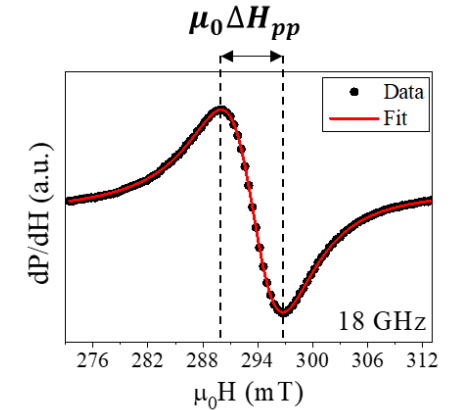
Sanchez-Manzano *et al.* Nature Materials (2022)

Dynamic coupling



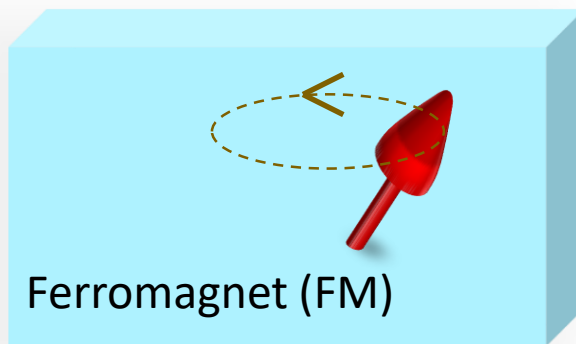
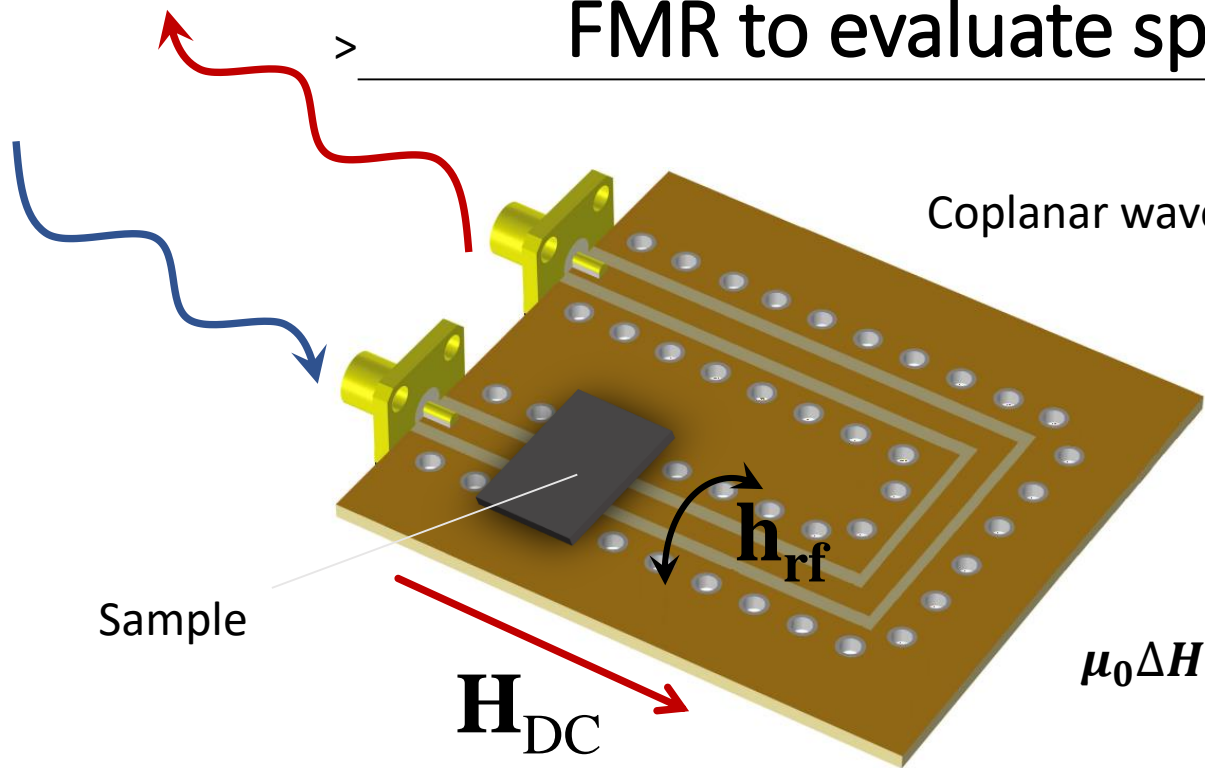
Tunable spin sink
d-wave effects

Carreira *et al.* PRB (2021)



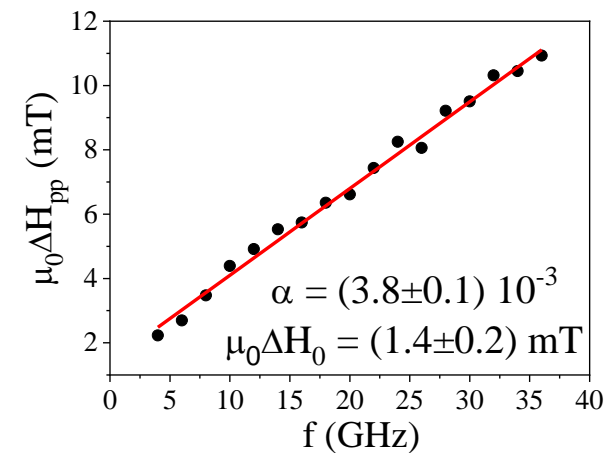
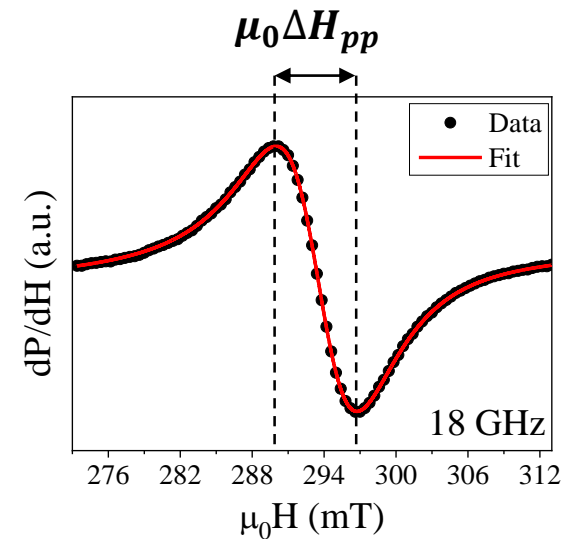
→ OPPORTUNITIES FOR HIGH- T_C SUPERCONDUCTING SPINTRONICS 30

FMR to evaluate spin absorption by SC

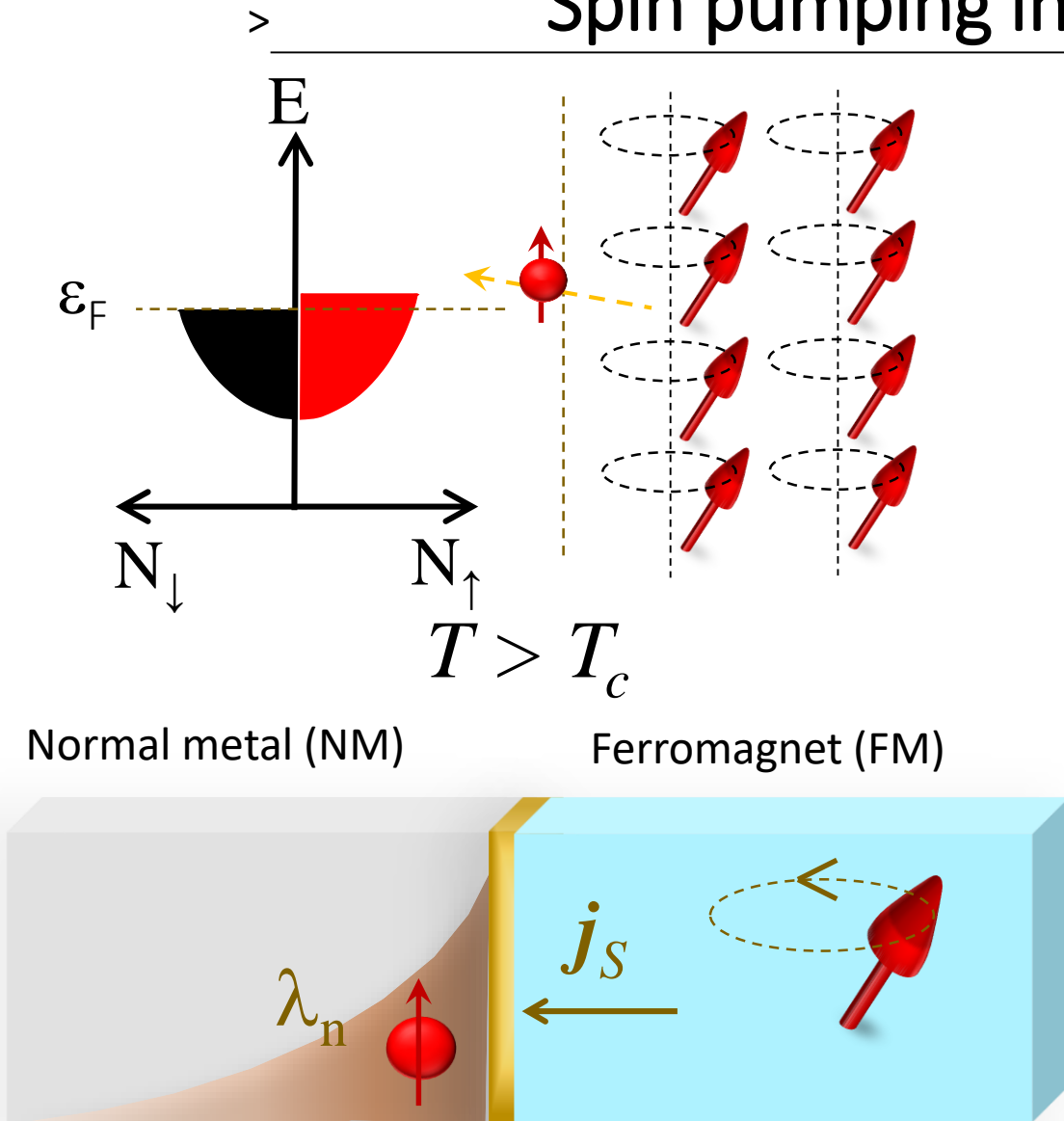


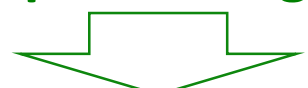
Damping Inhomogeneous broadening

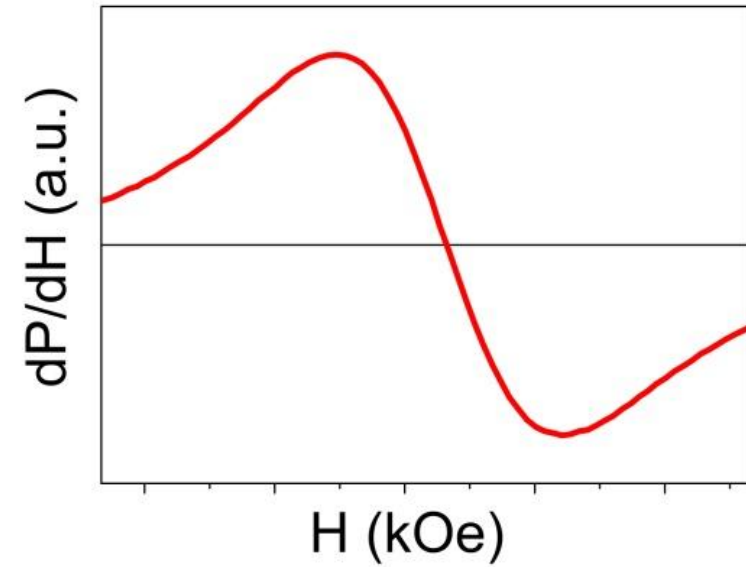
$$\mu_0 \Delta H_{pp} = \frac{2\alpha}{\sqrt{3}\gamma} f + \mu_0 \Delta H_0$$



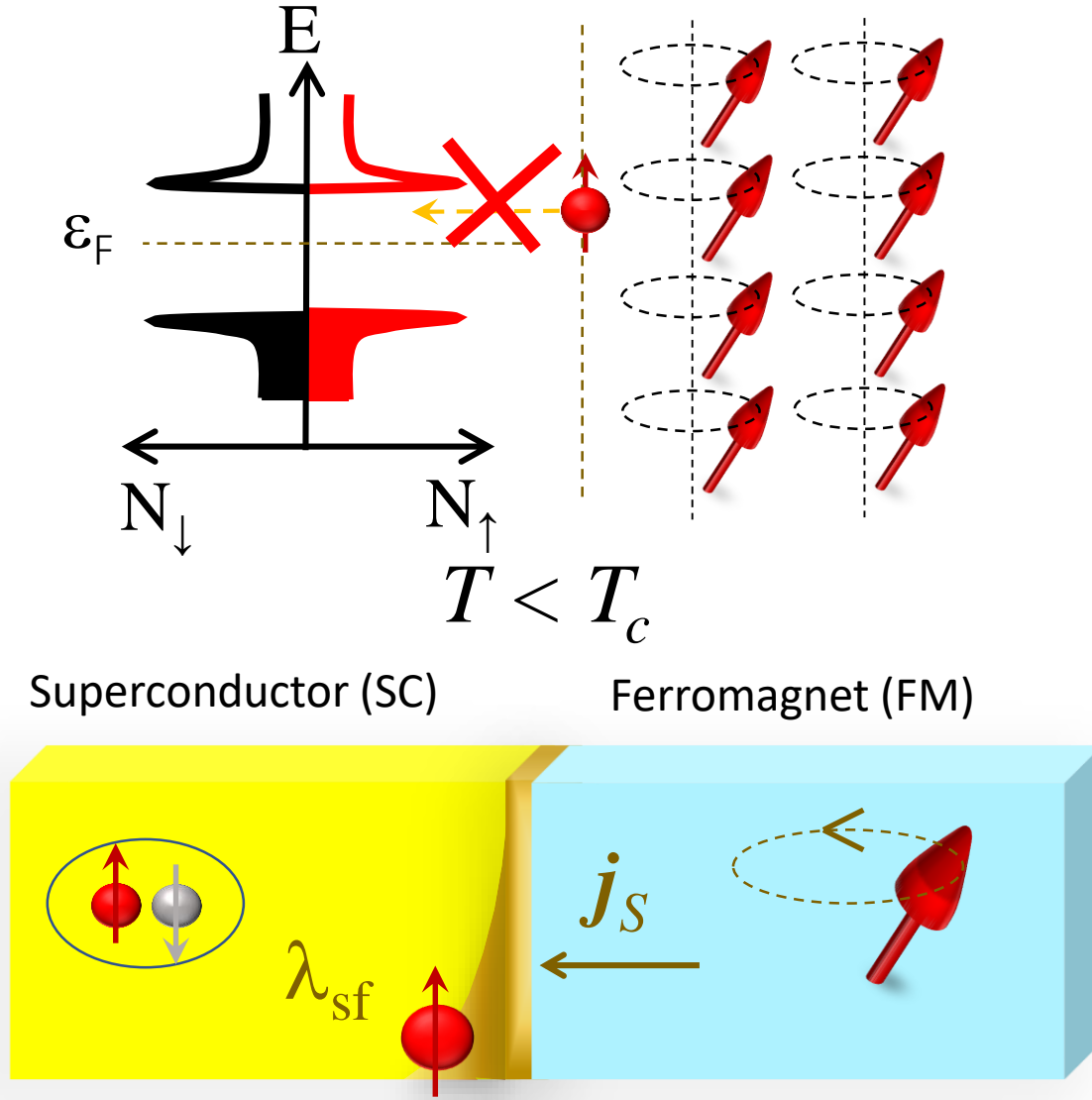
Spin pumping into normal-metal



Spin sinking

 linewidth broadening

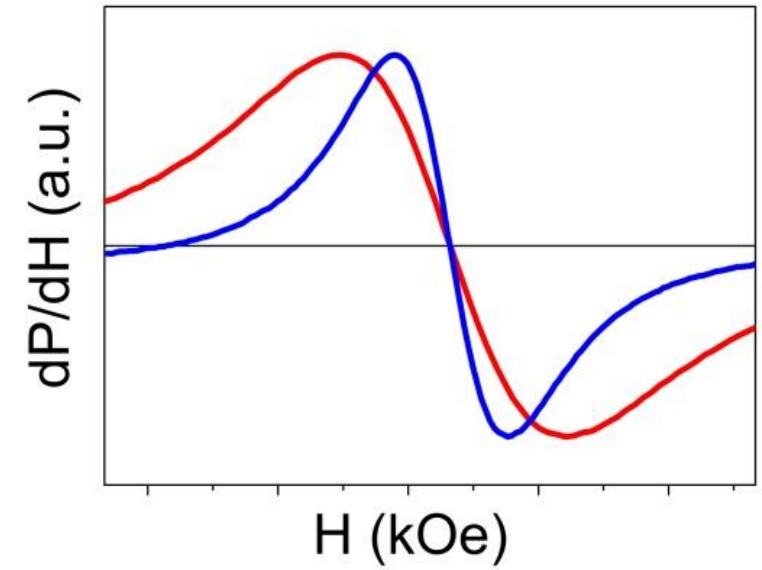


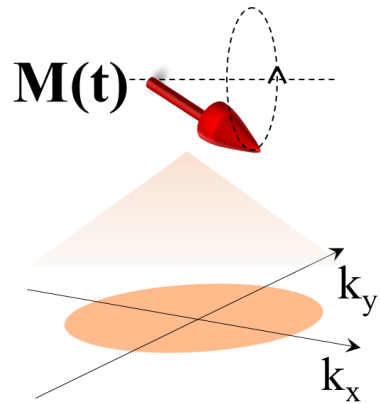
Spin pumping into a superconductor



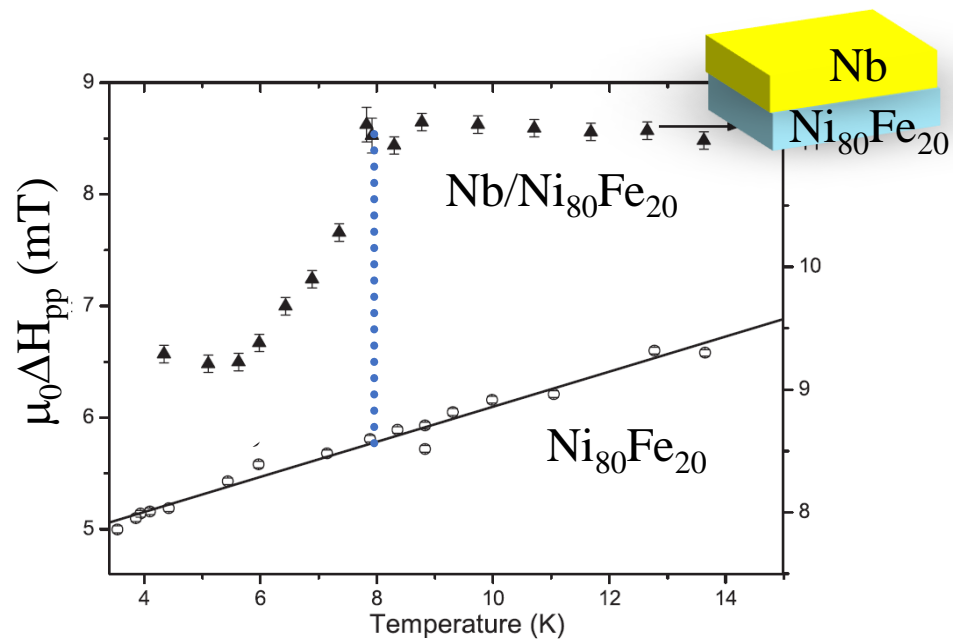
Vanishing DOS reduces spin sinking

↓
linewidth narrowing

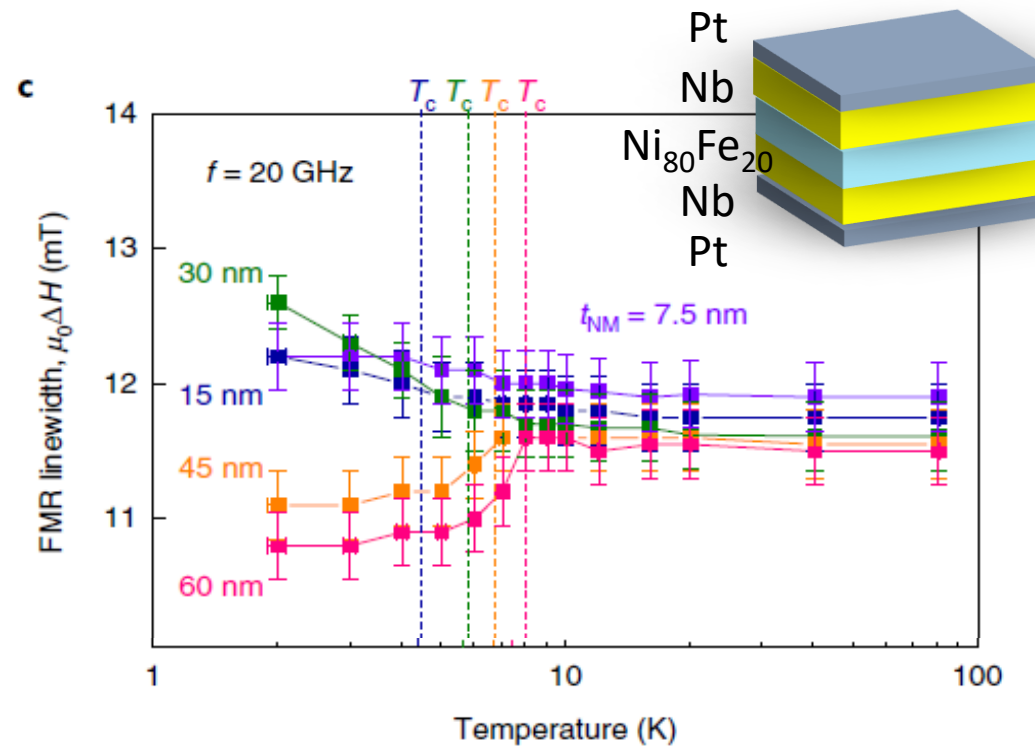




Experiments with s-wave superconductors

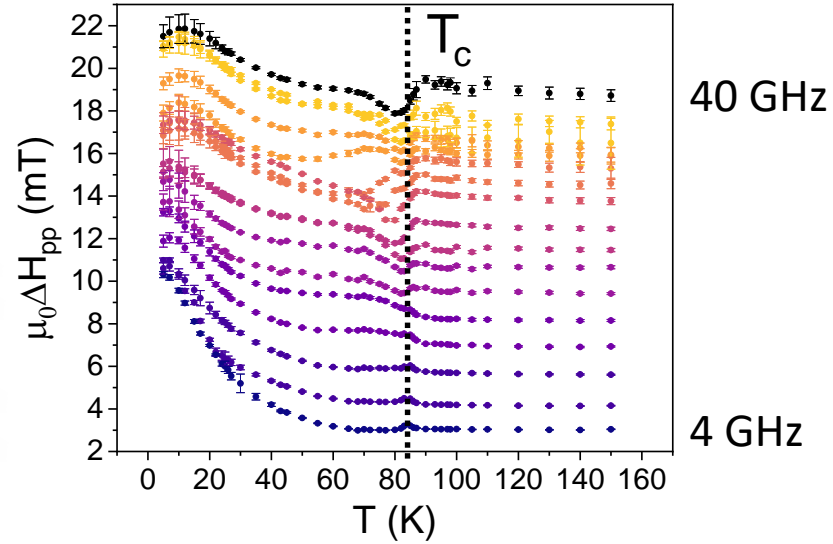
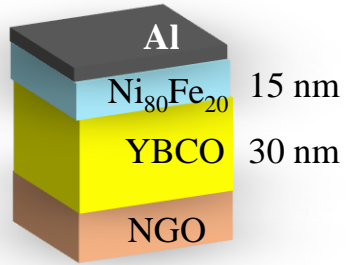
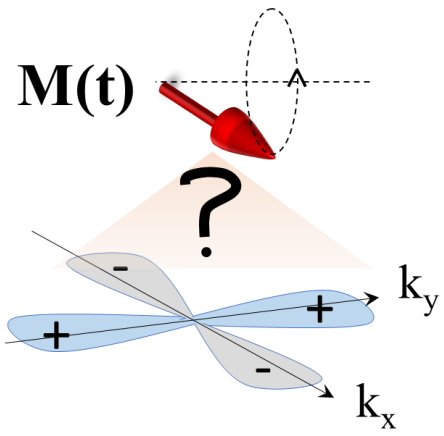


C. Bell et al, *Phys. Rev. Lett.* **100**, 047002 (2008)

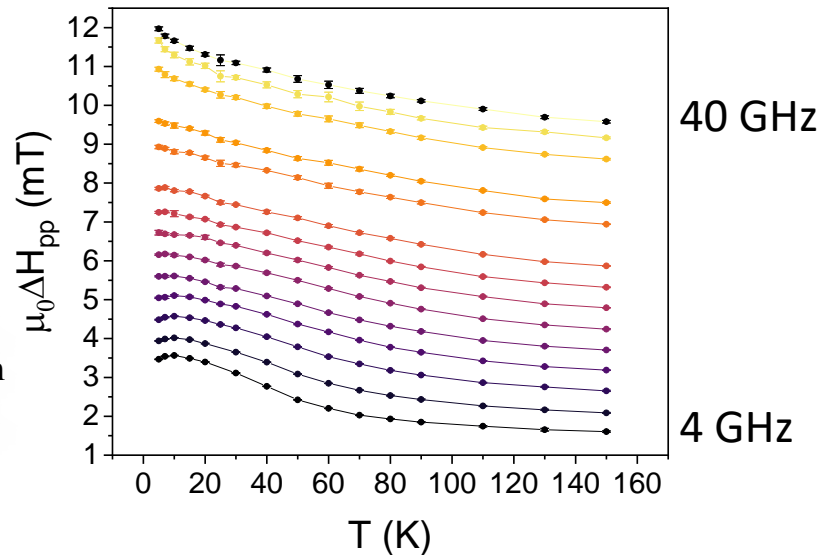
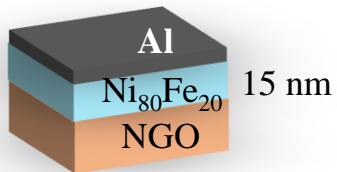


K. Jeon et al. *Nat. Mater.* **17**, 499–503 (2018)

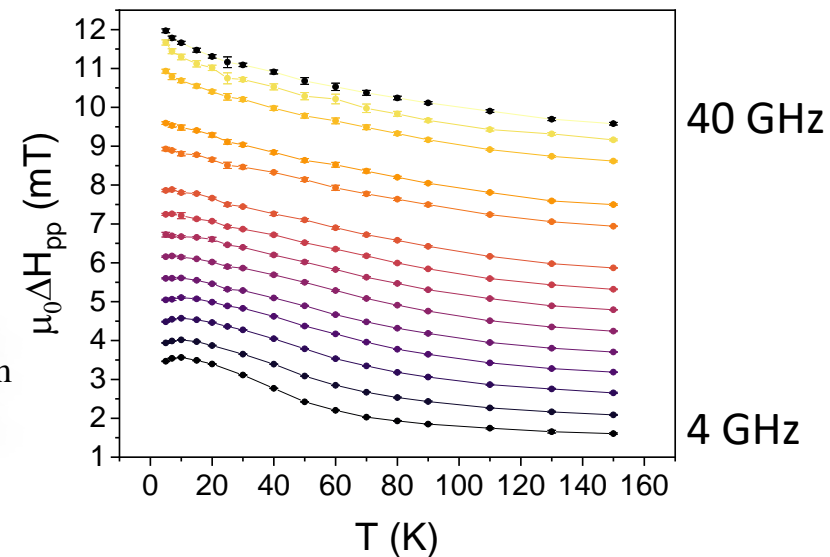
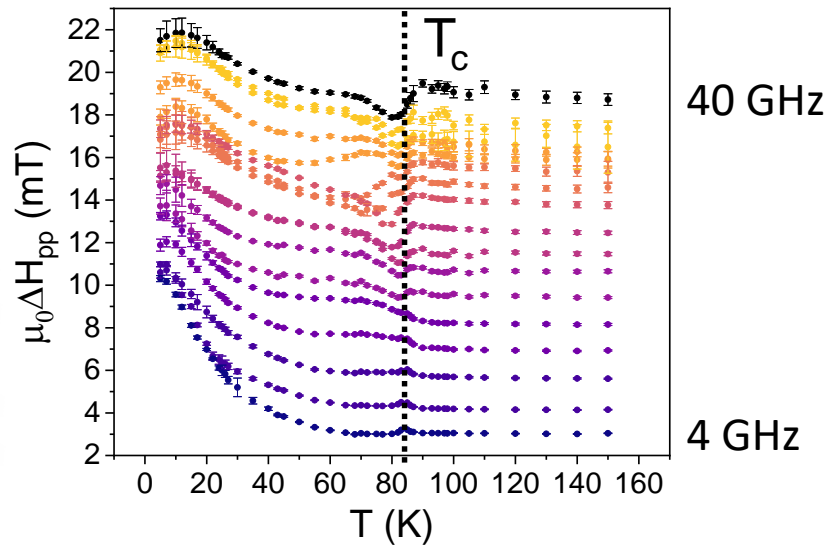
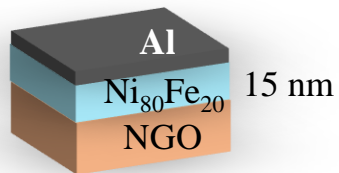
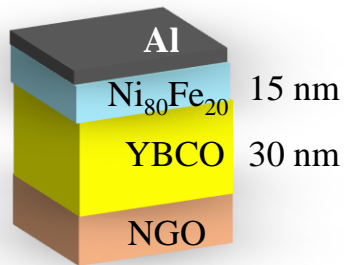
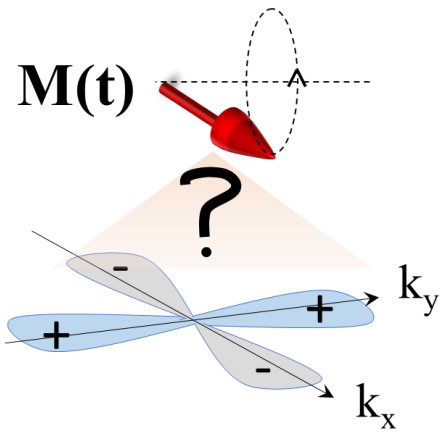
Experiments with d-wave superconductors



→ Drastic change below T_c
 → Frequency dependent

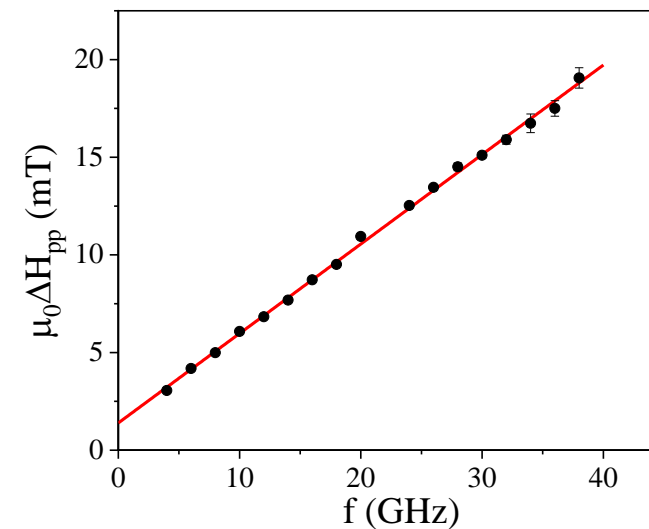


Experiments with d-wave superconductors

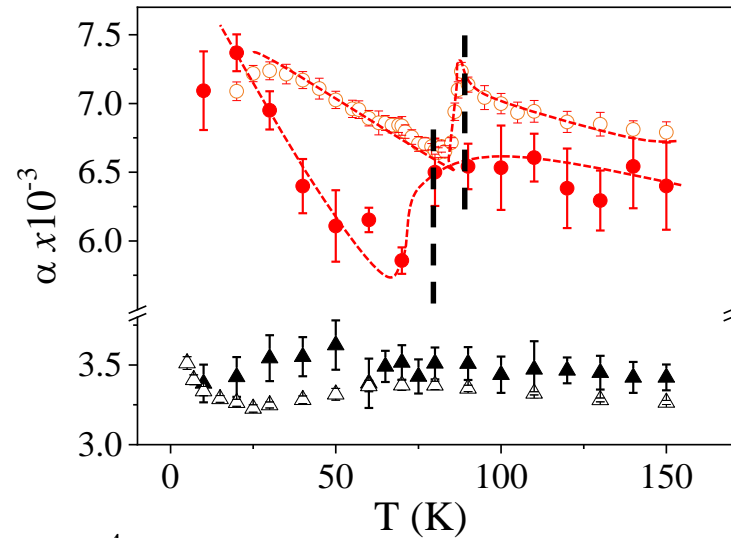
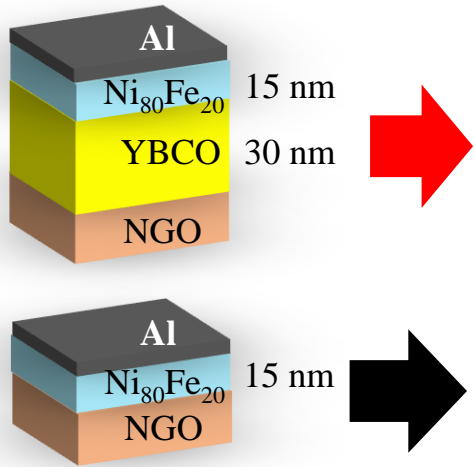


→ Drastic change below T_c
 → Frequency dependent

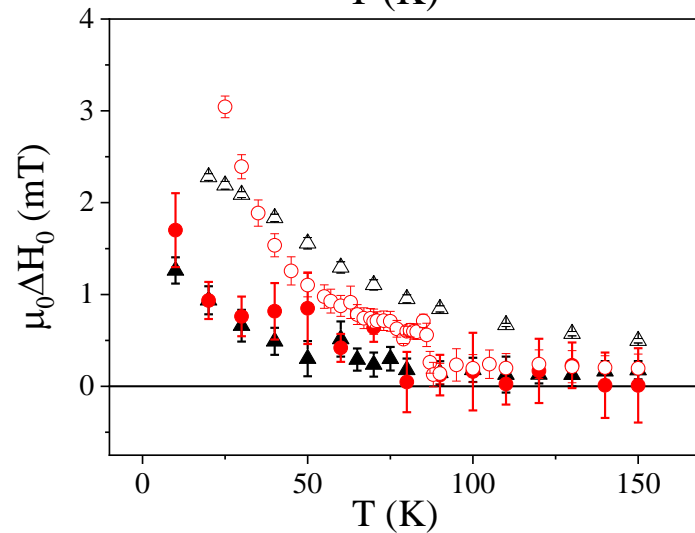
$$\Delta H_{pp} = \frac{2\alpha}{\sqrt{3}\gamma\mu_0} f + \Delta H_0$$



Experiments with d-wave superconductors

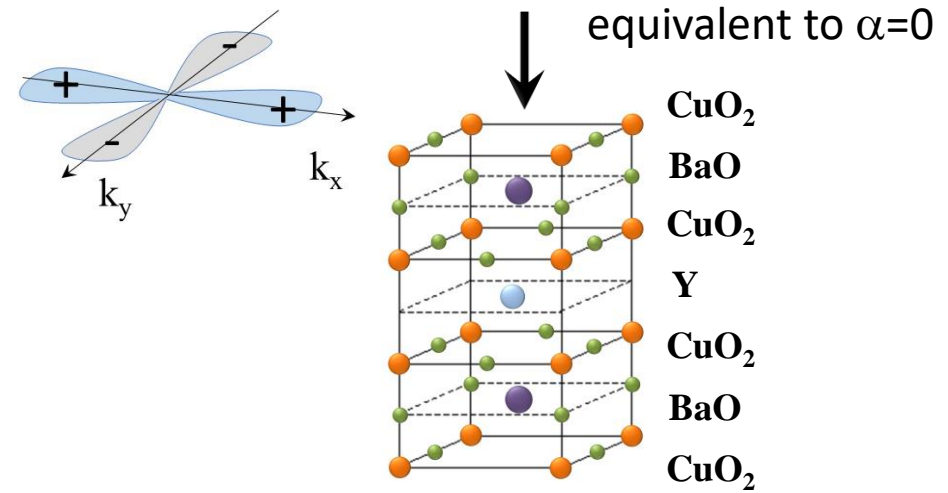
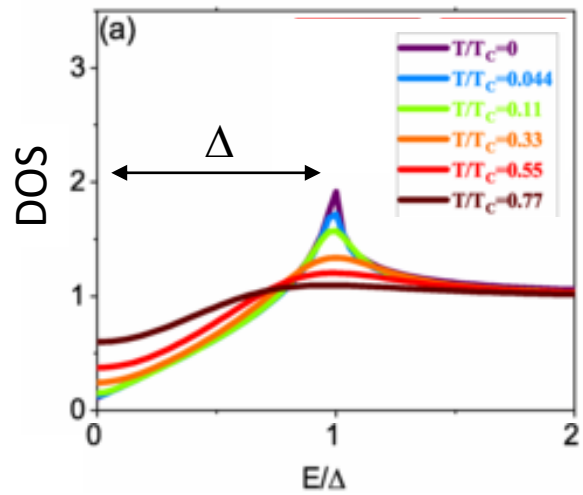


→ α drops at T_c
→ unexpected upturn further below

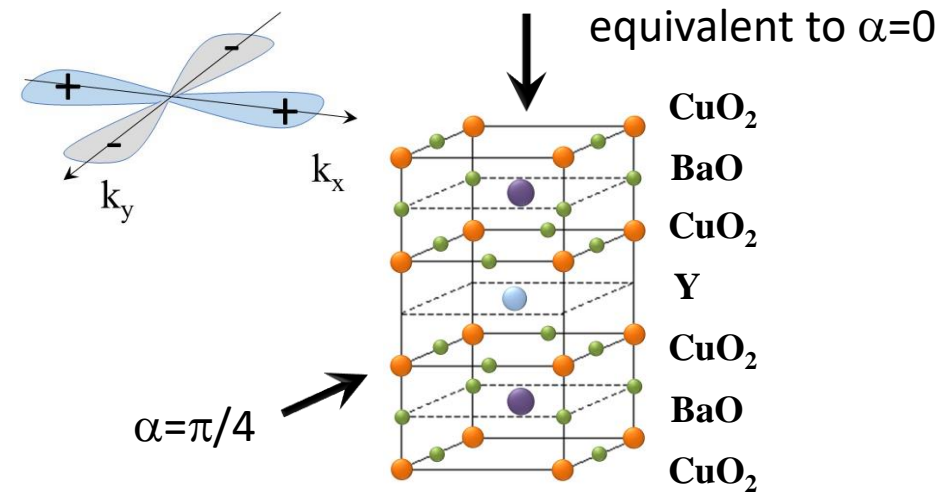
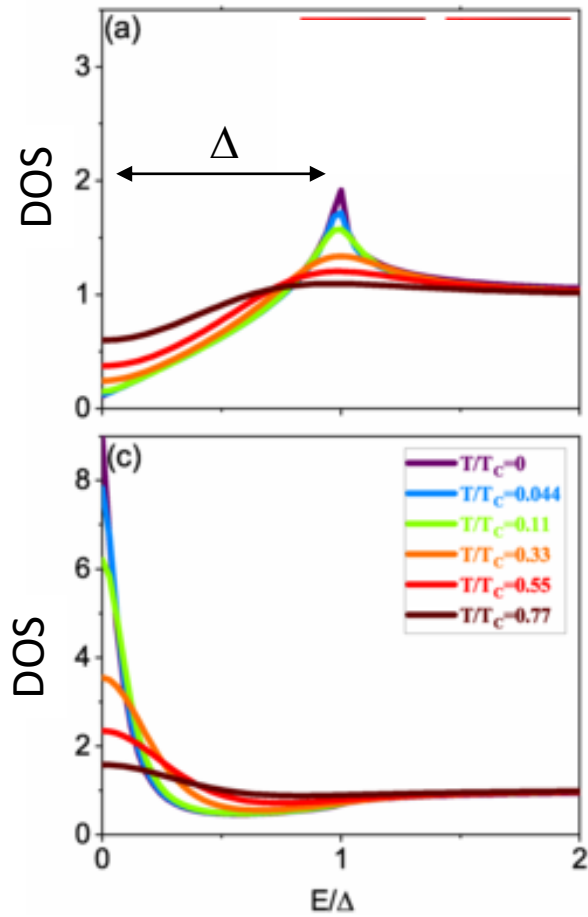


→ ΔH_0 not affected by SC

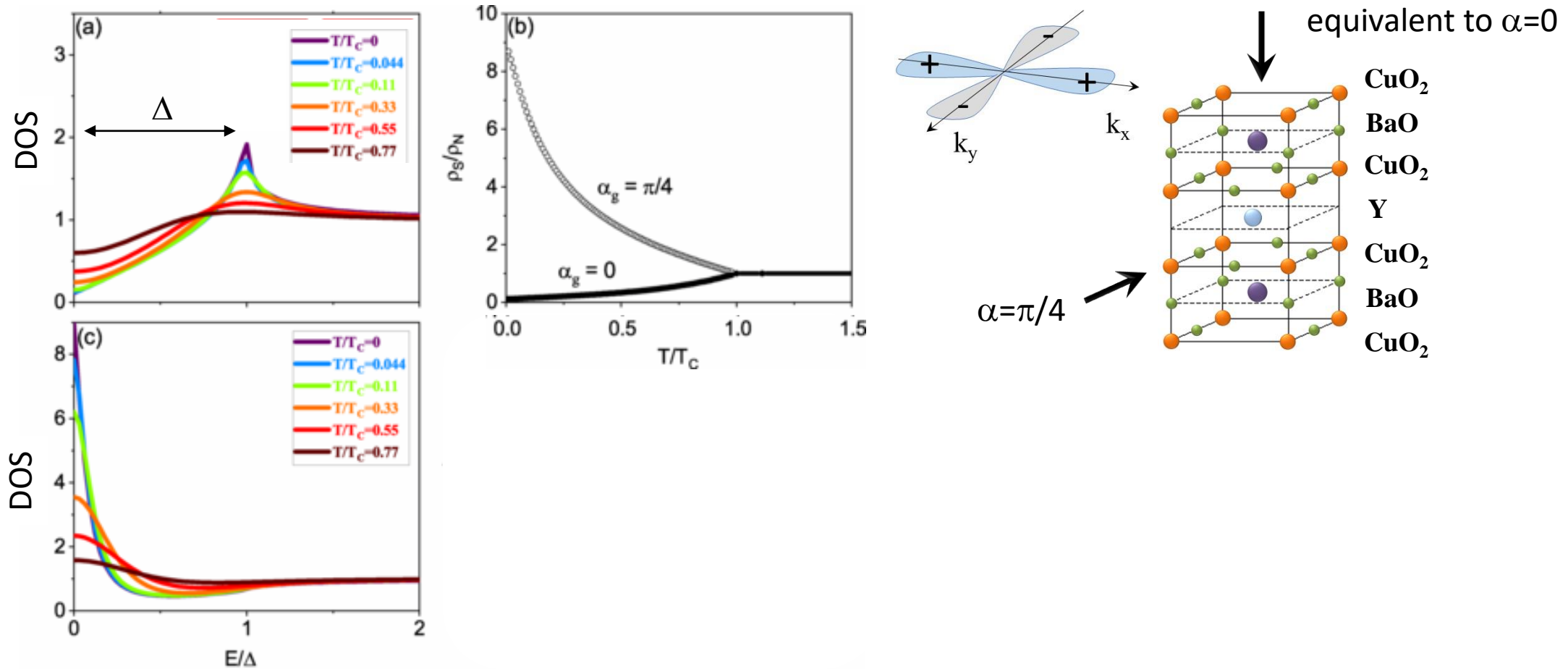
Anisotropic DOS as a function of temperature



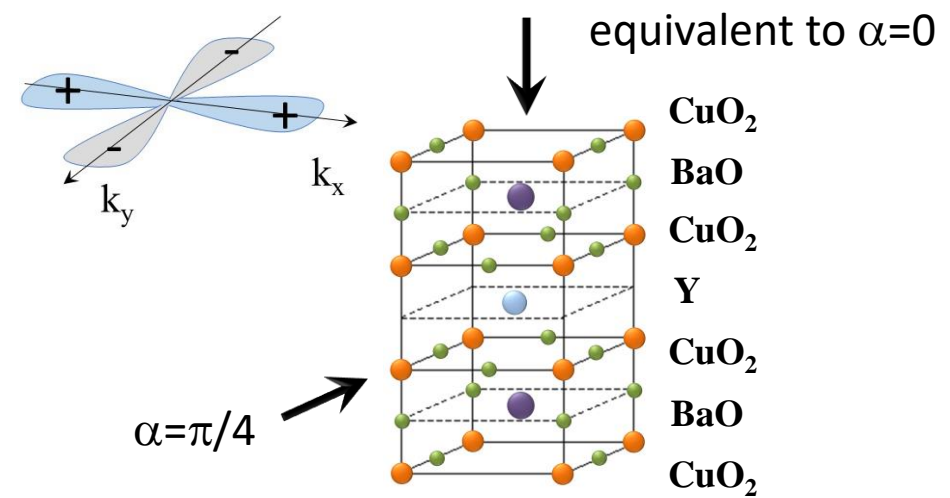
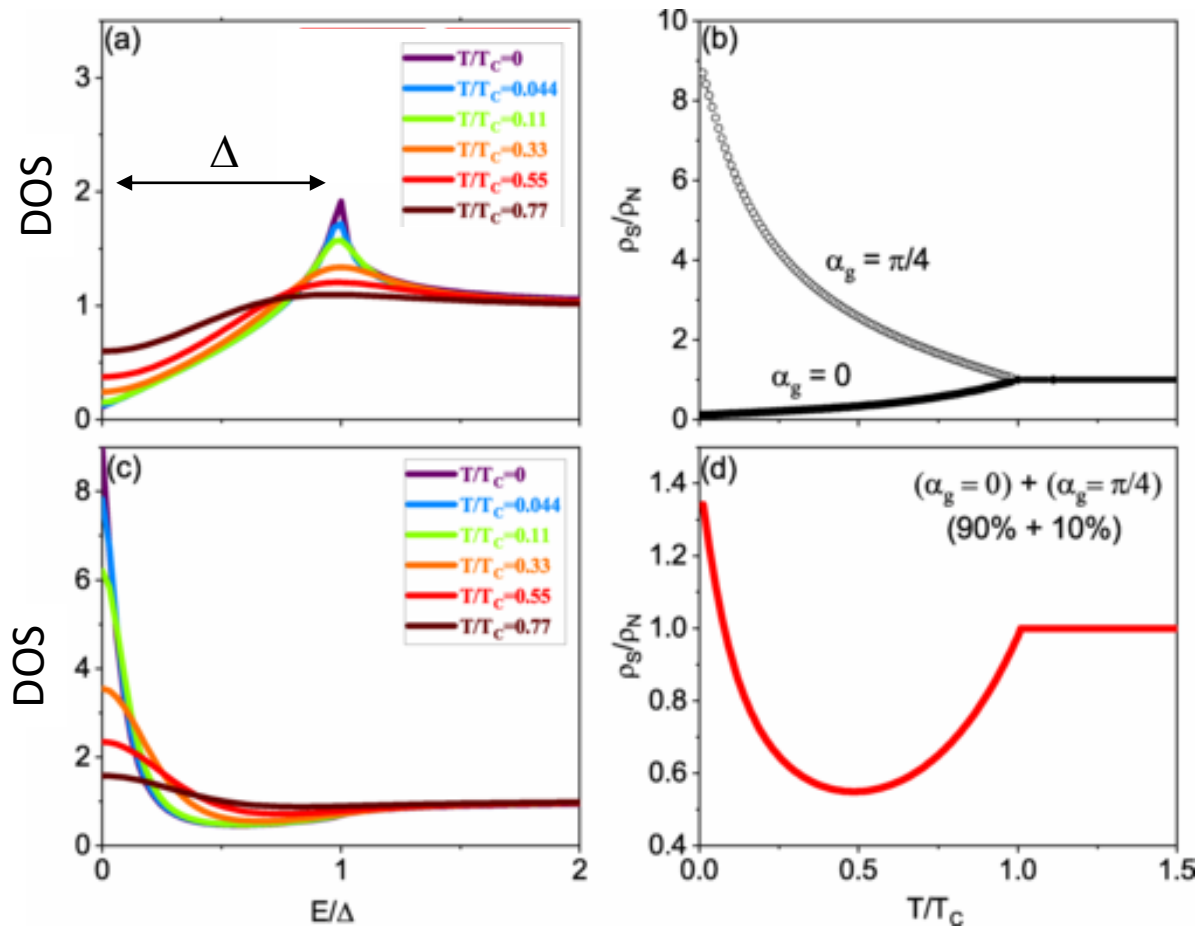
Anisotropic DOS as a function of temperature



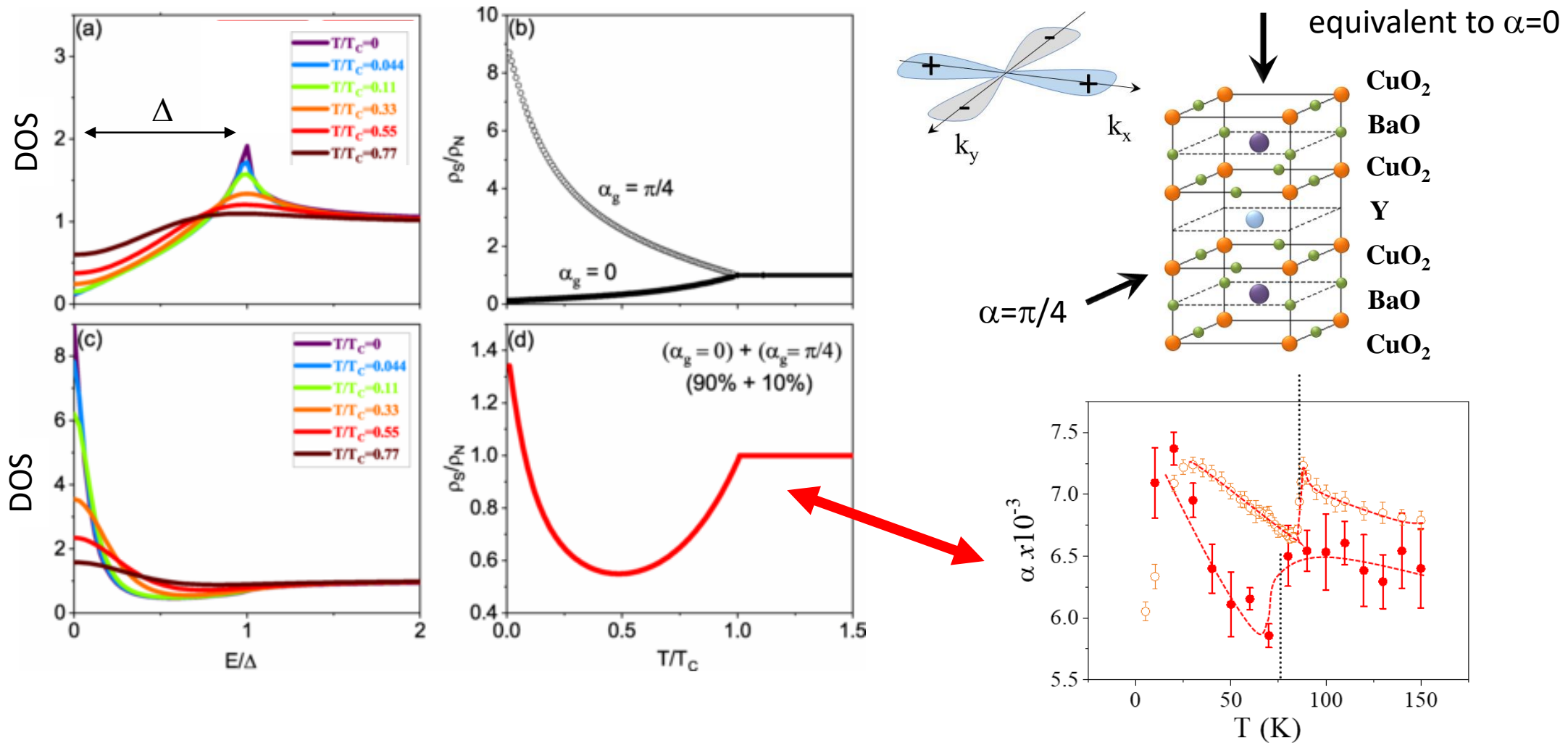
Anisotropic DOS as a function of temperature



Anisotropic DOS as a function of temperature

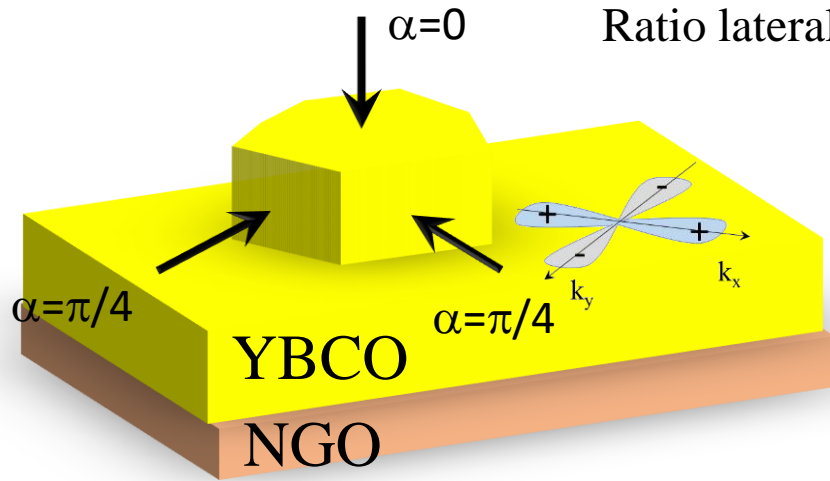
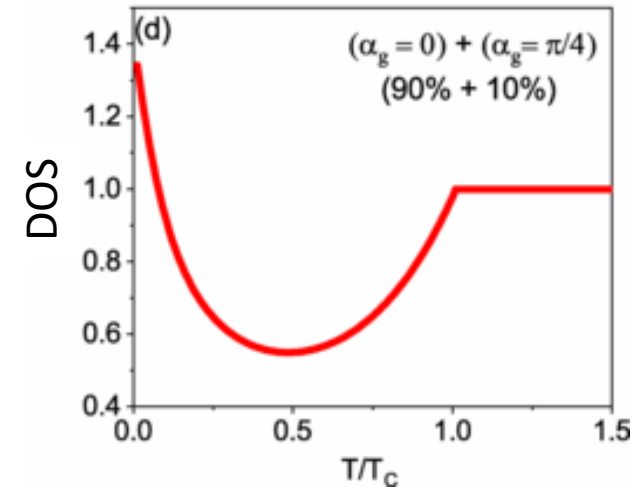
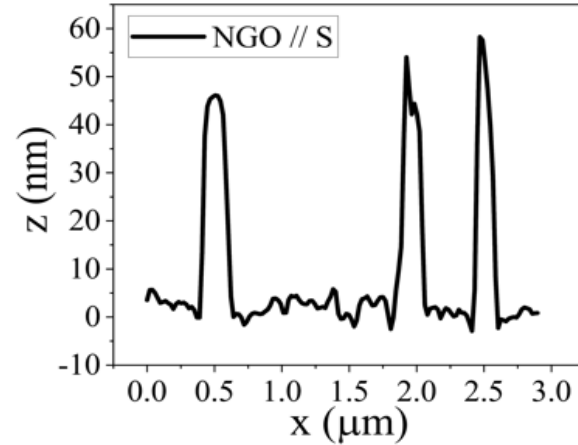
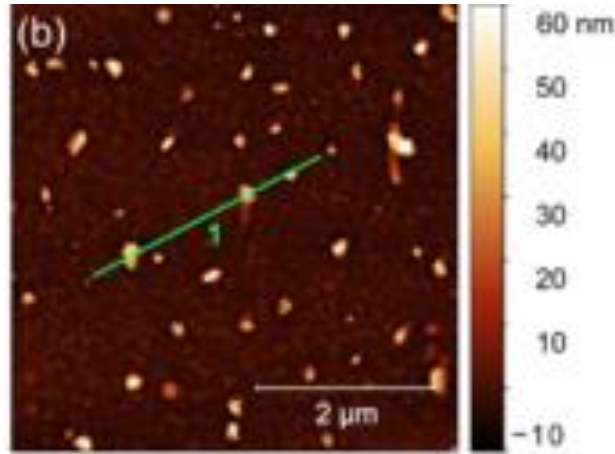


Anisotropic DOS as a function of temperature

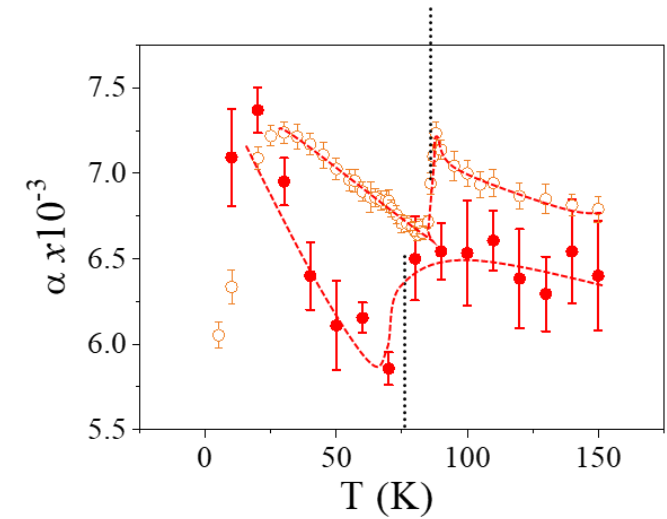
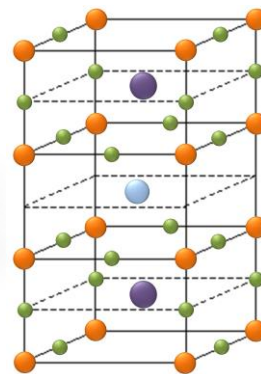


→ TEMPERATURE DEPENDENT QUASIPARTICLE DENSITY EXPLAINS $\alpha(T)$

Surface topography and effective DOS

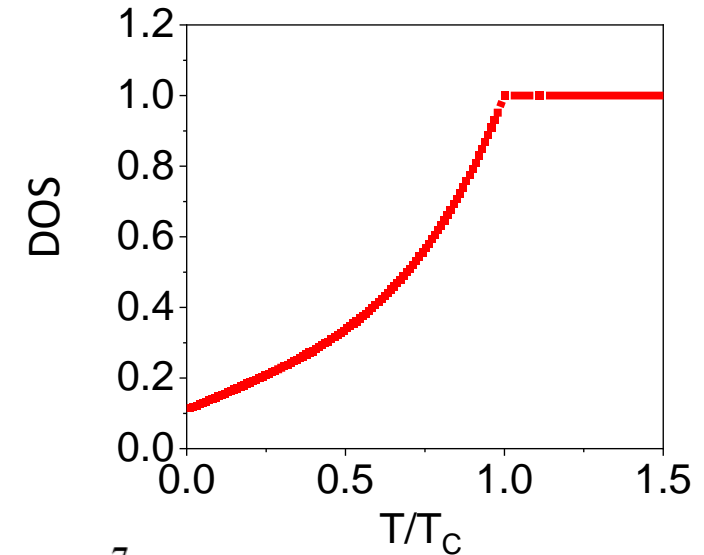
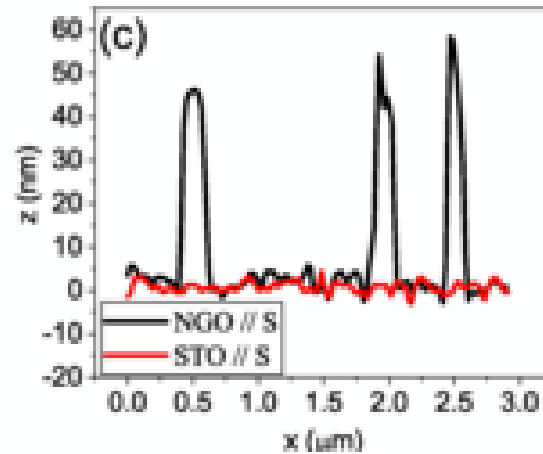
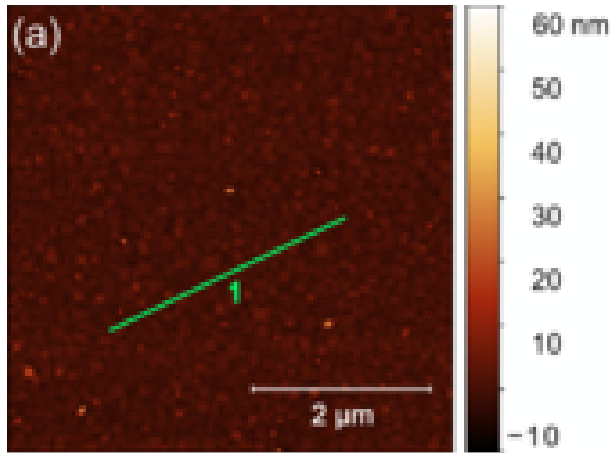


Ratio lateral/vertical surface $\approx 10\%$

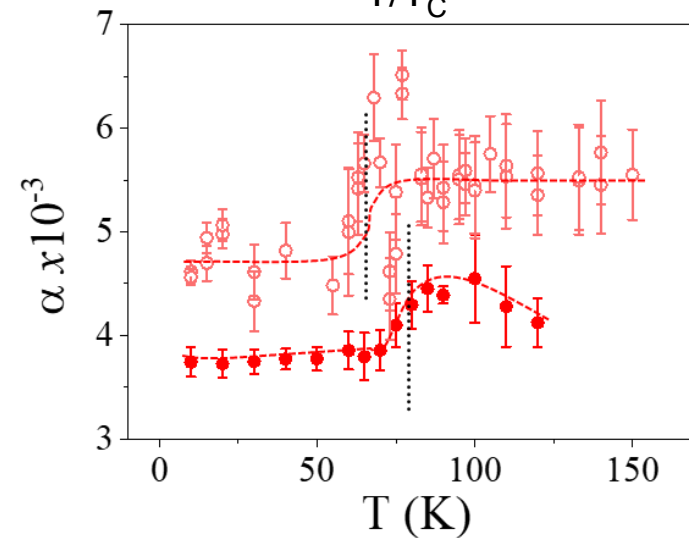
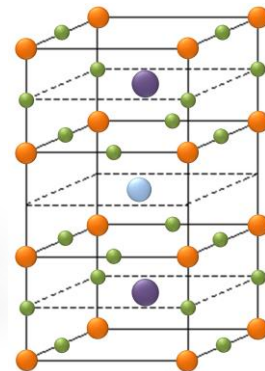
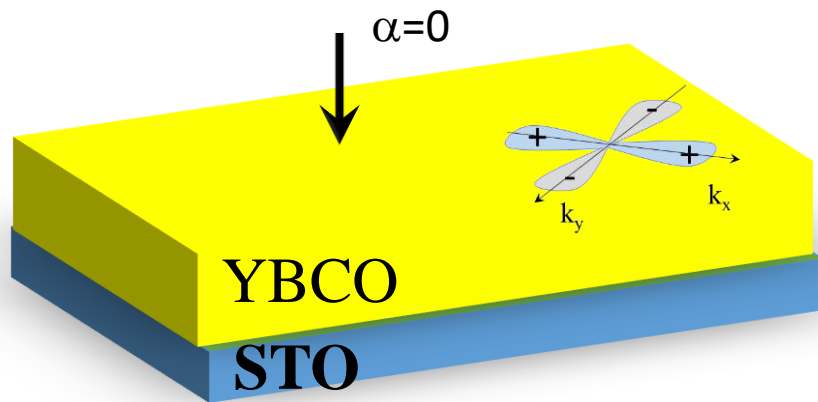


→ TOPOGRAPHY ALLOWS ACCESS TO LARGE QUASIPARTICLE DOS

Surface topography and effective DOS



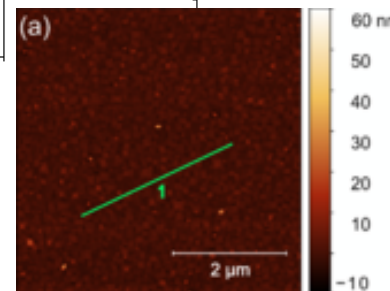
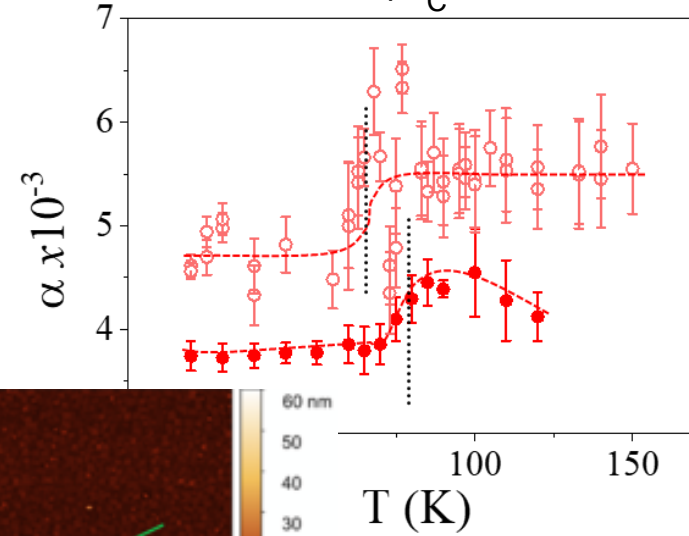
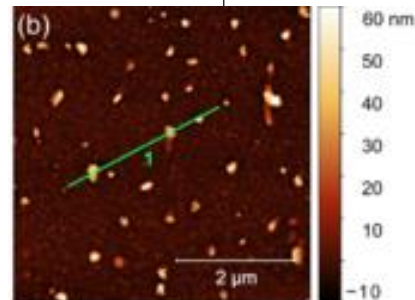
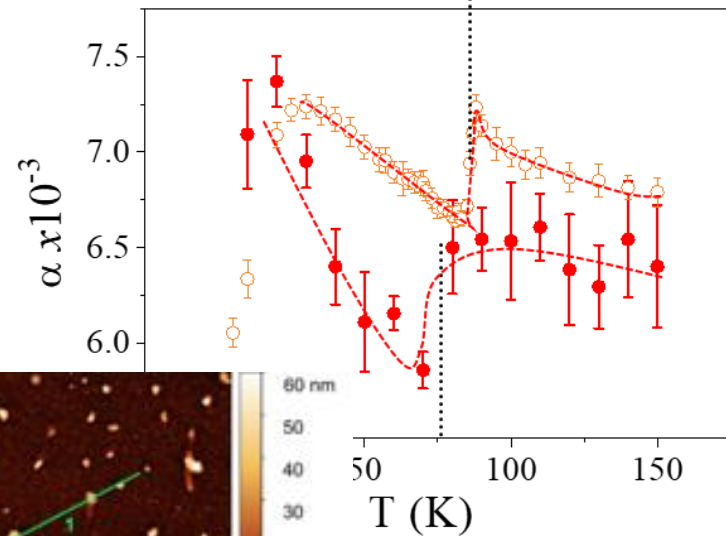
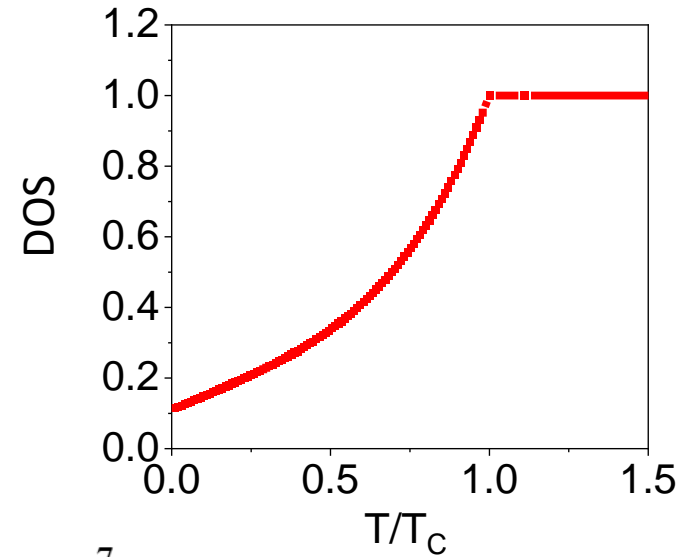
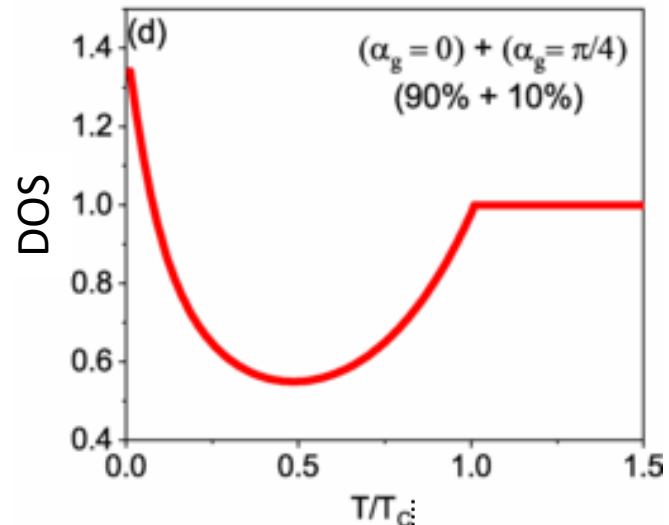
vertical surface $\approx 100\%$



→ FLAT SURFACE IMPEDES LIMITS ACCES TO QP BOUND STATES
 → BEHAVIOR AS WITH S-WAVE SUPERCONDUCTOR

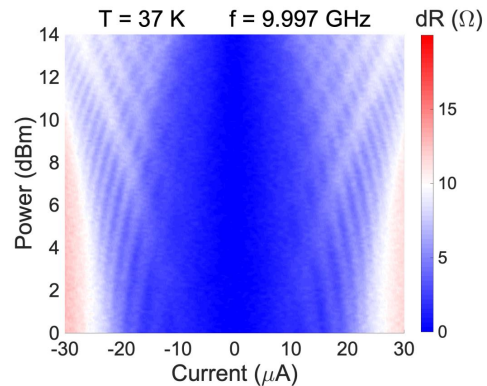
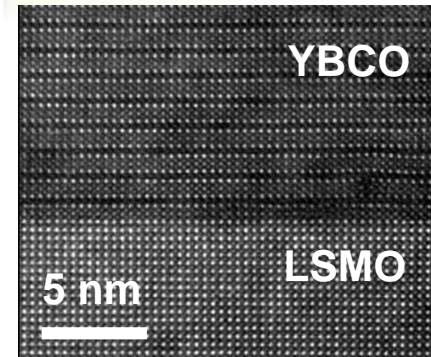
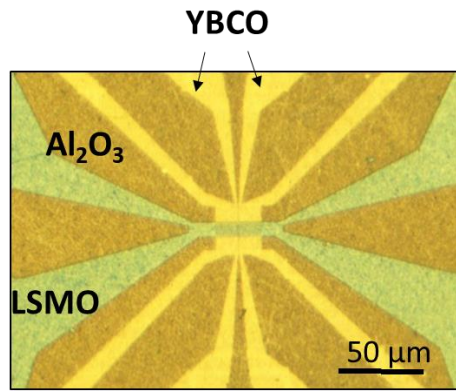
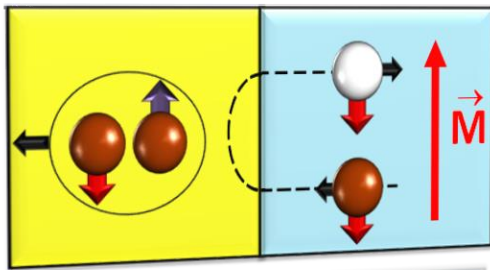
Surface topography and effective DOS

→ UNUSUAL
UPTURN
EXPLAINED BY
QP BOUND
STATES

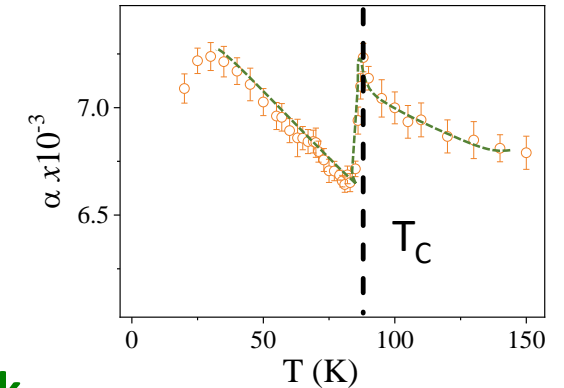
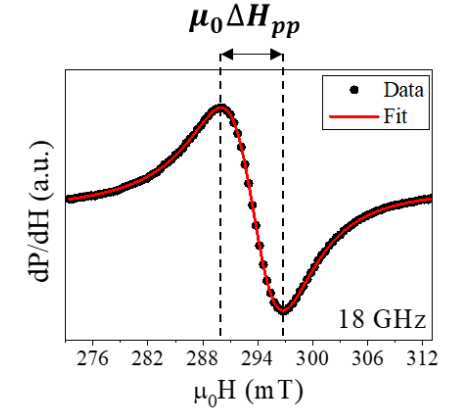
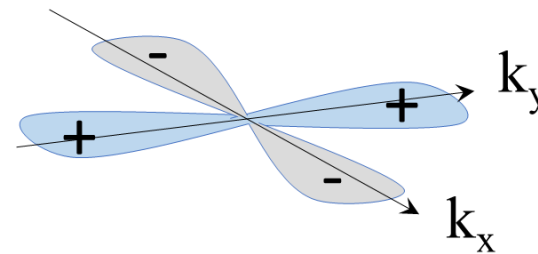
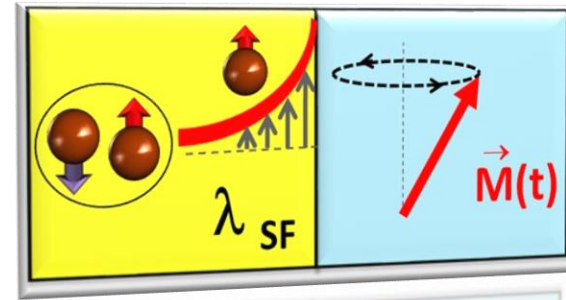


Conclusions

Proximity effect



Dynamic coupling



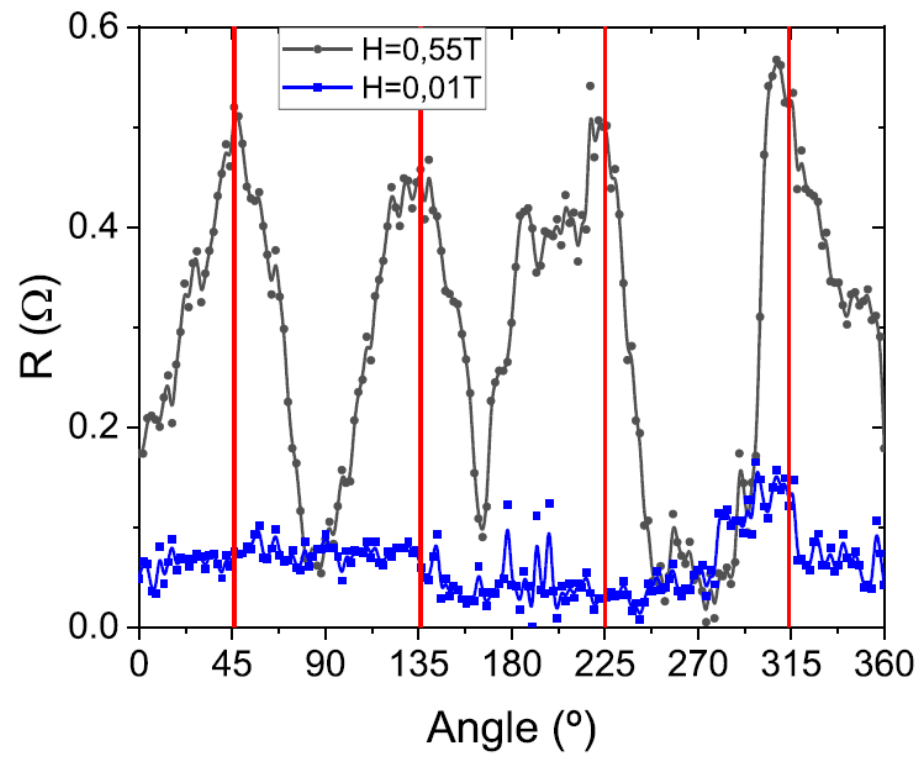
Fully spin-polarized, high- T_c Josephson supercurrents
Quantum phase coherence effects

Tunable spin sink
d-wave effects

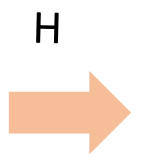
Sanchez-Manzano *et al.* Nature Materials (2022)

Carreira *et al.* PRB (2021)

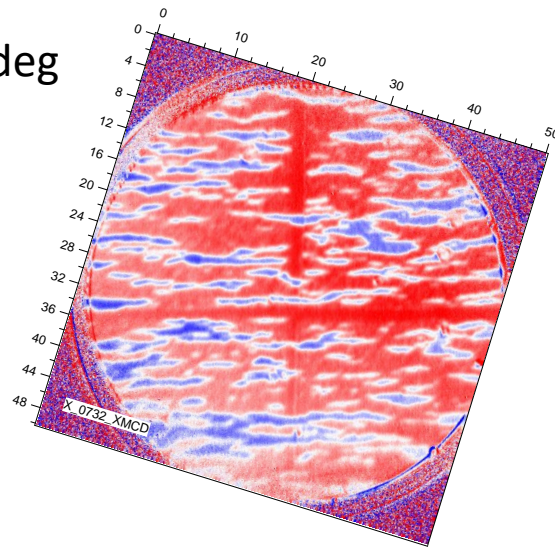
→ OPPORTUNITIES FOR HIGH- T_c SUPERCONDUCTING SPINTRONICS 46



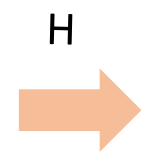
$\theta=45, 135, 225, 315$ deg



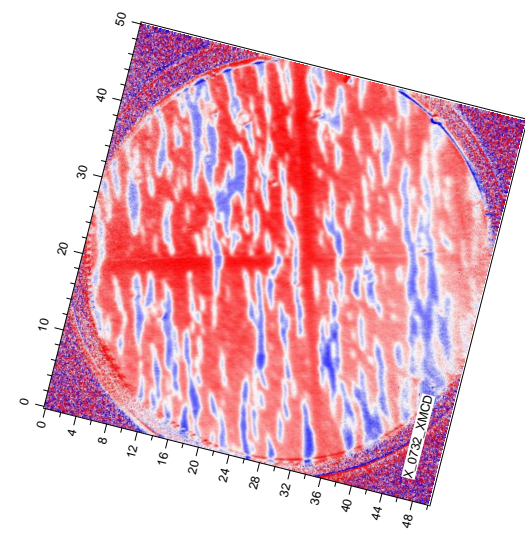
|| easy axis



$\theta=90, 180, 270, 360$ deg

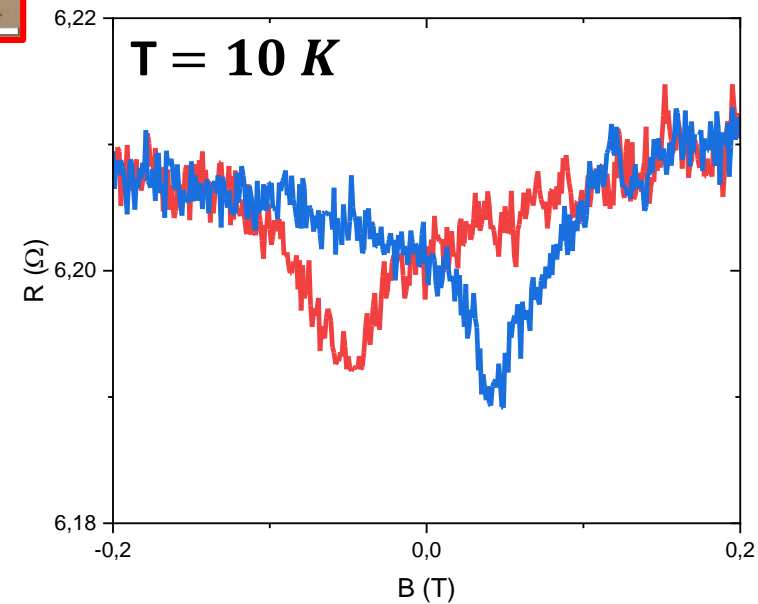
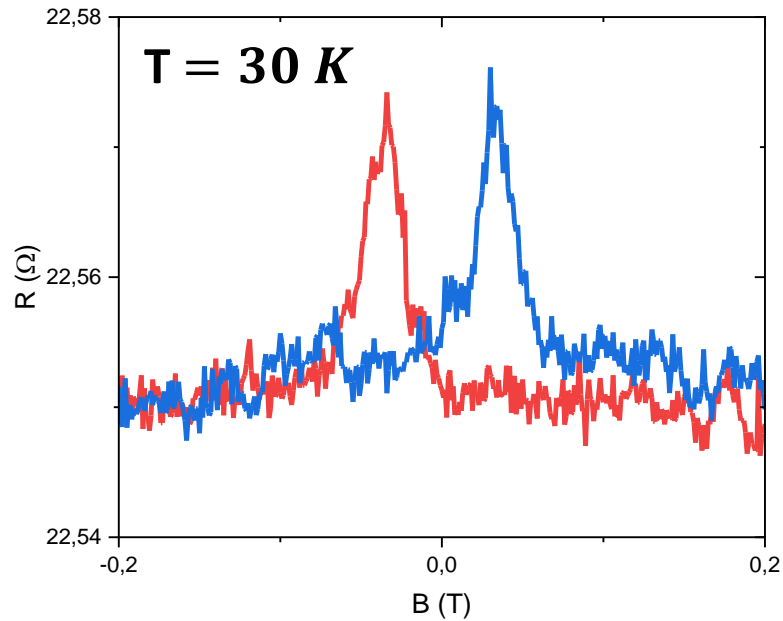
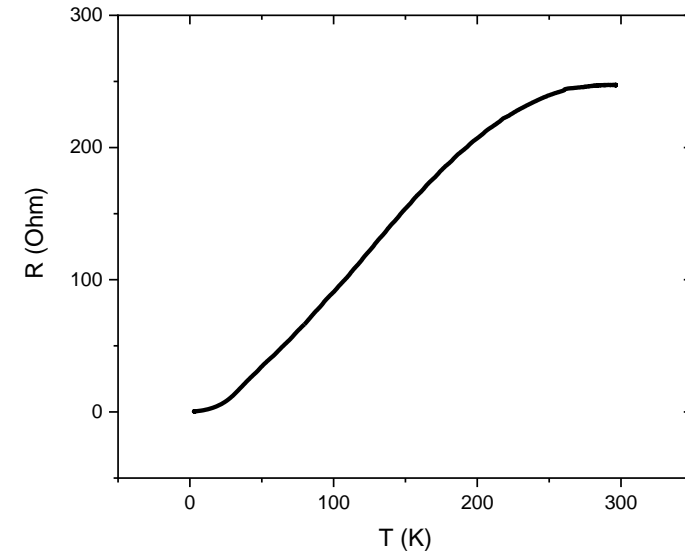
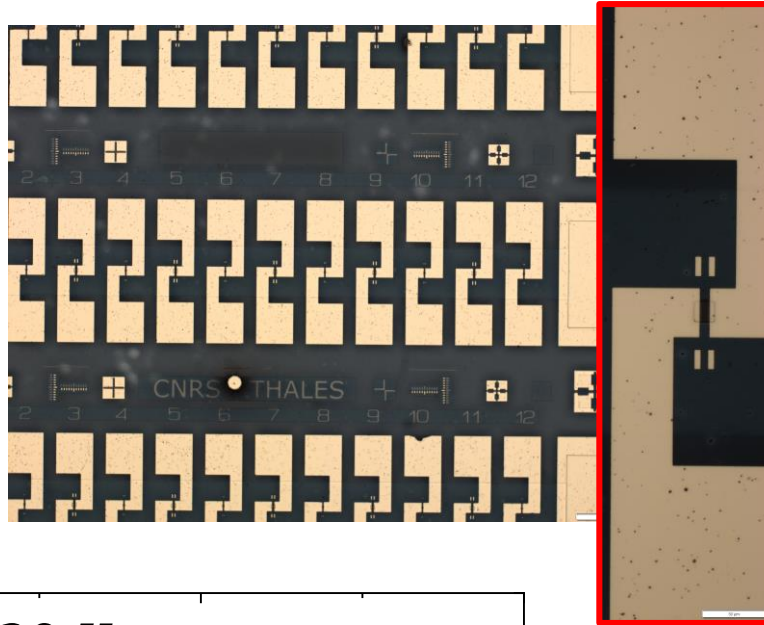
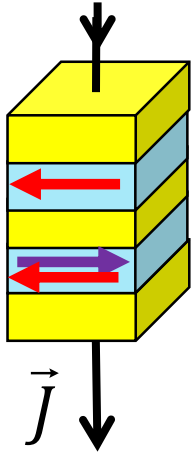


⊥ easy axis



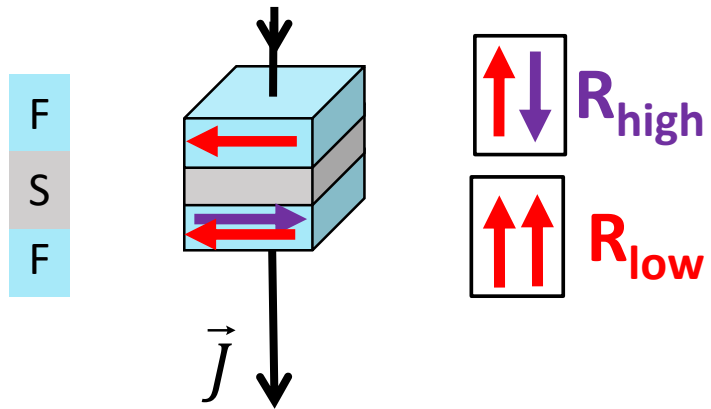
High- T_C Josephson spin valves: preliminary results

S
F
S
F
S

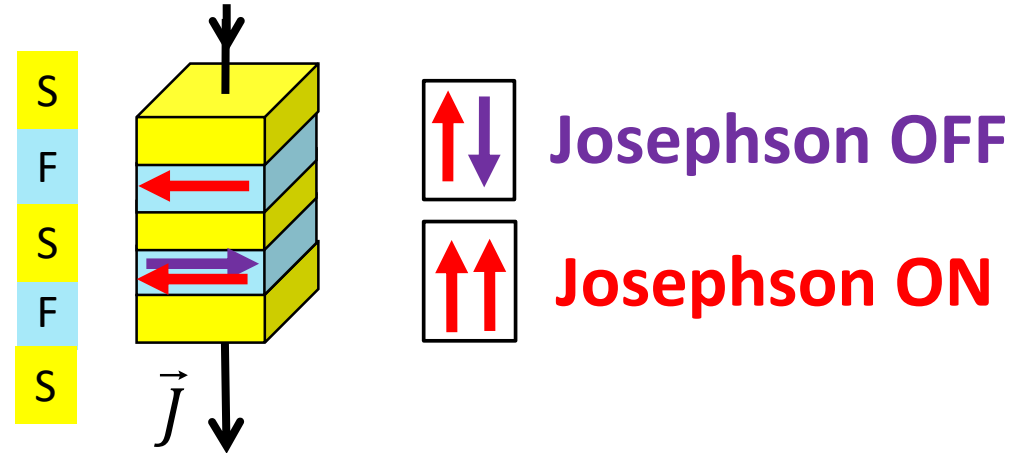


High- T_C Josephson spin valves

conventional spin valve

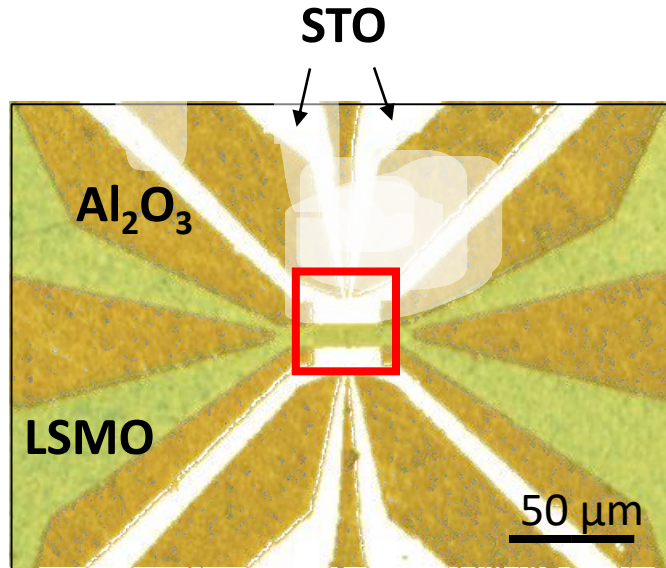
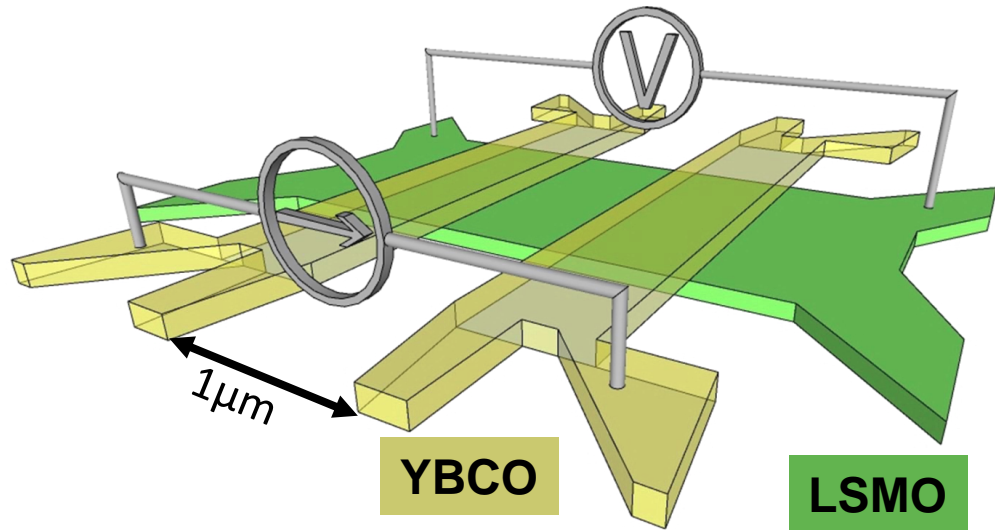


Josephson spin valve

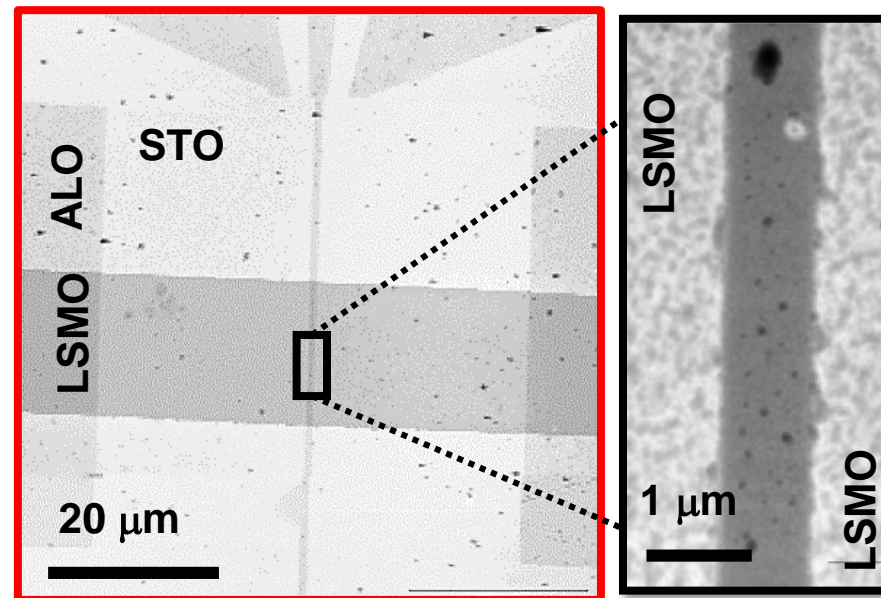


→ JOSEPHSON SPIN-VALVES... SPIN TORQUES, AND BEYOND?

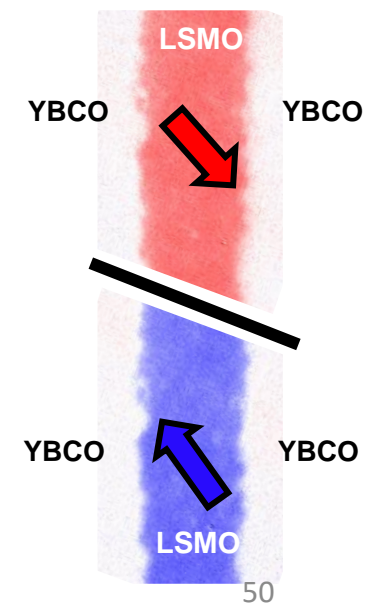
Fabrication of planar Josephson junctions



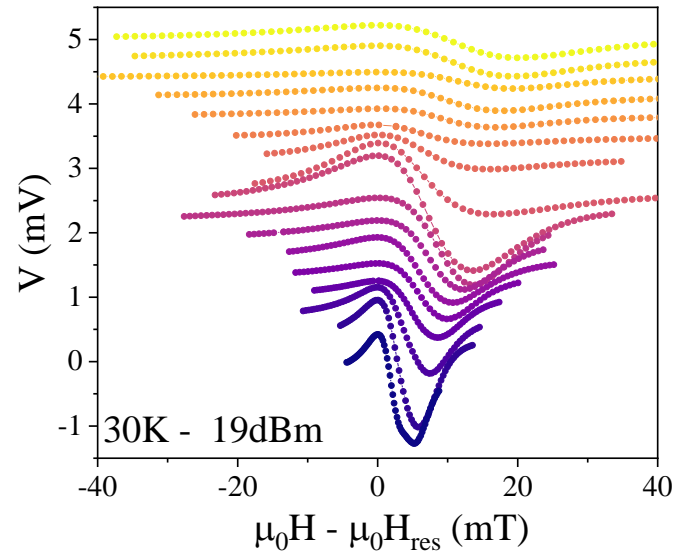
→ AMORPHOUS ALUMINA MASK
→ LSMO REMAINS MAGNETIC



XMCD-PEEM



FMR experiments – Damping and inhomogeneous broadening

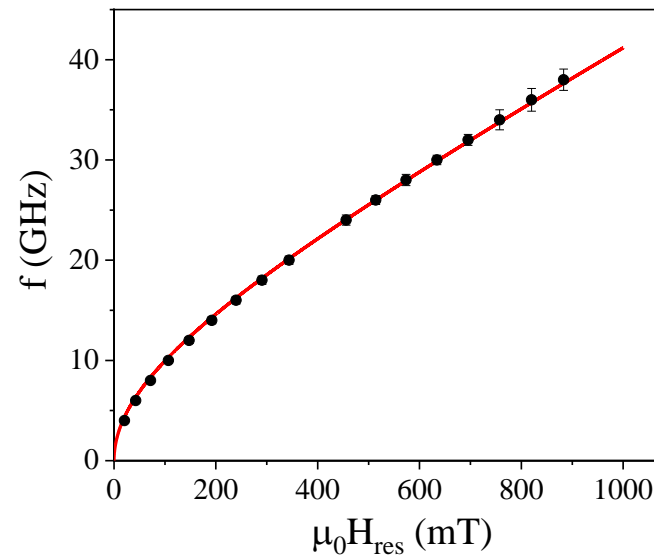
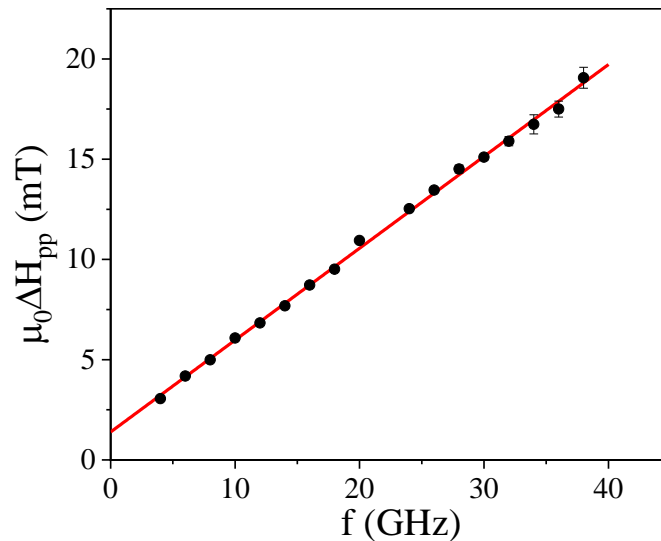


$$\Delta H_{pp} = \frac{2\alpha}{\sqrt{3}\gamma\mu_0} f + \Delta H_0$$

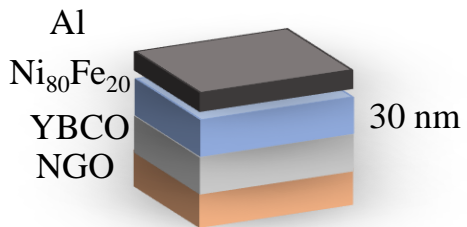
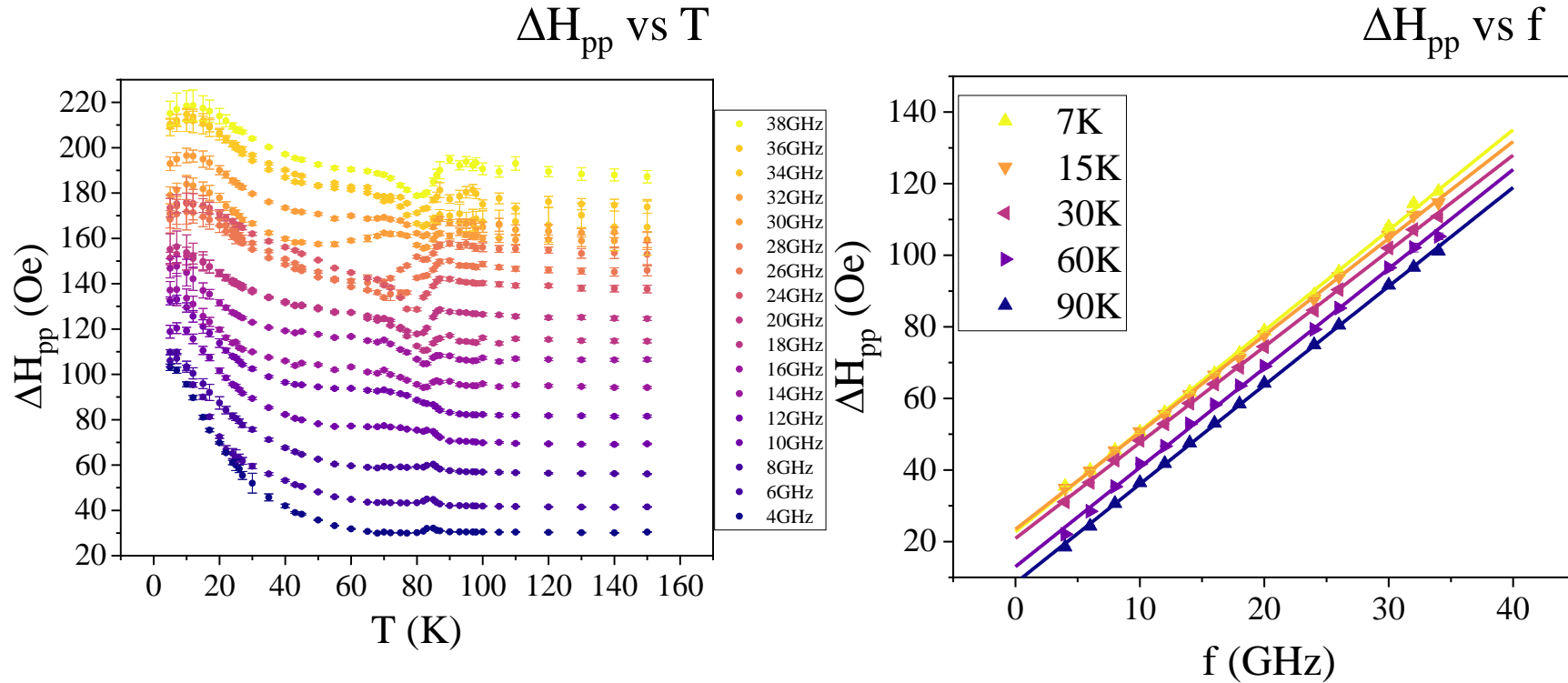
$$f = \gamma\mu_0 \sqrt{H_{res}(H_{res} + M_{eff})}$$

α : Gilbert damping

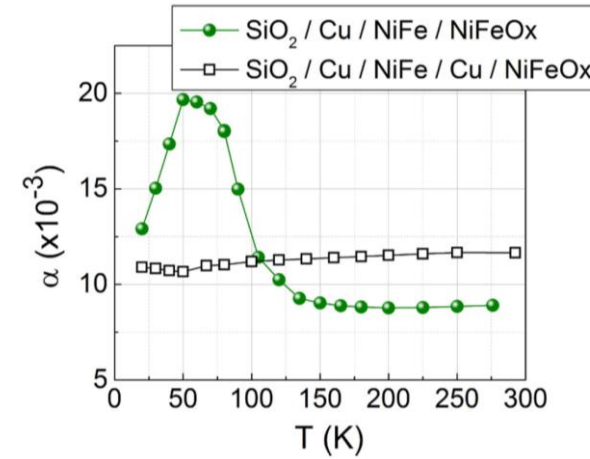
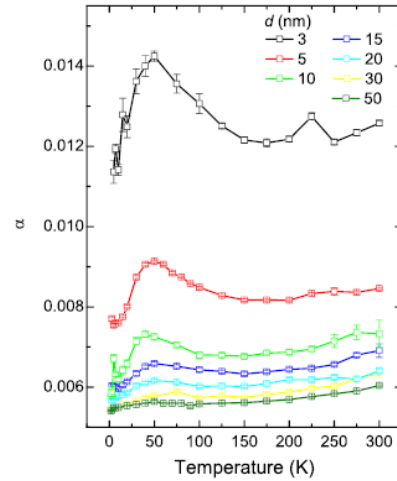
ΔH_0 : inhomogeneous broadening



Linewidth vs T and vs f for the sample grown on NGO



Intrinsic broadening of the linewidth at low temperatures in NiFe thin films



Y. Zhao et al, *Sci. Rep.* 6, 22890 (2016)

L. Frangou et al. *Phys. Rev. B* **95**, 054416 (2017)

Magnetic inhomogeneities at the interface due to the oxidation of the Py



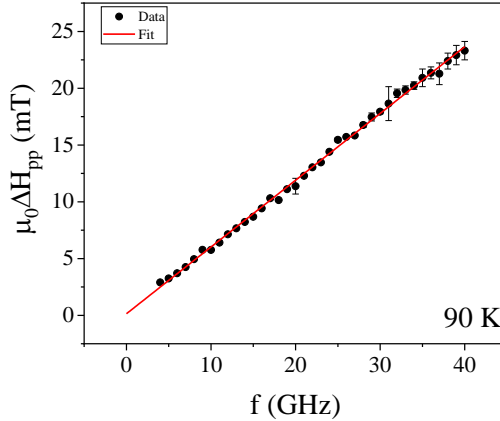
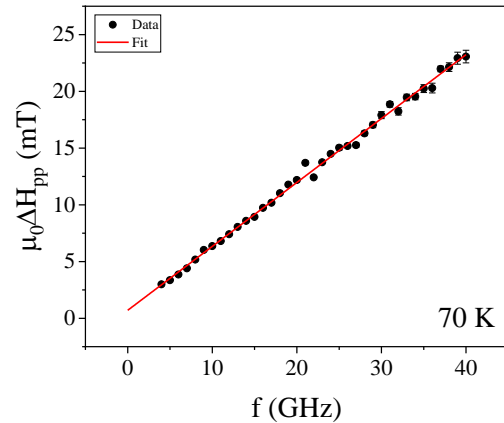
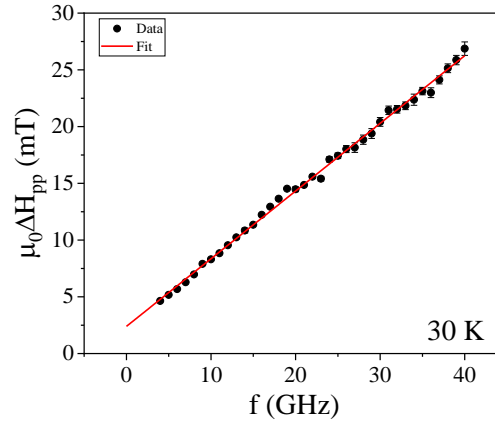
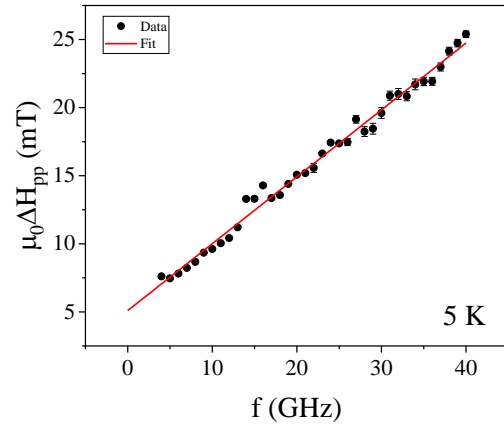
Opening of extrinsic relaxation channels



Linewidth increases at low temperatures



Ferromagnetic resonance experiments – Damping calculation

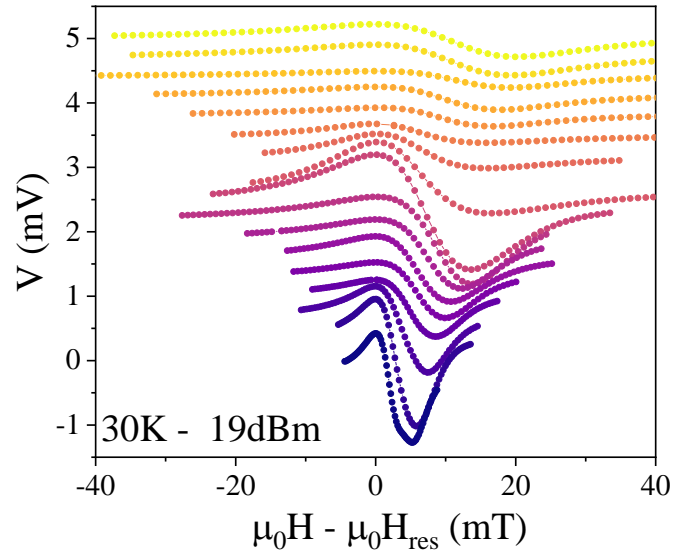


$$\Delta H_{pp} = \frac{2\alpha}{\sqrt{3}\gamma\mu_0} f + \Delta H_0$$

α : Gilbert damping

ΔH_0 : inhomogeneous broadening

FMR experiments – Damping and inhomogeneous broadening

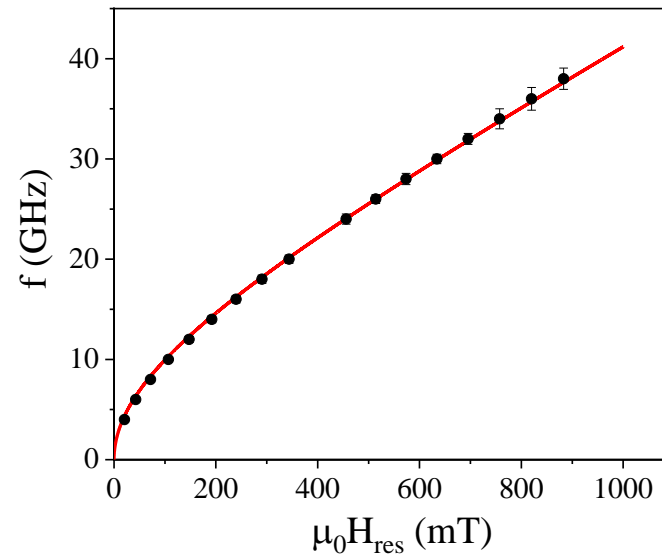
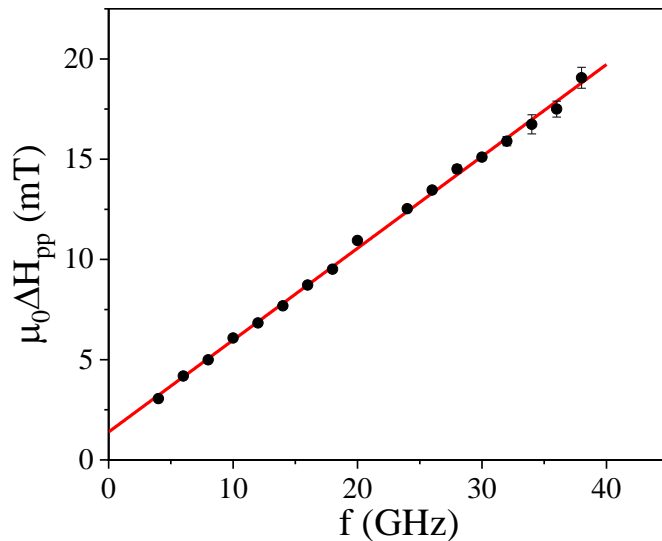


$$\Delta H_{pp} = \frac{2\alpha}{\sqrt{3}\gamma\mu_0} f + \Delta H_0$$

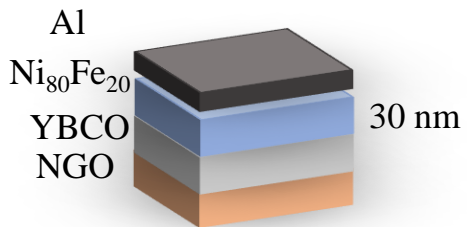
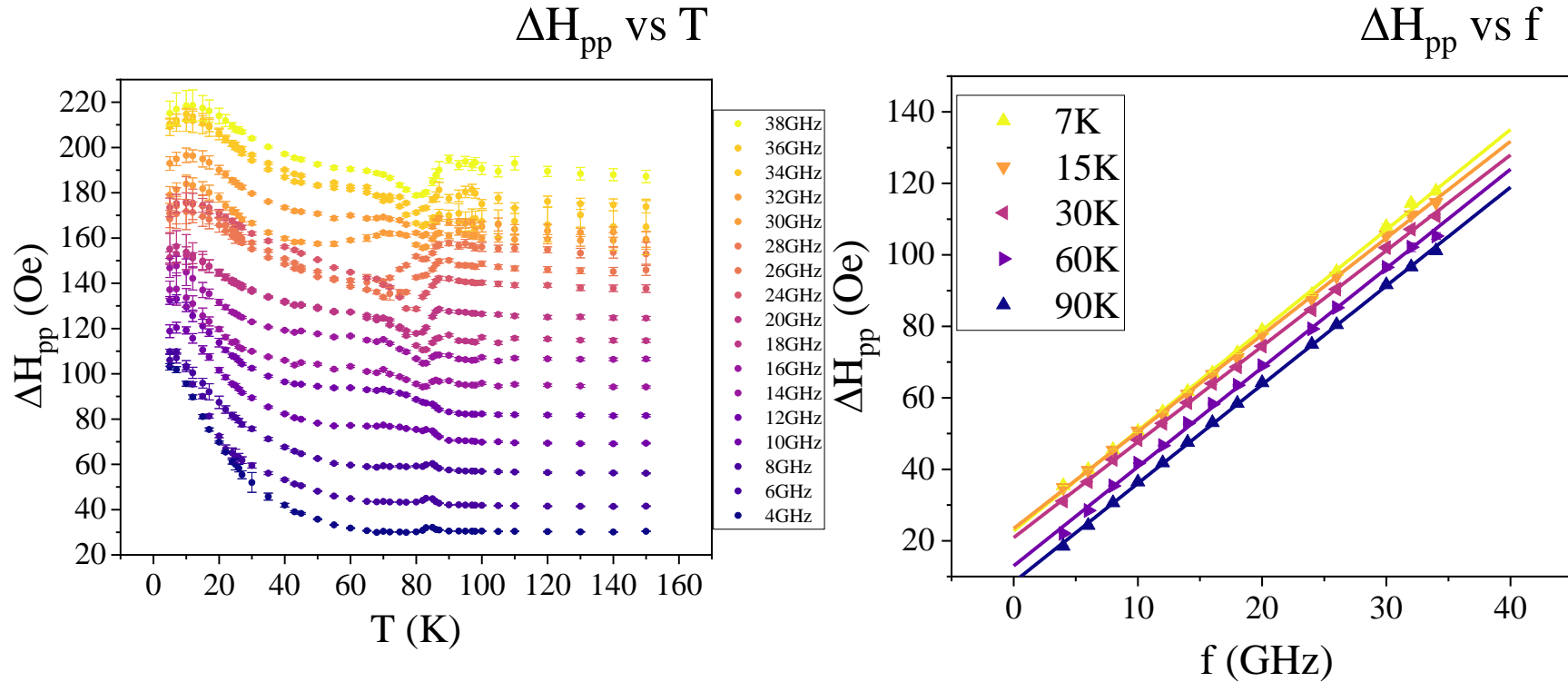
$$f = \gamma\mu_0 \sqrt{H_{res}(H_{res} + M_{eff})}$$

α : Gilbert damping

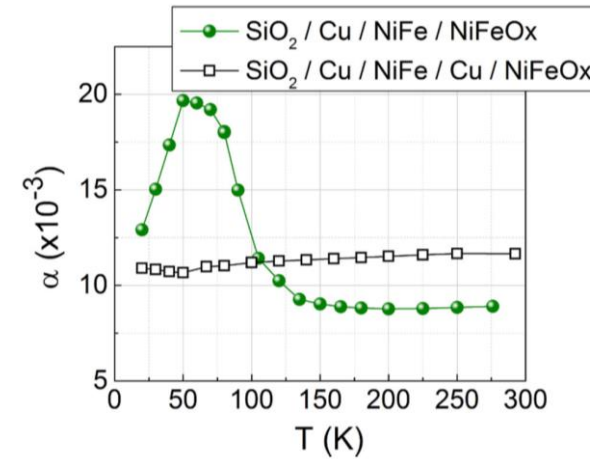
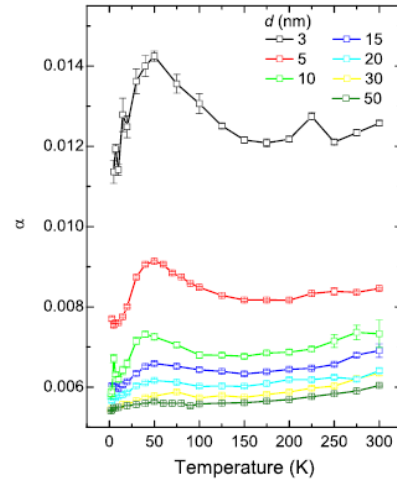
ΔH_0 : inhomogeneous broadening



Linewidth vs T and vs f for the sample grown on NGO



Intrinsic broadening of the linewidth at low temperatures in NiFe thin films



Y. Zhao et al, *Sci. Rep.* 6, 22890 (2016)

L. Frangou et al. *Phys. Rev. B* **95**, 054416 (2017)

Magnetic inhomogeneities at the interface due to the oxidation of the Py



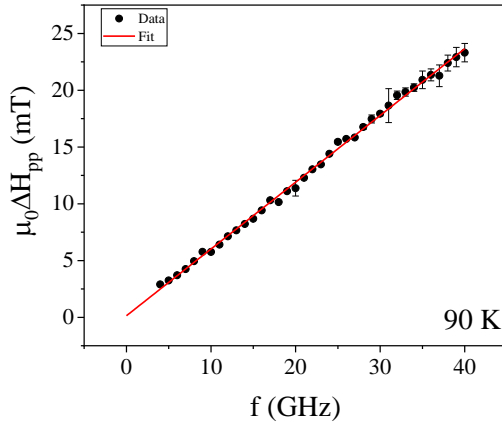
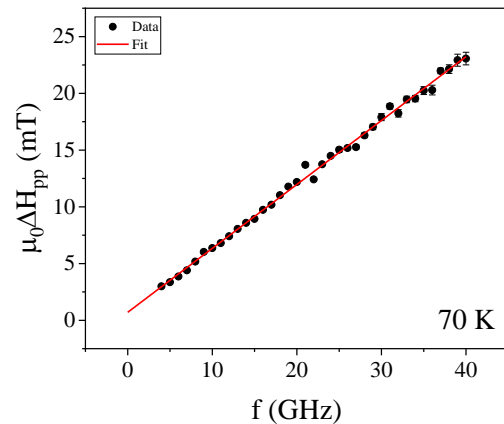
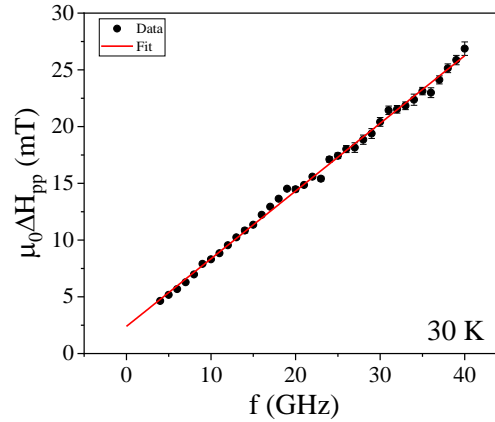
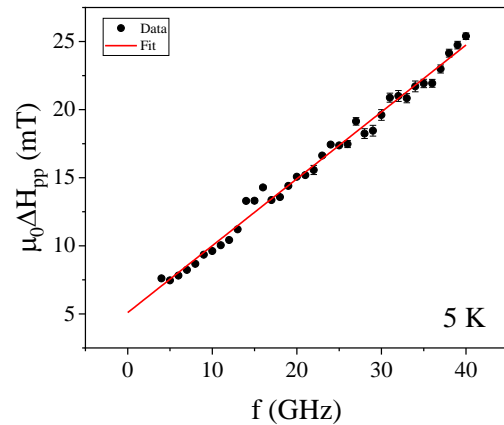
Opening of extrinsic relaxation channels



Linewidth increases at low temperatures



Ferromagnetic resonance experiments – Damping calculation

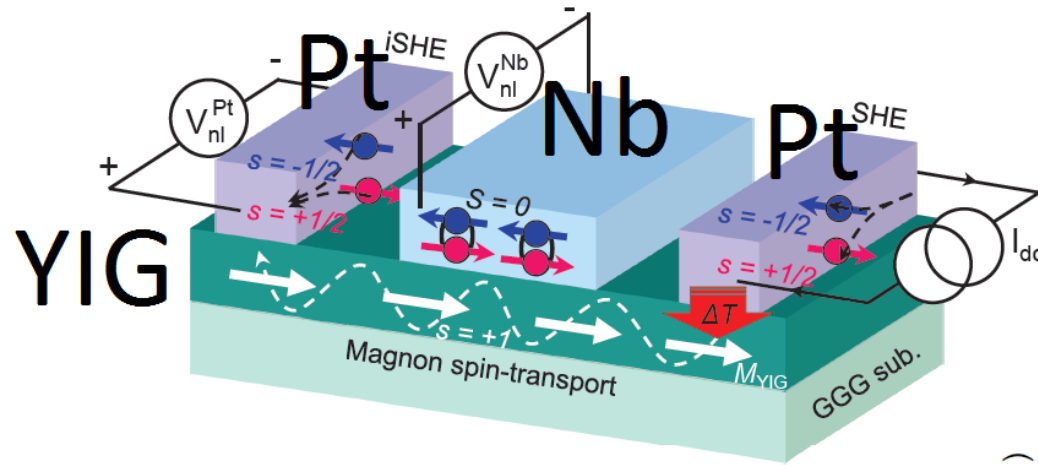


$$\Delta H_{pp} = \frac{2\alpha}{\sqrt{3}\gamma\mu_0} f + \Delta H_0$$

α : Gilbert damping

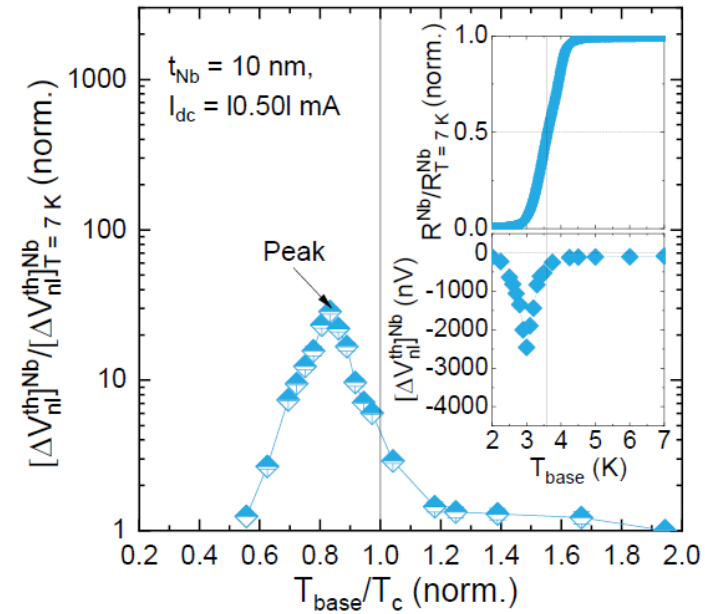
ΔH_0 : inhomogeneous broadening

Different designs to study spin injection in S/F hybrids



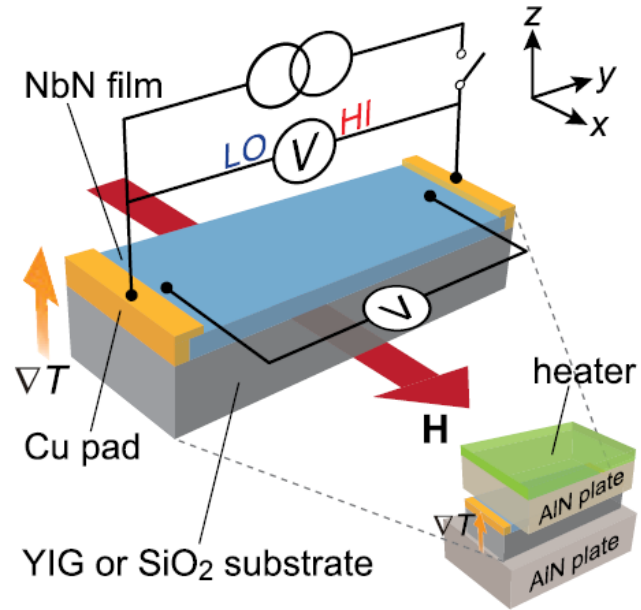
Non-local spin injection devices.
Inject angular momentum using magnons instead of spin polarized electrons

Spin injection efficiency in Nb increases below T_c !

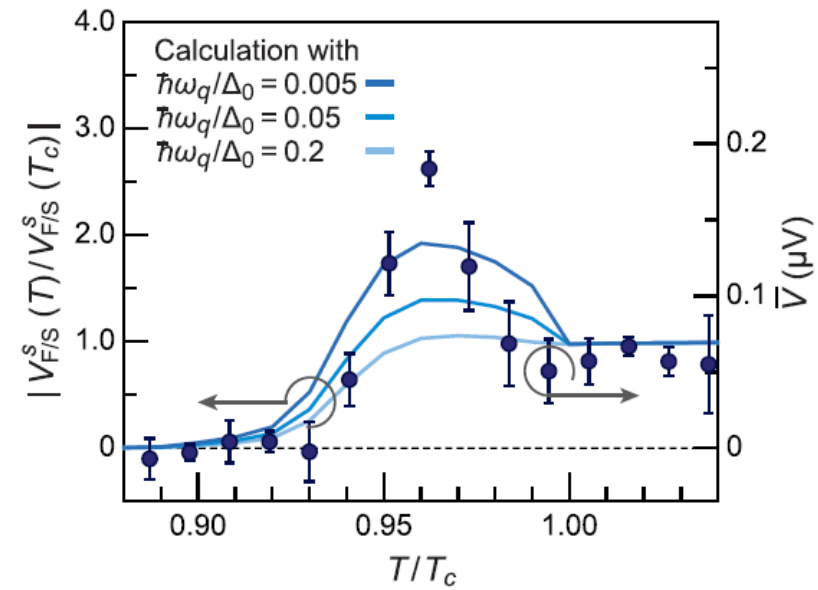


K.-R. Jeon *et al.* [arXiv:2004.09467](https://arxiv.org/abs/2004.09467) (2020)

Different designs to study spin injection in S/F hybrids



Spin injection using a thermal gradient
(Spin Seebeck effect)



M. Umeda *et al.* *Appl. Phys. Lett.* **112**, 232601 (2018)